UNIVERSITÉ DE METZ

Département de mathématique
UFR MIM

École doctorale IAEM Lorraine

Synthèse de commandes et d'observateurs pour les systèmes non-linéaires : Application aux systèmes hydrauliques

THÈSE

présentée et soutenue publiquement le 22 juin 2001

pour l'obtention du

Doctorat de l'université de Metz

(spécialité mathématiques appliquées - automatique)

par

Moez Feki

Composition du jury

Président :	Hassan Hammouri	Professeur de l'Université de Lyon
Rapporteurs :	Brigitte d'Andrea-Novel	Professeur de l'École des Mines de Paris
	Michel Zasadzinski	Professeur de l'Université de Nancy I - CRAN
Examinateurs :	Mohamed Darouach	Professeur de l'Université de Nancy I - CRAN
	Edouard Richard	Maître de Conférence de l'Université de Nancy I
	Gauthier Sallet	Professeur de l'Université de Metz (Directeur de thèse)
	Jean-Claude Vivalda	Chargé de Recherche INRIA Lorraine

Institue National de Recherche en Informatique et en Automatique

INRIA

UNIVERSITÉ DE METZ

Département de mathématique
UFR MIM

École doctorale IAEM Lorraine

Synthèse de commandes et d'observateurs pour les systèmes non-linéaires : Application aux systèmes hydrauliques

THÈSE

présentée et soutenue publiquement le 22 juin 2001

pour l'obtention du

Doctorat de l'université de Metz

(spécialité mathématiques appliquées - automatique)

par

Moez Feki

Composition du jury

Président :	Hassan Hammouri	Professeur de l'Université de Lyon
Rapporteurs :	Brigitte d'Andrea-Novel	Professeur de l'École des Mines de Paris
	Michel Zasadzinski	Professeur de l'Université de Nancy I - CRAN
Examinateurs :	Mohamed Darouach	Professeur de l'Université de Nancy I - CRAN
	Edouard Richard	Maître de Conférence de l'Université de Nancy I
	Gauthier Sallet	Professeur de l'Université de Metz (Directeur de thèse)
	Jean-Claude Vivalda	Chargé de Recherche INRIA Lorraine

Institue National de Recherche en Informatique et en Automatique

INRIA

Remerciements

I would like to thank Prof. Dr. Gauthier Sallet for having accepted my belonging to the members of Projet CONGE INRIA-Lorraine.

I would like to thank Dr. J-C Vivalda and Dr. E. Richard for the work we had carried out together.

Special thanks to Prof. Dr. Brigitte d'Andrea-Novel , Prof. Dr. Mohamed Darouach, Prof. Dr. Hassan Hammouri and Prof. Dr. Michel Zasadzinski for reading and commenting on the thesis and the honor they gave me by presiding the jury.

I want to express my deep gratitude to Dr. Rachid Outbib for having read and commented on this thesis and for all his valuable suggestions.

I am forever indebted to my parents for having made this possible, to my wife for her encouragements and patience and to my brothers and sisters for their support.

I am grateful to all my friends for the nice times we shared together.

Sincere thanks are also extended to everybody who has helped in the development of this thesis.

to . . .

My Parents for everything

My Olfa for her endless love

My Brothers and Sisters for their support

Table des matières

Table des figures

Première partie

Synthèse de commandes et d'observateurs pour les systèmes non-linéaires : Application aux systèmes hydrauliques

Chapitre 0

Résumé de la thèse

0.1 Introduction

L'objectif de ce travail consiste à résoudre certains problèmes d'automatique et de mathématiques appliquées issus des systèmes électrohydrauliques.

L'utilisation des systèmes à fluide sous pression est parfois le meilleur choix dans le cas d'applications qui nécessitent une grande puissance ainsi qu'une bonne précision. Pour cette raison, il est intéressant de développer des méthodes permettant de contrôler ces systèmes de manière automatique, de façon à améliorer leurs performances.

La première étape vers l'automatisation est l'élaboration d'un modèle mathématique. Cette modélisation est très importante tant pour les objectifs de simulation que pour les objectifs de synthèse de lois de commande. Un actionneur électrohydraulique simple se compose d'une servovalve et d'un vérin, et peut être caractérisé par les valeurs d'un certain nombre de variables (position du piston, vitesse du piston, pressions dans les chambres du vérin, ...) ; l'ensemble de ces variables étant appelé état du système. Notre approche consiste à considérer un modèle décrivant l'évolution au cours du temps de ces variables. Ce modèle consiste généralement en un système d'équations différentielles ordinaires portant sur l'état, ainsi que d'une équation d'observation (équation de sortie) :

$$\begin{aligned} \dot{x} &= f(x,u) \\ y &= h(x) \end{aligned}$$

où $x \in \mathcal{X} \subseteq \mathbb{R}^n$ représente le vecteur d'état , $u \in \mathcal{U} \subseteq \mathbb{R}^m$ représente le vecteur de commande appliqué au système, $y \in \mathcal{Y} \subseteq \mathbb{R}^p$ représente le vecteur de mesure (position du piston, force exercée par le piston...), f est l'expression de l'équation différentielle modélisant la dynamique de l'actionneur, et h est l'expression de l'équation d'observation modélisant les mesures.

Si l'on dispose d'un modèle et de la connaissance d'un état initial $x(t_0)$ à l'instant t_0, il est possible, en théorie, de prévoir l'état futur, $x(t)$, du système à n'importe quel instant t. L'automaticien est alors conduit à concevoir des techniques de commande pour contrôler ces systèmes électrohydrauliques, ce thème de recherche suscite depuis toujours un grand intérêt dans la communauté automaticienne.

En général, les méthodes de synthèse de commande en boucle fermée exigent la connaissance de tout l'état. Cependant, pour des raisons techniques ou financières, les variables d'état ne peuvent être toutes mesurées. Cela rend impossible l'utilisation de certain lois de commande ; notons par ailleurs que les mesures disponibles peuvent être bruitées.

Pour pallier ces difficultés, une solution consiste à développer un système auxiliaire qui, à partir des mesures expérimentales, donnera une estimation des variables d'état, (notée $\hat{x}$ dans la suite). Ce système auxiliaire, appelé observateur dans le language de l'automatique, permet de fournir une estimation des variables d'état qui seront utilisées tant pour la synthèse de lois de commande que pour la détection des pannes.

Si l'observateur fournit une connaissance exacte de l'état, alors une loi de commande utilisant l'état de l'observateur parviendrait à stabiliser le système. Cependant, les variables d'état ne sont pas, en général, parfaitement estimées, ce qui amène la question suivante : Si une loi de commande par retour d'état, $u_s(x)$, stabilise le système, $u_s(\hat{x})$ le stabilisera-t-elle encore ? La réponse à cette question est positive dans le cas des systèmes linéaires, on dit qu'il y a un principe de séparation, mais est en générale négative pour les systèmes non-linéaires. Pour ce dernier type de systèmes, trouver des conditions suffisantes assurant la validité de ce principe est un domaine d'étude important.

Cette thèse s'inscrit dans ce contexte : étude d'un système électrohydraulique constitué d'une servovalve alimentant un vérin double tige, agissant sur une charge modélisée par l'association d'une masse, une raideur, et un frottement. Ce travail comporte quatre parties et est organisé comme suit :

Le deuxième chapitre est consacré à la modélisation d'un actionneur hydraulique. On y propose un nouveau modèle permettant de reproduire de manière satisfaisante les caractéristiques statiques d'une servovalve et ne nécessitant que quelques paramètres que l'on ajuste à partir des courbes habituellement fournies par les constructeurs [20].

Le troisième chapitre concerne la synthèse de commande pour les systèmes dynamiques non-linéaires. On y présente quatre méthodes différentes existant dans la littérature à savoir, la linéarisation autour d'un point de fonctionnement, linéarisation entrée-sortie, méthode passive, et mode de glissement. Concernant ce dernier point, une nouvelle méthode y est proposée pour le choix d'une surface de commutation non-linéaire. Pour comparer les performances de ces différentes lois de commande, elles sont appliquées à l'actionneur électrohydraulique et des simulations numériques sont présentées.

Le quatrième chapitre, fait le point de la théorie des observateurs non-linéaires et dans le cinquième chapitre, on propose trois différents observateurs. Le premier est une modification de l'observateur de Gauthier *et. al.* [32], le deuxième repose sur l'idée de la synchronisation de l'observateur en le conduisant avec l'entrée et la sortie du système, et le troisième observateur proposé est basé sur la technique "mode glissant". La synthèse de cet observateur est motivée par la nécessité de concevoir un observateur robuste aux mesures bruitées et/ou aux erreurs de modélisation. Pour comparer les performances de ces observateurs, des simulations numériques sont présentées.

Le sixième chapitre aborde le problème du principe de séparation, un nouveau résultat concernant la stabilisation des systèmes non-linéaires par retour d'état estimé est établi.

Pour finir, on rapporte quelques remarques de conclusion, et on donne des perspectives de recherches futures.

0.2 Modèle statique de l'étage à tiroir d'une servovalve

Les servovalves de commande d'écoulement sont largement répandues dans les servomécanismes électrohydrauliques. Pour cette raison, l'élaboration d'un modèle mathématique pour ces servovalves est très importante tant pour les objectifs de simulation que pour les objectifs de synthèse de lois de commande. La pluspart des modèles considèrent la géométrie de la servovalve comme idéale. La géométrie idéale implique qu'il n'y ait pas de jeu entre le tiroir et la chemise, et donc il n'y a aucun écoulement de fuite. Bien qu'une telle perfection ne soit pas possible dans la pratique, la grande majorité des applications, où des modèles de servovalve sont employés, négligent l'écoulement de fuite. Par conséquent, dans ce cas, l'équation de l'écoulement du fluide à travers un orifice est donnée par

$$Q = ki\sqrt{\Delta P}$$

où Q est le débit à travers l'orifice, k est une paramètre de la servovalve , i est le courant de commande et ΔP est la chute de pression à travers l'orifice. Selon cette expression le débit à travers la servovalve est nul quand le courant d'entrée est nul. Le modèle idéal peut être satisfaisant pour certaines applications. Cependant, les expériences montrent qu'en réalité la présence d'un jeu entre le tiroir et la chemise induit un débit de fuite significatif qui ne peut être ignoré quand la commande est nulle. En effet, dans plusieurs applications telles que l'asservissement de position ou d'effort, où une bonne précision est nécessaire, négliger l'écoulement de fuite peut dégrader sévèrement les performances de commande.

Dans ce travail, on s'intéressera uniquement à la modélisation statique. C'est à dire au modèle donnant les débits fournis par la servovalve en fonction des chutes de pressions et de la grandeur de commande. Il existe actuellement deux types de modélisation de servovalves : le premier est un modèle très simple ne considérant pas les fuites dans les jeux fonctionnels et qui ne permet pas de reproduire correctement les caractéristiques statiques des servovalves [18]. Le deuxième type de modèle est très élaboré et fait appel à une métrologie dimensionnelle du composant. Le modèle intermédiaire que nous allons proposer est dû à E. Richard [20], il permet de reproduire de manière satisfaisante les caractéristiques statiques de la servovalve, et ne nécessitant que quelques paramètres à ajuster à partir des courbes habituellement fournies par les constructeurs.

Contrairement à beaucoup d'autres modèles, on suppose ci-dessus que l'écoulement est laminaire dans le jeu entre le tiroir et la chemise. On supposera aussi que la relation entre le déplacement du tiroir et le courant de commande est linéaire

$$x = \xi i$$

0.2.1 Restriction en recouvrement

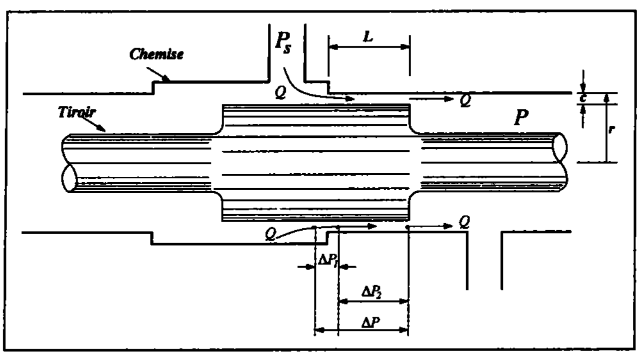

FIG. 0.1 – Tiroir-chemise en position de recouvrement

La figure 0.1 schématise une restriction en position de recouvrement d'un étage à tiroir. On considère que le fluide subit une perte de charge ΔP_1 correspondant à un écoulement laminaire dans un orifice à bord étroit à l'entrée de la restriction, puis une perte de charge ΔP_2 due à un écoulement laminaire dans une conduite annulaire le long des portées du tiroir. Le débit Q traversant l'orifice est alors donné par :

$$Q = \alpha \Delta P_1 \quad \text{où} \quad \alpha = \frac{\pi c^2 (2\pi r)}{32\mu} > 0 \tag{0.1}$$

pour la perte de charge localisée en entrée de l'orifice et

$$Q = \frac{\beta}{L}\Delta P_2 \quad \text{où} \quad \beta = \frac{\pi r c^3}{6\mu} > 0 \tag{0.2}$$

pour la perte de charge dans la conduite annulaire. A partir des deux relations précédentes et compte tenu de $\Delta P = \Delta P_1 + \Delta P_2$, et du fait que L est positive $L = \xi|i|$, on obtient l'expression de débit suivante :

$$Q_c(i, \Delta P) = \frac{\alpha}{1+\gamma|i|}\Delta P \quad \text{où } \gamma = \xi\frac{\alpha}{\beta} = \frac{3\pi}{8}\frac{\xi}{c} \tag{0.3}$$

0.2.2 Restriction en découvrement

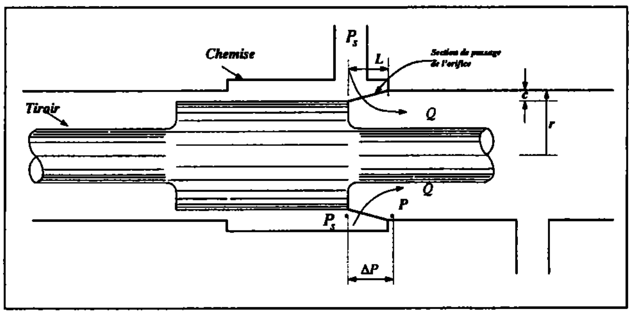

FIG. 0.2 – Tiroir-chemise en position de découvrement

La figure 0.2 représente une restriction d'un étage à tiroir en position de découvrement. Dès que le découvrement est suffisamment grand et la chute de pression relativement importante l'écoulement est en régime turbulent. L'expression du débit est alors donnée par :

$$Q(i, \Delta P) = k|i|\sqrt{\Delta P}$$

Pour assurer la continuité de l'expression du débit en $i = 0$ on doit avoir $\lim_{i \to 0} Q(i) = \alpha \Delta P$. Afin que cette condition soit vérifiée on ajoute à l'expression précédente le terme $\frac{\alpha}{1+\gamma|i|}\Delta P$. Ce terme, décroissant rapidement lorsque i augmente permet d'assurer la continuité de l'expression du débit et la transition entre le régime laminaire et le régime turbulent. Finalement l'expression retenue pour le débit d'une restriction en découvrement est :

$$Q_o(i, \Delta P) = k|i|\sqrt{\Delta P} + \frac{\alpha}{1+\gamma|i|}\Delta P \tag{0.4}$$

0.2.3 Modèle d'un étage à tiroir à centre critique

En examinant la figure ci-dessus, et compte tenu des expression (0.3) et (0.4) des débits, de l'hypothèse de symétrie totale, il est aisé d'exprimer les débits $Q_1(i, P_1)$ et

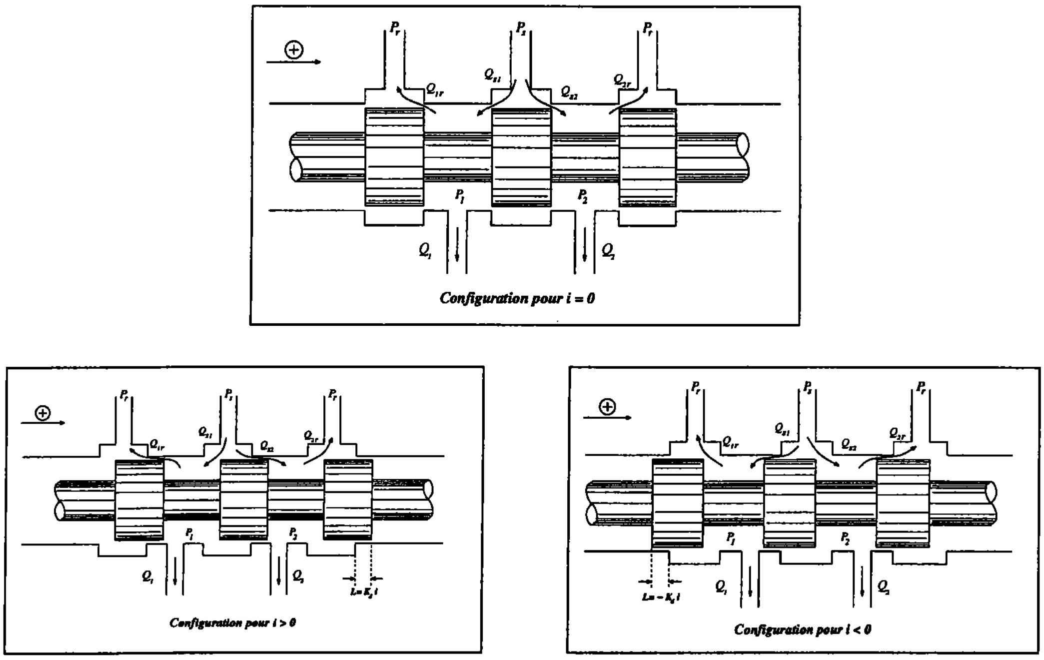

FIG. 0.3 – Configuration d'un tiroir à centre critique

$Q_2(i, P_2)$.

$$Q_1 = Q_{s1} - Q_{1r} \qquad Q_2 = Q_{s2} - Q_{2r}$$

$$Q_1(i, P_1) = \begin{cases} ki(P_s - P_1)^{1/2} + \frac{\alpha}{1+\gamma i}(P_s - P_1) - \frac{\alpha}{1+\gamma i}(P_1 - P_r) & \text{si } i \geq 0 \\ ki(P_1 - P_r)^{1/2} + \frac{\alpha}{1-\gamma i}(P_s - P_1) - \frac{\alpha}{1-\gamma i}(P_1 - P_r) & \text{si } i < 0 \end{cases} \tag{0.5}$$

$$Q_2(i, P_2) = \begin{cases} -ki(P_2 - P_r)^{1/2} + \frac{\alpha}{1+\gamma i}(P_s - P_2) - \frac{\alpha}{1+\gamma i}(P_2 - P_r) & \text{si } i \geq 0 \\ -ki(P_s - P_2)^{1/2} + \frac{\alpha}{1-\gamma i}(P_s - P_2) - \frac{\alpha}{1-\gamma i}(P_2 - P_r) & \text{si } i < 0 \end{cases} \tag{0.6}$$

0.3 Synthèse de commande par retour d'état

La stabilisation des systèmes non-linéaires a été l'objet d'un intérêt particulier pour de nombreux chercheurs au cours de ces deux dernières décennies. Actuellement, trois méthodes sont principalement utilisées : la linéarisation entrée/sortie, la méthode passive, et le mode glissant.

La commande de systèmes non-linéaires affine a largement fait appel aux techniques de linéarisation entrée/sortie [38] [54]. Lorsqu'on effectue un changement de coordonnées, et lorsque le degré relatif r est inférieur à l'ordre n du système, les difficultés rencontrées sont généralement liées à la stabilité de la dynamique résiduelle après avoir appliqué le retour linéarisant. La méthode passive concerne davantage les systèmes non-linéaires non-affines en la commande, cette méthode repose sur l'hypothèse que le système non contrôlé est stable. Cette hypothèse peut être restrictive mais lorsqu'elle est satisfaite, une commande non-linéaire peut être conçue sans recours à la linéarisation. Le problème avec ces deux méthodes réside dans la compensation des erreurs qui peuvent provenir soit de la modélisation, soit des perturbations et des inexactitude qui affectent les mesures. Cette compensation n'est pas toujours possible.

Pour résoudre ce problème, de nombreux chercheurs ont proposé la méthode "mode glissant". Certes, cette méthode n'échappe pas à quelques difficultés, mais c'est une loi de commande très intéressante pour sa rapidité de réponse, ses bonnes performances en régime transitoire, et surtout pour sa robustesse par rapport aux variations des paramètres du modèle, aux perturbations non modélisées, et aux perturbations externes.

Dans ce chapitre, nous faison d'abord quelques rappels de stabilité des systèmes, ensuite des lois de commande par retour d'état sont synthétisées, en utilisant les méthodes précédemment évoquées. Plus précisément notre but est de réaliser un suivi de trajectoire : nous voulons que la force exercée par le piston suivre un profil donné. Notre apport dans ce chapitre est la construction d'une surface de commutation pour la méthode "mode glissant".

0.3.1 Construction d'une surface de glissement

Soit le système dynamique non-linéaire suivant :

$$\dot{x} = f(x) + g(x)\varphi(x,u)u \tag{0.7}$$

où l'origine est un point d'équilibre, $f(.)$ et $g(.)$ sont des champs de vecteurs réguliers, et $\varphi(.,.)$ une fonction non-linéaire.

On rappelle qu'une fonction $\phi : \mathbb{R}^+ \to \mathbb{R}^+$ est dite de classe $\mathcal{K}$ $(\phi \in \mathcal{K})$, si elle est continue, strictement croissante et $\phi(0) = 0$; elle est dite de classe $\mathcal{K}^\infty$ $(\phi \in \mathcal{K}^\infty)$ si $\phi \in \mathcal{K}$, et $\lim_{r\to+\infty} \phi(r) = +\infty$.

On suppose qu'il existe une loi de commande stabilisante $\gamma(x)$ tel que le système autonome

$$\dot{x} = f(x) + g(x)\varphi(x,\gamma(x))\gamma(x) \tag{0.8}$$

est uniformément asymptotiquement stable. Cette hypothèse assure l'existence d'une fonction de Lyapunov $V(x)$ pour le système (0.8) et de trois fonction α_i $(i = 1, 2, 3)$ de classe $\mathcal{K}$ tel que

(i) $\alpha_1(\|x\|) \leq V(x) \leq \alpha_2(\|x\|)$

(ii) $\dot{V}(x) \leq -\alpha_3(\|x\|)$
(iii) $\sup_x \left\| \frac{\partial V(x)}{\partial x} \right\| < \infty$.
Si l'on choisit une surface de commutation

$$\sigma(x) = L_g V(x) = 0$$

la relation

$$\begin{aligned} \dot{V}(x) &= L_f V(x) + L_g V(x) \varphi(x, \gamma(x)) \gamma(x) \\ &= L_f V(x) \\ &\leq -\alpha_3(\|x\|) \end{aligned}$$

est vérifiée sur cette surface.

On peut donc dire que si les états sont restreints à la surface de commutation, le système (0.7) devient asymptotiquement stable et ses trajectoires glissent vers le point d'équilibre. Ceci signifie que le point d'équilibre doit être sur la surface de commutation.

De plus, d'après les équations précédentes on peut conclure que les incertitudes dans les paramètres utilisés pour calculer la loi de commande $\gamma(x)$ n'auront pas d'effets sur le comportement du système lorsqu'il évolue sur la surface de commutation.

Une condition nécessaire pour que les trajectoires du système (0.7) évoluent sur la surface de commutation est l'attractivité de cette dernière, donc il suffit que

$$\sigma \dot{\sigma} < 0$$

soit vérifiée sur tout le domaine de fonctionnement. Pour cela on peut choisir

$$\dot{\sigma} = -W \text{sign}(\sigma), \quad W > 0 \, , \tag{0.9}$$

ce qui mène à $\sigma\dot{\sigma} = -W|\sigma| < 0$. Sachant que

$$\dot{\sigma} = \frac{\partial \sigma}{\partial x} f(x) + \frac{\partial \sigma}{\partial x} g(x) \varphi(x, u) u \, , \tag{0.10}$$

il suffit de résoudre l'équation suivante

$$-W \text{sign}(\sigma) = \frac{\partial \sigma}{\partial x} f(x) + \frac{\partial \sigma}{\partial x} g(x) \varphi(x, u(x)) u(x) \, . \tag{0.11}$$

pour obtenir la loi de commande qui assure l'attractivité de la surface de commutation.

Remarque 0.1 *La synthèse d'une loi de commande par mode glissant est une synthèse en deux temps : le premier consiste en le choix d'une surface de commutation qui assure la stabilité du mode de glissement et le second assure l'attractivité de ce mode de glissement par le choix de la loi de commande.*

Des simulations numériques du système hydraulique contrôlé par les lois de commande issues des différentes méthodes sont présentées dans le troisième chapitre. On peut voir la robustesse du mode de glissement par rapport aux autres méthodes. Cette commande est valable aussi bien en suivi de trajectoire qu'en asservissement. Cependant, le problème de la stabilité de l'actionneur en suivi de trajectoire en utilisant le modèle non-affine reste posé car nous n'avons pas trouvé une fonction de Lyapunov pour la synthèse de la loi de commande. Néanmoins, nos recherche dans cette direction se poursuivent.

0.4 Synthèse d'observateurs non-linéaires

Depuis l'apparition des méthodes de l'espace d'état dans les techniques de synthèse de lois de commande, la recherche a prouvé que la technique par retour d'état donne plus de degrés de liberté au concepteur que la technique par retour de sortie. C'est évident, puisque la sortie est en général une fonction des variables d'état et probablement du temps. Cette technique de synthèse de loi de commande par retour d'état repose sur une exigence : l'accès à toutes les variables d'état.

Cette condition peut parfois être réalisée grâce à des mesures directes, cependant il existe des cas où, pour des raisons financières ou techniques, il est impossible de mesurer toutes les variables d'état. Dans ce cas il est nécessaire de réviser la technique de commande ou de reconstruire les variables d'état manquantes.

Si on adopte cette dernière solution, le problème de la reconstruction de l'état est fondé sur la conception d'un système dynamique auxiliaire appelé "observateur d'état" qui donne une estimation des variables d'état en utilisant seulement les variables mesurées, en l'occurrence la sortie et l'entrée du système.

Cet observateur d'état, ne sera pas seulement utilisé pour les objectifs de synthèse de lois de commande [6] [11] [35] [53], mais servir aussi au diagnostic de système [1], et pour la détection des pannes [33] [37] [16].

Alors que le problème de la synthèse des observateurs des systèmes linéaires stationnaires est complètement résolu depuis les années 60 [46] [47], c'est un problème largement ouvert pour les systèmes non-linéaires bien qu'il ait été étudié depuis les années 70. Plusieurs méthodes ont été utilisées pour cela; de la méthode de grand gain à la méthodes de mode glissant en passant par les méthodes adaptatives.

Une première contribution systématique à la théorie d'observateurs des systèmes non-linéaires a été offerte par la méthode de Thau [76]. Les systèmes non-linéaires considérés sont constitués d'une partie linéaire observable à laquelle est ajoutée une fonction non-linéaire Lipschitzienne. Un observateur de type Luenberger est conçu et des conditions suffisantes pour la stabilité asymptotique de l'erreur peut être dérivée. Cette méthode a été étendue par Tsinias [80] et par Ciccarella *et. al.* [12].

Plus tard Krener, Isidori et Respondek [92] [30] ont considéré la méthode de linéarisation par un changement non-linéaire des coordonnées, ainsi un observateur de type Luenberger peut être élaboré pour de tels systèmes. Zeitz [92] a également développé un observateur pour les systèmes non-linéaires dans ce sens .

Une autre contribution aux observateurs non-linéaires, celle d'une classe de systèmes affines en la commande appelée systèmes bilinéaires a été présenté dans le travail de Williamson [90]. Ce résultat a été étendu ensuite par Sallet *et. al.* [10].

Un observateur non-linéaire différent appelé observateur à grand gain basée sur l'annulation approximative de la non-linéarité a été présenté par Tornambè [79], et a été ensuite amélioré par J.P. Gauthier *et. al* [32] [30]. Les observateurs "mode glissant" ont été présentés par Utkin [83] pour les systèmes linéaires. Cette méthode a été étendue par Slotine *et. al* [67] et Edwards et Spurgeon [15] pour le cas des systèmes non-linéaires. Les observateurs "mode glissant" sont basés sur la théorie des systèmes à structure variables, et sont connus pour leur robustesse par rapport aux variations des paramètres du modèle et aux perturbations externes.

Un autre genre d'observateur peut être employé dans le cas des systèmes non-linéaires avec des paramètres inconnus : il s'agit de l'observateur adaptatif présenté par Marino et Tomei [51] [50]. Ces auteurs considèrent les systèmes qui peuvent être transformés en un certain forme canonique. Les observateurs adaptatifs aident à estimer simultanément les états du système et les paramètres inconnus.

Dans ce chapitre nous exposerons notre propre contribution à la théorie des observateurs non-linéaire.

0.4.1 Observateur à grand gain

On considère le système dynamique non-linéaire

$$\dot{x} = Ax + Bu + f(x,u) \quad ; u \in \mathbb{R}^m, \tag{0.12a}$$

$$y = Cx \quad ; y \in \mathbb{R}^p, \tag{0.12b}$$

où A, B et C sont des matrices de dimensions appropriée et le champ de vecteur non-linéaire $f = (f_1, f_2, \ldots, f_n)^T$ (x^T est le transposé de x) est Lipschitzien et régulier, avec $f(0,0) = 0$.

On considère ensuite le système suivant

$$\dot{\hat{x}} = A\hat{x} + Bu + f(\hat{x}, u) + \zeta S^{-1} C^T (y - C\hat{x}) \tag{0.13a}$$

$$0 = -\theta S - A^T S - SA + C^T C \tag{0.13b}$$

où θ est suffisamment grand et $\zeta \geq 1$

Remarque 0.2 *La matrice $S(\theta)$ peut être considérée comme la solution stationnaire de l'équation différentielle*

$$\dot{S}_t(\theta) = -\theta S_t(\theta) - A^T S_t(\theta) - S_t(\theta) A + C^T C \ ,$$

avec une condition initiale S_0 définie positive. $S(\theta) = \lim_{t \to \infty} S_t(\theta)$, où $S_t(\theta) \in S^+$ est la cône des matrices symétriques définies positives.

Théorème 0.1 *Si le système défini par (0.12) satisfait les hypothèses suivantes*

($\mathcal{H}1$) *il existe une constante positive γ_1 telle que*

$$\|f(x, u) - f(\hat{x}, u)\| \leq \gamma_1 \|x - \hat{x}\|$$

$\forall (x, \hat{x}) \in \mathbb{R}^{n \times n}$ *et* $\forall u \in \mathbb{R}^m$

($\mathcal{H}2$) *la paire (C, A) est observable*

($\mathcal{H}3$) *on peut choisir $\theta > 0$ et $\zeta \geq 1$ telles que*

$$\gamma_1 < \frac{\lambda_{\min}(\theta S + (2\zeta - 1) C^T C)}{2 \lambda_{\max}(S)} \tag{0.14}$$

$\lambda_{\min}(.)$ *et* $\lambda_{\max}(.)$ *sont la plus petite et la plus grande valeur propre de la matrice* $(.)$ *respectivement.*

Alors le système défini par (0.13) est un observateur pour le système (0.12) avec

$$\|x(t) - \hat{x}(t)\| \leq \sqrt{\frac{\lambda_{\max}(S)}{\lambda_{\min}(S)}} \exp(-\alpha_0 t) \|x(0) - \hat{x}(0)\| \ ,$$

où $\alpha_0 = \dfrac{\lambda_{\min}(\theta S + (2\zeta - 1) C^T C)}{2 \lambda_{\max}(S)} - \gamma_1$. □

Ce résultat représente un prolongement du résultat présenté par Hammami [35], où la borne de la constante de Lipschitz était $\gamma_1 < \frac{\theta}{2} \frac{\lambda_{\min}(S)}{\lambda_{\max}(S)}$. En effet, il est clair que pour $\zeta > 1$ on a

$$\gamma_1 < \frac{\theta}{2} \frac{\lambda_{\min}(S)}{\lambda_{\max}(S)} \leq \frac{\lambda_{\min}(\theta S + (2\zeta - 1) C^T C)}{2 \lambda_{\max}(S)}$$

0.4.2 Observateur "mode glissant"

Soit le système non-linéaire

$$\Sigma \begin{cases} \dot{x} &= Ax + f(x,u) + B\Phi(x)\mu \ , \\ y &= Cx \ . \end{cases}$$

où $x \in \mathbb{R}^n$ est le vecteur d'état, $u \in \mathbb{R}^m$ est le vecteur d'entrée de commande et $y \in \mathbb{R}^p$ représente le vecteur de sortie $p < n$. A, B et C sont des matrices de dimensions appropriés, $f : \mathbb{R}^n \times \mathbb{R}^m \to \mathbb{R}^n$ est un champ de vecteur régulier. $\Phi : \mathbb{R}^n \to \mathbb{R}^{p\times p}$ est une fonction bornée, et $\mu \in \mathbb{R}^p$ est un vecteur de paramètres inconnus.

Soit encore le système dynamique

$$\hat{\Sigma} \begin{cases} \dot{\hat{x}} &= A\hat{x} + f(\hat{x},u) + \zeta S^{-1}C^T(y - C\hat{x}) + \Lambda v \ , \\ \hat{y} &= C\hat{x} \ , \\ 0 &= -\theta S - A^T S - SA + CC^T \ . \end{cases}$$

On suppose que les hypothèses suivantes sont satisfaites

($\mathcal{H}1$) (C, A) est une paire observable

($\mathcal{H}2$) $f(x,u)$ vérifie

$$\|f(x,y) - f(\hat{x},u)\| \leq \gamma_f \|x - \hat{x}\| \ .$$

($\mathcal{H}3$) le vecteur des paramètres inconnus est borné

$$\sup_{t>0} \|\mu(t)\| \leq \gamma_\mu \ .$$

($\mathcal{H}4$) $\|\Phi(x)\| \leq \gamma_\Phi \qquad \forall x \in \mathbb{R}^n$.

($\mathcal{H}5$) on peut choisir $\theta = \bar{\theta}$ et $\zeta = \bar{\zeta}$ telles que

$$\gamma_f < \frac{\bar{\theta}}{2} \frac{\lambda_{\min}(S)}{\lambda_{\max}(S)} < \frac{\lambda_{\min}\Big(\bar{\theta}S + (2\bar{\zeta} - 1)C^T C\Big)}{2\lambda_{\max}(S)}$$

($\mathcal{H}6$) il existe une matrice D de dimension $p \times p$ telle que

$$\Lambda D = B$$

Notre résultat est résumé par le théorème suivant

Théorème 0.2 *Considérons les systèmes dynamiques Σ et $\hat{\Sigma}$ avec B et C des matrices de rang maximal, si les hypothèses $(\mathcal{H}1) - (\mathcal{H}6)$ sont satisfaites et si on choisit Λ telle que*

$$\Lambda = S^{-1}C^TW^{-1}$$

avec W une matrice définie positive qui vérifie

$$\lambda_{\min}(W) > \|D\|\gamma_\Phi\gamma_\mu \frac{\lambda_{\max}(CS^{-1}C^T)}{\lambda_{\min}(CS^{-1}C^T)} .$$

Alors $\hat{\Sigma}$ est un observateur asymptotique pour Σ. □

0.5 Sur la stabilisation des systèmes non-linéaires par retour d'état estimé

La commande par retour d'état des systèmes dynamiques non-linéaires a été étudiée par de nombreux auteurs. Dans les références [43] [63] [48] on suppose que l'on a accès à toutes les variables d'état ; dans [84] [81], on travaille avec des estimations (fournies par un observateur) de ces variables. La question qui se pose est la suivante : une loi de commande stabilisante calculée non pas à partir des valeurs exactes des variables d'état mais à partir d'une estimation de celles-ci continue-t-elle de stabiliser le système ? La réponse est positive dans le cas des systèmes linéaires mais reste un sujet de recherche pour les systèmes non linéaires. La référence [84] propose une loi de commande $\gamma(x)$ stabilisant un système non linéaire $\dot{x} = f(x,u)$ (i.e., O est un point d'équilibre asymptotiquement stable pour $\dot{x} = f(x, \gamma(x))$), cette loi γ étant telle que, si z est une estimation de l'état x, $\gamma(z)$ continue de stabiliser $\dot{x} = f(x,u)$. Dans [84], γ est supposée continûment différentiable, dans [48] cette hypothèse a été affaiblie : γ est seulement supposée continue. L'objet de ce travail est d'affaiblir encore les hypothèse sur γ ; nous supposons seulement que cette fonction est bornée et continue par morceaux.

0.5.1 Rappels Théoriques

On considère un système non-linéaire de la forme :

$$\dot{x} = f(x,u), \quad x \in \mathbb{R}^n, \quad u \in \mathbb{R}^m \tag{0.15a}$$
$$y = h(x), \quad y \in \mathbb{R}^k. \tag{0.15b}$$

où $f : \mathbb{R}^n \times \mathbb{R}^m \to \mathbb{R}^n$ est un champ de vecteur C^∞, et $h : \mathbb{R}^n \to \mathbb{R}^k$ est une fonction suffisamment dérivable. On suppose que l'origine $(0,0) \in \mathbb{R}^n \times \mathbb{R}^m$ est un point d'équilibre pour f, et que l'espace des entrées contient les fonctions bornées $u : \mathbb{R}^+ \to \mathbb{R}^m$, cette borne M est définie comme $\|u\| \leq M$.

Définition 0.1 *Le système (0.15) est dit faiblement détectable s'il existe une fonction continue $g : \mathbb{R}^n \times \mathbb{R}^k \times \mathbb{R}^m \to \mathbb{R}^n$ ($g(0,0,0) = 0$), une fonction $W : \mathbb{R}^n \times \mathbb{R}^n \to \mathbb{R}^+$ continûment differentiable, et trois fonctions ψ_i $i = 1,2,3$ $\psi_i \in \mathcal{K}^\infty$, telles que $f(x,u) = g(x,h(x),u)$, $\forall (x,u) \in \mathbb{R}^n \times \mathbb{R}^m$ et de plus*

$$\psi_1(\|x-z\|) \leq W(x,z) \leq \psi_2(\|x-z\|) , \tag{0.16}$$

$$\frac{\partial W}{\partial x} f(x,u) + \frac{\partial W}{\partial z} g(z,h(x),u) \leq -\psi_3(\|x-z\|) , \tag{0.17}$$

$\forall u \in \mathbb{R}^m$ et dès que $x - z \in \mathbb{R}^n$ est suffisamment petit.

Ainsi si le système (0.15) est faiblement détectable, alors le système dynamique $\dot{z} = g(z,h(x),u)$ est un estimateur d'état du système (0.15).

Définition 0.2 *[72] Le système (0.15) est dit stable entrée-état (SEE) si et seulement s'il admet une fonction SEE-Lyapunov . C'est-à-dire, s'il existe une fonction $V : \mathbb{R}^n \to \mathbb{R}^+$ continûment differentiable, $\alpha_1, \alpha_2 \in \mathcal{K}^\infty$ et $\alpha_3, \theta \in \mathcal{K}$ telles que*

$$\alpha_1(\|x\|) \leq V(x) \leq \alpha_2(\|x\|) , \tag{0.18}$$

pour $x \in \mathbb{R}^n$ et

$$\nabla V(x).f(x,u) \leq -\alpha_3(\|x\|) , \tag{0.19}$$

pour $x \in \mathbb{R}^n$ et $u \in \mathbb{R}^m$ vérifiant $\|x\| \geq \eta(\|u\|)$.

Remarque 0.3 *[72] Il est facile de voir qu'une fonction V est SEE-Lyapunov pour (0.15) si et seulement s'il existe $\alpha_i \in \mathcal{K}^\infty$ $i = 1,2,3,4$ telles que la condition (0.18) est vérifiée, et*

$$\nabla V(x).f(x,u) \leq -\alpha_3(\|x\|) + \alpha_4(\|u\|) . \tag{0.20}$$

Soit $\gamma(x)$ une loi de commande admissible pour le système (0.15). On entend par admissible, n'importe quelle loi de commande pour laquelle l'équation $\dot{x} = f(x,\gamma(x))$ est bien posée, et qui admet pour chaque condition initiale $x(0) \in \mathbb{R}^n$ une unique solution absolument continue. Soit $\rho \in \mathcal{K}^\infty$, une loi de commande est dite bornée par ρ si pour chaque $x \in \mathbb{R}^n$, $\|\gamma(x)\| \leq \rho(\|x\|)$.

Dans la suite on examine la question suivante : si $u = \gamma(x)$ stabilise (0.15) en $0 \in \mathbb{R}^n$ sous quelles conditions la loi de commande $u = \gamma(z)$ stabilise-t-elle le système :

$$\begin{pmatrix} \dot{x} \\ \dot{z} \end{pmatrix} = \begin{pmatrix} f(x,\gamma(z)) \\ g(z,h(x),\gamma(z)) \end{pmatrix} \tag{0.21}$$

en $(0,0) \in \mathbb{R}^n \times \mathbb{R}^n$?

Cette question a été traitée par de nombreux chercheurs, mais notre résultat constitue une amélioration des résultats existant.

0.5.2 Résultat principal

Nous considérons le système (0.15), le théorème ci-dessous constitue le principal résultat de cette partie

Théorème 0.3 *Si le système (0.15) est faiblement détectable et stable entrée-état alors il existe une loi de commande bornée* $u = \gamma(x)$, $\gamma(0) = 0$ *qui stabilise (0.15) et telle que le système (0.21) est asymptotiquement stable.*

Ce résultat expose la possibilité d'utiliser les états estimés pour contrôler des systèmes dynamiques stabilisables par des lois de commande discontinues. Notre résultat constitue une amélioration d'autres résultats exigeant que la loi de commande soit continûment différentiable ou au moins continue.

0.6 Conclusion

Au terme de ce travail, nous voudrions souligner nos apports sur le plan théorique et envisager quelques perspectives.

L'objectif de cette thèse est l'étude du comportement d'un actionneur électrohydraulique. Elle comprend deux grandes parties, la première partie porte sur la modélisation de ce type de système, la seconde traite la commande automatique de cet actionneur et de sujets connexes, en l'occurrence, synthèse d'observateur et principe de séparation.

En ce qui concerne la modélisation , on a développé un nouveau modèle pour la servovalve qui suffisamment simple pour permettre son analyse mathématique, et permet de décrire le comportement réel, y compris les débits de fuite généralement négligés dans d'autres modèles.

Il s'avère que le système électrohydraulique est fortement non-linéaire, par conséquent, l'utilisation directe des méthodes existantes pour la synthèse de lois de commande n'est pas évidente. Pour cette synthèse on a utilisé les avantages de la méthode passive et la robustesse du mode glissant pour concevoir une nouvelle méthode de construction de la surface de commutation. Cette méthode aide à la synthèse de loi de commande robuste pour les système non-linéaires et non-affines en la commande.

En effet, les lois de commande appliquées au système électrohydraulique, exigent toutes les informations position, vitesse et pressions dans les chambres du vérin. Par ailleurs en pratique, on ne peut mesurer facilement que le déplacement. Nous avons donc pallié cet inconvénient en proposant la construction de trois observateurs non-linéaires, dont un basé sur le mode glissant et il a montré une robustesse en présence de paramètres inconnus. Le cinquième chapitre constitue notre apport dans ce domaine.

Finalement, nous avons étudié le problème de la stabilisation par retour d'état estimé. Ce travail prolonge les travaux de Vidyasagar et Tsinias.

Sur le plan des perspectives, quelques résultats proposés dans cette thèse peuvent être améliorés.

Dans le domaine de la modélisation, on peut espérer qu'un modèle dynamique au lieu de statique de la servovalve apportera de meilleurs résultat surtout dans les applications ou l'actionneur est soumis à de relativement hautes fréquences. Terminer l'étude théorique et l'application de la stabilité en suivi de trajectoire avec la méthode passive serait également un résultat intéressant. On peut aussi améliorer la robustesse de l'observateur à grand-gain par l'estimation de paramètres inconnus. Il serait sans doute souhaitables de pouvoir estimer le paramètre du frottement sec en ne mesurant que le déplacement du piston.

Deuxième partie

Nonlinear controller and observer design : Application to electrohydraulic systems

Chapitre 1

Introduction

In applications where high power is needed with a requirement for precision control, it is inevitable that a fluid power system will be used. The diversity of applications from robotics to heavy industrial systems has made electrohydraulic manipulators widely utilized in many industrial fields. Electrohydraulic manipulators are systems that produce hydraulic power outputs in response to electrical signal inputs.

1.1 Automation

A simple electrohydraulic manipulator consists of a servovalve and a piston. One main preoccupation in industrial applications, is to automatically control such systems. These manipulators can be characterized by values of several variables (pressure applied to the piston, piston position, piston velocity...) The set of all variables describing the dynamics of the system are denoted as state variables. The first approach to automation is to extract a mathematical model describing the time evolution of these state variables. The model consists, in general, of a system of ordinary differential equations, in addition to an algebraic equation called the output or the observation equation.

$$\begin{aligned} \dot{x} &= f(x,u) \\ y &= h(x) \end{aligned}$$

where $x \in \mathcal{X} \subseteq \mathbb{R}^n$ stands for the state vector, $u \in \mathcal{U} \subseteq \mathbb{R}^m$ represents the electrical input signal, $y \in \mathcal{Y} \subseteq \mathbb{R}^p$ is the measured output (piston position, piston force...), f is the expression of the differential equations describing the dynamics of the electrohydraulic manipulator and h is the expression of the observation equation modeling the measured output.

1.2 Modeling

Modeling is in its own a large field of study that attracted the attention of many researchers [59] [64]. Extracting a mathematical model to an application system is very crucial and the success or failure of the behaviour of a controlled system directly depends on it. The required mathematical model precision to describe the dynamical behaviour of a given system depends on its purpose. Indeed, fields where high precision is needed, and where faults are less tolerated (robots that are to send to the space), require very fine models in which all aspects are meticulously respected. However, fields where only little precision is required (civil engineering machinery) we can simplify complicated geometrical shapes and neglect phenomena that slightly contribute to the main dynamics (leakage, heat...). In both cases designers have been faced to difficulties. While in the first case the model may be too complex and represent a hindrance towards designing a controller, in the second case the model may be too simple to correctly describe the system behaviour. Therefore, an intermediate model is always appreciated. A model that reflects as best the dynamics of the system and can mathematically be handled. In modeling an electrohydraulic system consisting of a servovalve and a piston, the main concern is the fluid flow through the servovalve, and the piston motion.

1.3 Systems output and output control

The role of all machines (systems), in real life, is to perform a desired task (output). The system output is usually a response to the system input. In some applications, the system requires human interference, thus the system is said to be controlled in open-loop manner, that is the input signal is provided by the user and is in a way independent off the output. However, in other applications the system is autonomous and the input depends on the output, that is the system behaves according to the fact that a desired output is attained or not. This is denoted as the closed-loop control. In general, when using the closed-loop control approach, the input signal is an algebraic combination of the state variables.

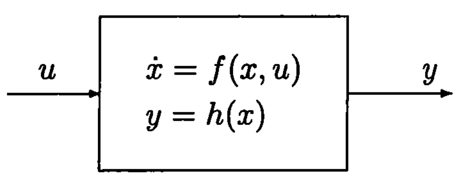

FIG. 1.1 – Open-loop controller scheme

Controllability of dynamical systems has been addressed by many researchers. In particular the control design for hydraulically actuated manipulators. Their highly nonlinear and complicated features, and the need to obtain a specified performance, namely a given piston position or a prescribed piston force, were considered to be challenging.

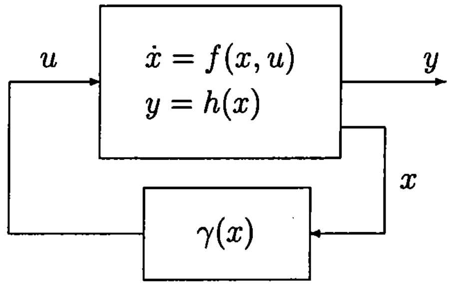

FIG. 1.2 – Closed-loop controller scheme

1.4 Observation of the system

The closed-loop control methods, which are in general more efficient than open-loop approaches, require the accessibility to all different state variables. However, technical reasons or cost usually present an obstacle towards obtaining a trustworthy measurements of all state variables. Therefore, we generally measure only a limited number of outputs ($p < n$). In the electrohydraulic system we can easily and precisely measure the piston position, simply by installing a sensor next to it. However, measuring the pressure applied to the piston inside the cylinder chambers requires further manufacturing which can be expensive and may alter the system behaviour.

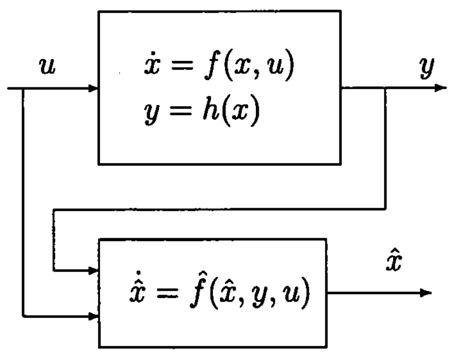

FIG. 1.3 – System observer

A remedy to these limitations is to construct an auxiliary system which can estimate the state variables from the knowledge of the input and the measured outputs. The state estimator dubbed as state observer in control theory, enables to reconstruct the state variables which will thereafter be used to build the input controller. Should the estimated states be exactly equal to the real states, one can expect the controller constructed from estimated states to yield to the desired task. Despite this is true in linear systems, it is not a straightforward conclusion for general nonlinear systems. This problem is addressed as the separation principle.

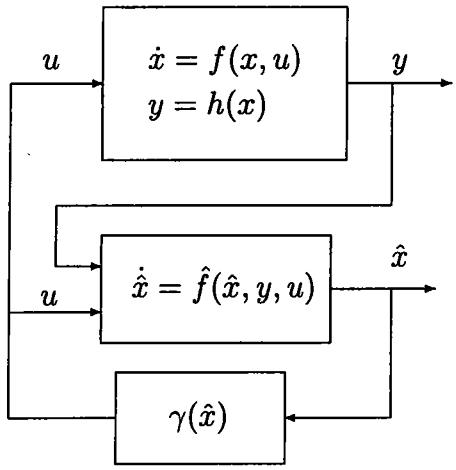

FIG. 1.4 – Controller using estimated states

1.5 Motivations

The main motivation of this work was the development of electrohydraulic servovalve model that can describe the fluid flow without neglecting leakage occurring due to manufacturing imperfections. Next, the model will be used to control the force exerted by a hydraulic piston on a given load. In fact, the design of reliable control systems involves more than system modeling and design of control laws to satisfy performance objectives. A control system should possess the capability of reacting favorably and promptly to unexpected changes like parameter variations and component failures that tend to degrade overall system performance. In essence, we need to design a robust control law. This need, inherently requires the construction of state observers, and again robust observers are preferred.

1.6 Thesis contribution

This dissertation has a four-fold focus namely

- Development of a servovalve model.
- Constructing a robust controller using sliding method.
- Improving the performance of an existing high-gain observer and designing of two new nonlinear observers, one of which is robust and uses the siding method.
- Proving a new result on the separation principle.

This thesis attempts to bring these ideas together in a form that will give an insight to the reader on the function of an electrohydraulic manipulator. The challenge is to design robust controllers and observers appropriate for real applications.

1.7 Thesis outline

Chapter 2 introduces flow fundamentals of fluids, then presents how we construct the servovalve model. Next we show results of its experimental validation [20]. Using the servovalve model an overall model describing the dynamics of a piston-valve combination is derived.

In chapter 3 we review definitions and theorems concerning the stability theory. We then state some different controller design methods existing in literature. Next some of these methods are applied to the electrohydraulic system developed in chapter 2 [21]. An other robust method to design controllers based on sliding mode methods is presented and applied to the electrohydraulic system [23].

Chapter 4 represents an overview to observability theory and to different nonlinear observer design approaches.

Chapter 5 is devoted to the construction of new nonlinear observer, and their application to the electrohydraulic system. A first observer constitutes an improvement of another existing one [24]. The second is a new simple observer that does not cover a wide range of applications but correctly works in the case of our system [25]. The third observer was developed based on the sliding method [22].

The separation principle is revisited in chapter 6 where we present a new result on nonlinear system controlling via estimated states [27].

Conclusions of the thesis and future research options are explored in chapter 7.

Chapitre 2

Including leakage in the servovalve static model

2.1 Introduction

The role of the hydraulic power modulator consists in modulating, with respect to an electrical input signal, the inlet orifices between the pressure source and the actuator housings and the outlet orifices between the tank return pressure and the actuator housings. This modulation can be achieved in general by a sliding spool. Figure 2.1 shows a representation of the spool valve and the modulated orifices $R_{s1}, R_{1r}, R_{s2}, R_{2r}$. These orifices forme a Wheatstone bridge as delineated by the next figure.

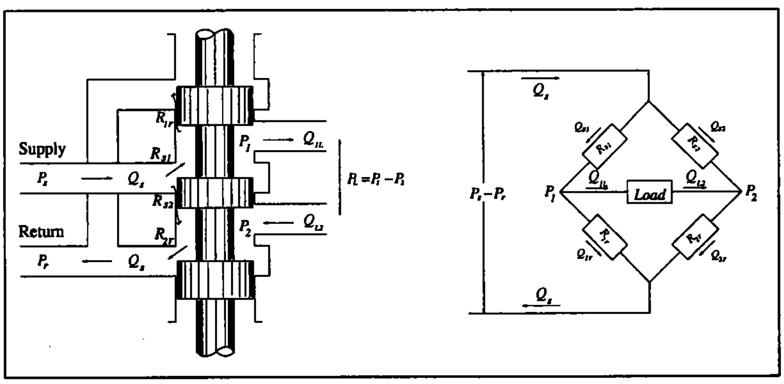

FIG. 2.1 – Wheatstone bridge

Valves may be classified by a feature of their construction, however, they are best classified by their function. Three broad functional types can be distinguished : pressure control valves, directional control valves and flow control valves. Pressure control valves act to regulate pressure in a circuit. Directional control valves direct or prevent a flow through a selected passage. They can be controlled by solenoids which generate the force necessary to open or close the valve. Removal of the solenoid voltage allows the spool to return to its original position under the action of an opposite spring. The proportional valves have developed from the directional control valves. They were obtained by incorporating a position transducer connected to the spool, thereby allowing accurate closed-loop position control of the spool. In the case of high flow, a double-stage setup is used, where in the first stage a first valve is utilized to control the spool position of the second valve which is subjected to the hydraulic forces. Electrohydraulic flow control servovalves usually consist of two stages. They contain a hydraulic preamplifier first stage, thus the electrical control signal needed is considerably low ($< 30mA$). Two-stage servovalves may be classified by the type of feedback used inside. Spool position feedback two-stage servovalves are by far the most common. Due to its construction, the dynamical performance of the electrohydraulic servovalves are much higher than that of the directional control valves and the proportional valves.

Extracting a mathematical model for the electrohydraulic servovalve is very significant as well for the simulation aims as for the objectives of synthesis of control laws. In this chapter we will be interested only in the static models. That is we will deal with models expressing the flows provided by the electrohydraulic servovalve according to the pressures in the housings of the actuator and the input control. Actually there are two approaches to model these components. A first very simple model not considering the leakage due to functional clearances and not providing the correct static characteristics of the component [52] [89] [70] [18]. And a second very refined model making use of the physical dimensions of the component [17]. Herein, we propose an intermediate model [20] allowing a satisfactory reproduction of the static characteristics of the components and only requiring to adjust few parameters using some curves usually provided by the manufacturers. We start by giving basics on spool valves and flow theory, then we establish our model of the electrohydraulic servovalve.

2.2 A spool valve power modulator

2.2.1 Description

There are different types of servovalves, however, the most widely used is the sliding valve employing spool type construction. Figure 2.2 shows some typical spool valve configurations. Spool valves can be classified by different ways, namely, the number of ways

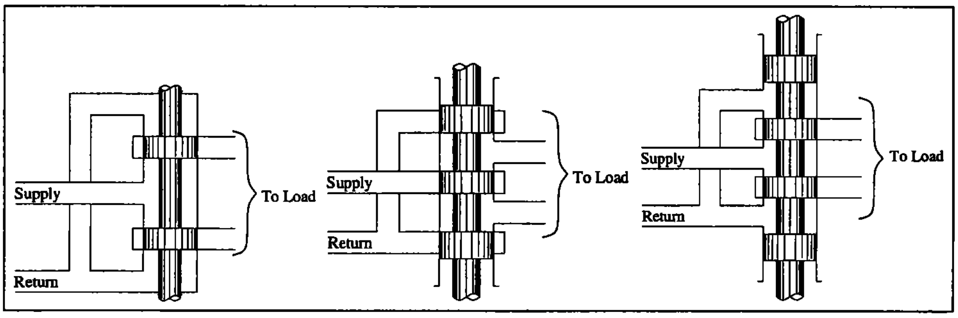

FIG. 2.2 – Typical hydraulic servovalves

flow enter and leaves the valve, the number of lands in the spool and the type of center when the valve spool is in neutral position. Because all valves require a supply, a return and at least one line to the load, most valves are either three-way or four-way. In this chapter we will be interested in the four-way valves. A four-way valve has a supply, a return and two lines to the load, see Figure 2.2. The number of lands vary according to the application, and herein we will be restricted to the three-land valves.

Using the classification according to the type of center, we can distinguish three type of valves.

Open center spool valve (or Underlapped spool valve) This corresponds to having land width smaller than the port width in the sleeve, thus having open orifices when the spool is at neutral. This produces a considerable leakage flow and a steeper slope of the flow gain curve in the underlap region arising from opening the supply port and closing the return port in the case of positive input current ($i > 0$) and vice versa in the case of negative input current ($i < 0$). Figure 2.3 depicts an open center spool valve.

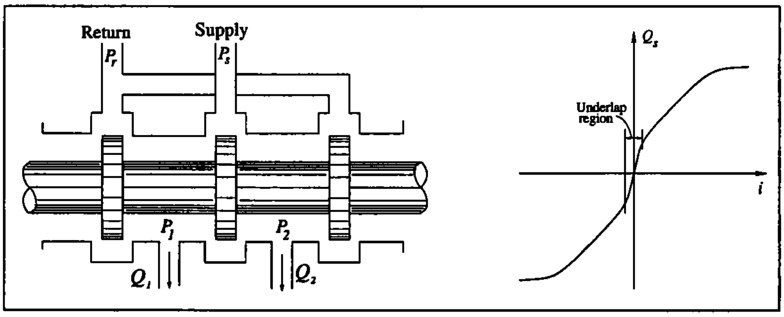

FIG. 2.3 – Open center spool valve

Closed center spool valve (or Overlapped spool valve) Contrary to the previous case, here the land width is larger than the port width, thus making it necessary to move the spool before having any type of flow other than the internal leakage through the clearance between the spool and the valve sleeve. This type of configuration reduces the leakage flow at the neutral position and introduces a dead zone (overlap region) in the characteristic of the flow curve. A closed center spool valve configuration is shown in Figure 2.4.

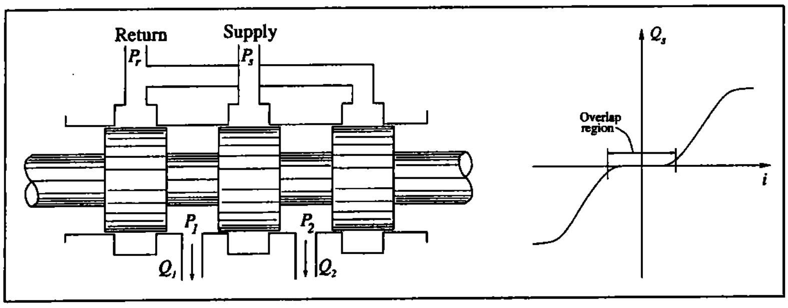

FIG. 2.4 – Closed center spool valve

Critical center spool valve (or Critically lapped spool valve) In this configuration the valve lands are critically lapped, that is the lands and ports are exactly matched such that the smallest movement of the spool allows flow through the valve. Figure 2.5 shows a critical center spool valve.

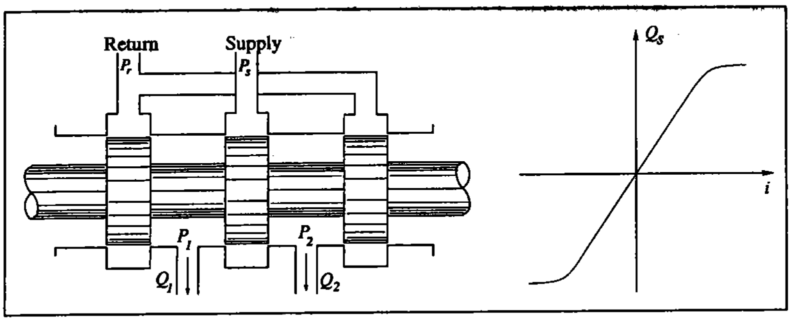

FIG. 2.5 – Critical center spool valve

2.2.2 Static characteristics

Since electrohydraulic servovalves have a major part to play in feedback control systems, it is worth considering some of the features of such devices. Servovalves are mainly characterized by some rated values in addition to the flow gain, the null leakage and the pressure gain [77].

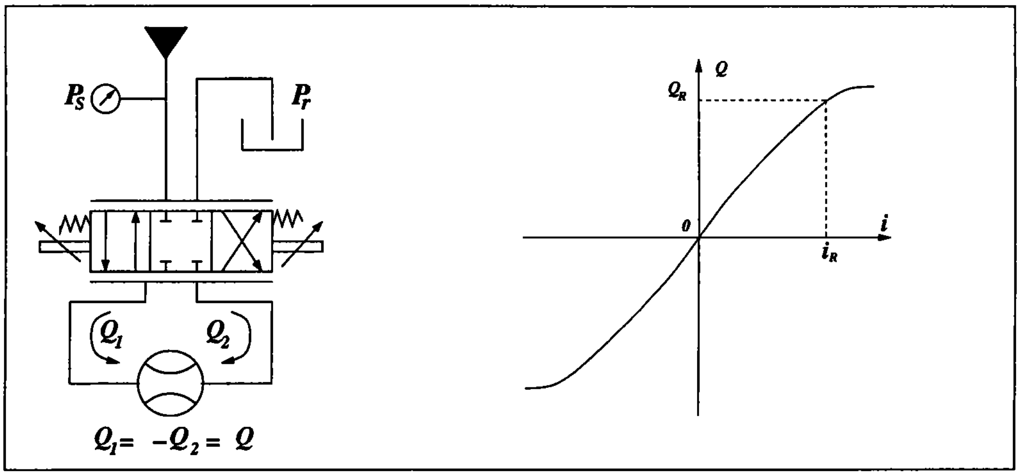

FIG. 2.6 – (a) Setup of the control flow measurement. (b) Flow curve

2.2.3 Rated values

The rated current i_R expressed in mA, is the input current required to produce rated flow Q_R which is itself the maximum control flow before flow saturation effects occur [77]. Rated flow is normally specified as the no-load flow and is expressed in liters per minute. Rated values are usually measured at a specific valve pressure drop which is the sum of the differential pressures present across the control orifices. Valve pressure drop is $\Delta P_v = P_s - P_1 + P_2 - P_r$. Usually the no-load valve pressure drop used to measure the rated values is $70bar$.

Flow gain

The essential role of the spool valve is to use a low electrical power input to move the spool that governs a hydraulic flow and thus gives a high power output. Clearly, for the sake of simplicity, the relationship between the input current, i, and the output flow rate Q, has to be as linear as possible. This aim can be reached by a critically lapped valve with ideal geometry. However, ideal geometry implies that the orifice edges are perfectly square with no rounding and that there is no radial clearance between the spool and the sleeve, which is practically impossible. Nevertheless, it is always possible to construct a valve with a relatively linear flow. The flow curve is obtained by plotting the flow through the control ports, with a load pressure drop $P_1 - P_2 = 0$, versus the input current as the spool performs a complete cycle between plus and minus rated current value. Therefrom, the flow gain is the slope of the linear part of the flow curve [77]. Figure 2.6-a shows a technical diagram that represents the setup used to obtain the flow gain curve, whereas Figure 2.6-b sketches the flow gain curve.

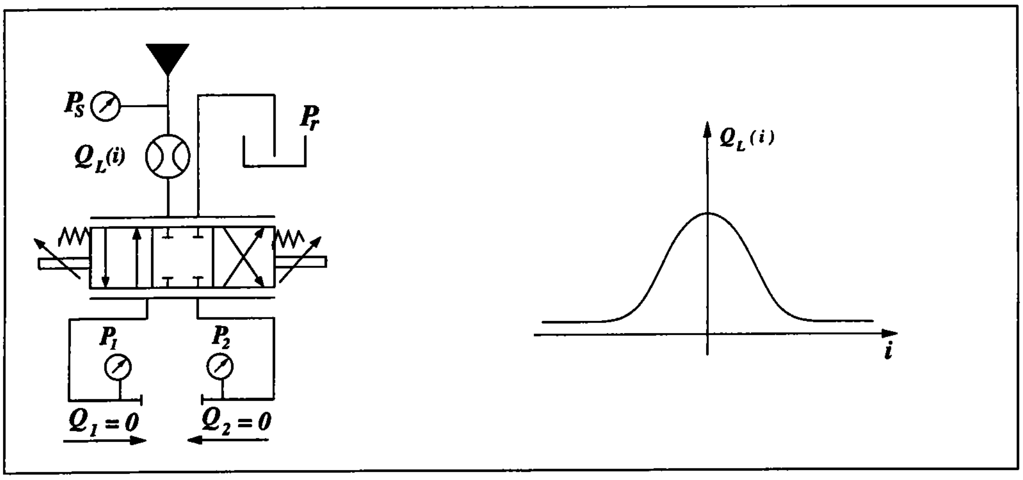

FIG. 2.7 – Setup to measure the internal leakage flow

Leakage flow

It is the leakage characteristics that actually differentiate a practical from an ideal critically lapped valve. The ideal valve has zero leakage flows, whereas the practical valve has radial clearance and hence a leakage flow exists. The leakage flow curves can be obtained by obstructing both load lines, then measuring the total flow rate used up, which is actually a leakage flow since load flow is zero. Figure 2.7 shows a technical diagram of the setup and a sketch of a typical leakage flow. The leakage flow is maximum when the input current is nil (null leakage), and decreases rapidly with increasing input current (valve stroke) because the spool land overlaps the return valve orifices. This curve is a measure of hydraulic power loss.

Block-line pressure sensitivity

The block-line pressure sensitivity curve is a measure of the change in the load pressure drop ($P_L = P_1 - P_2$), with zero control flow (control ports blocked), as the spool is stroked around the null region [77]. The block-line pressure sensitivity curve can be obtained by the same setup as used for the leakage flow measurement. The load pressure drop quickly increases to near full supply pressure for a very small input current (very small spool displacement). The pressure gain is defined to be the average slope of the pressure sensitivity curve in the region between $\pm 40\%$ of maximum load pressure drop. This curve is of great importance and is generally provided by the constructors.

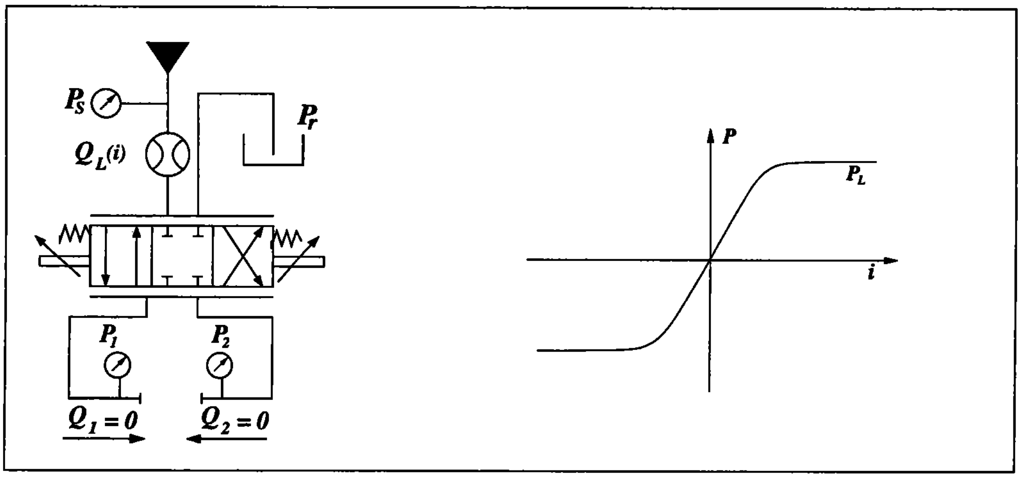

FIG. 2.8 – Block-line pressure sensitivity curve

2.3 Flow fundamentals of incompressible fluid

Knowledge of the fundamental laws and equations which govern the flow of fluid is indispensable to extract mathematical model for the dynamical hydraulic systems.

An accurate analytic description of general fluid flow has always been a challenging aim to be achieved. Although some attempts were promising, see [52] and the references therein, the complexity of the nonlinear partial differential equations describing the fluid motion made it nearly impossible to find a general solution. Thus, in many instances certain approximations can be made to reduce the complexity of these equations and permit solutions accurate enough for most applications.

For instance, the equation governing the motion of a one-dimensional, steady, incompressible, frictionless flow with no body forces is given by

$$u\frac{\partial u}{\partial x} = -\frac{1}{\rho}\frac{\partial P}{\partial x} \tag{2.1}$$

where x and u are the displacement and the velocity, ρ is the mass density and P is the pressure. The integration of this equation leads to the so called Bernoulli's equation

$$\frac{u^2}{2} + \frac{P}{\rho} = constant \tag{2.2}$$

Another important equation describing the fluid flow results from the law of conservation of mass. Let us assume a control volume V undergoing a mass flow rate $\mathcal{M}$ in and out of the volume. Let the accumulated mass inside V be m with density ρ. The rate at which mass is stored is equal to the incoming mass flow rate minus the outgoing mass flow rate. Therefore

$$\sum \mathcal{M}_{in} - \sum \mathcal{M}_{out} = \frac{dm}{dt} = \frac{d(\rho V)}{dt} \tag{2.3}$$

This equation is called the continuity equation.

Several other equations may be needed to fully describe the fluid motions, but will not be included herein, see [52] [89]. This section will discuss the types of flows, flows through conduits will be mentioned, however we will focus on flow through orifices.

2.3.1 Types of fluid flow

Since a general solution of fluid flow has not been found yet, different particular situations have been distinguished to promote the use of approximation. Based on practical use, flow in closed conduits is of particular interest, this includes several types of which we will only cover the flow in pipes and the flow through sharp edged orifices. Besides, fluid can also be discerned according to the type of forces affecting it. Though the flow can be subjected to many types of forces, it is tenable to consider forces due to fluid inertia and forces arising from viscosity as more significant in most cases.

Flow dominated by viscosity forces is referred to as *laminar* or viscous flow. Laminar flow is characterized by an orderly, smooth parallel line motion of the fluid. Inertia dominated flow is generally *turbulent* and characterized by irregular, eddylike paths. Nevertheless, in some cases inertia dominated flow behaves in an ordered fashion if we neglect the boundary layer next to the solid. This type of flow is called potential or *streamline*, this is can be observed in case of flow through an orifice.

2.3.2 Reynolds number

The existence of two types of flow make rise to a question : When can we say if a flow is viscosity or inertia dominated? Therefore, it is indeed necessary to define a quantity which weights the relative significance of these two forces in a given flow situation. The dimensionless ratio of inertia force to viscous force is called Reynolds number and defined by

$$\mathcal{R}e \stackrel{def}{=} \frac{\text{inertia force}}{\text{viscous force}} = \frac{\rho \bar{u} D_h}{\mu} \tag{2.4}$$

where ρ is fluid mass density, μ is absolute viscosity, $\bar{u}$ is the average velocity of flow, and D_h is the hydraulic diameter defined by

$$D_h = 4\frac{A}{S}$$

where A is the flow section area and S is the flow section perimeter.

The Reynolds number helps to describe the transition from viscous to inertia dominated flows. A simple interpretation of equation (2.4) shows that Reynolds number is small if viscosity forces are preponderant, whereas it is large if inertia forces are preponderant. Though inertia dominated flows can be turbulent or streamline, the term turbulent is generally used to describe flows with large Reynolds numbers.

2.3.3 Flow through conduits

Flow in pipes may be laminar or turbulent. The hydraulic diameter of a pipe is the inside diameter $D_h = D$ and the average velocity is volumetric flow rate divided by pipe area, that is

$$\bar{u} = \frac{Q}{A} = \frac{4Q}{\pi D^2} \tag{2.5}$$

Therefore the Reynolds number is given by :

$$\mathcal{R}e = \frac{\rho \bar{u} D_h}{\mu} = \frac{4\rho Q}{\pi \mu D} \tag{2.6}$$

Empirical values of $\mathcal{R}e$ for flow through pipes are $\mathcal{R}e \leq 2000$ for laminar flow and $\mathcal{R}e \geq 4000$ for turbulent flow. Transition between laminar to turbulent flow occurs inside that range $2000 < \mathcal{R}e < 4000$.

Laminar flow in pipes

These pipes usually termed capillary tubes because of their small diameter which results in laminar flow. If we consider steady laminar flow then we have a constant velocity profile $\bar{u}$ at the entrance of the pipe. The fluid velocity at the pipe wall is zero, hence this fluid layer exerts forces on the inner layers whose velocities increase to satisfy the law of continuity and henceforth until the center of the pipe is reached. The velocity profile

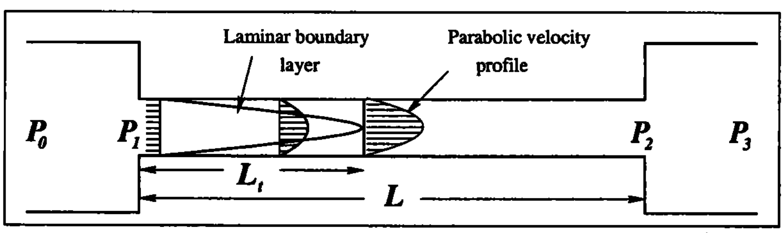

FIG. 2.9 – Laminar flow in a pipe

becomes parabolic after a certain transition length is reached, and remains parabolic throughout the pipe. The peak velocity u_0 for a parabolic profile is $2\bar{u}$. Experimental observations showed that the transition length for a laminar flow is $L_t = 0.0575D\mathcal{R}e$ so that for a laminar flow at $\mathcal{R}e = 2000$; $L_t = 115$ times the pipe diameter. For pipe length greater than transition length, the pressure drop can be approximated, if we consider losses due to sharp edged entrances, by (see [52]).

$$P_0 - P_3 = \frac{128\mu LQ}{\pi D^4}\left(1 + 0.0434\frac{D\mathcal{R}e}{L}\right) \tag{2.7}$$

Turbulent flow in pipes

The equations describing the turbulent flow in pipes are mainly based on experimental observations. As flow enters the pipe the boundary layer becomes turbulent after a very

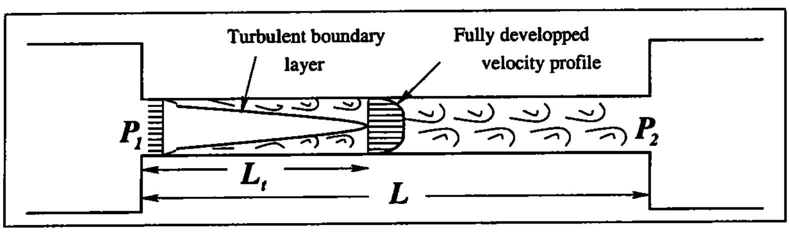

FIG. 2.10 – Turbulent flow in a pipe

short distance. As this boundary layer advances inside the pipe it increases in thickness to the center of the pipe until it reaches a certain thickness after a transition length of about 25 to 40 pipe diameter, this is delineated in Figure 2.10. The pressure drop for fully developed turbulent flow has been empirically obtained and is expressed as :

$$P_1 - P_2 = f\frac{L}{D}\frac{\rho\bar{u}^2}{2} \tag{2.8}$$

where f is the friction factor that depends on Reynolds number and pipe roughness.

2.3.4 Flow through orifices

An orifice is a sudden restriction of short length in a flow passage and may have a fixed or variable area. Since this type of restriction is widely used in preventing or letting a flow pass, orifices are considered a basic means for the control of fluid power. Therefore, knowledge of the flow characteristics of orifices is essential. Again two types of flow are prevailing, depending whether inertia or viscous forces dominate.

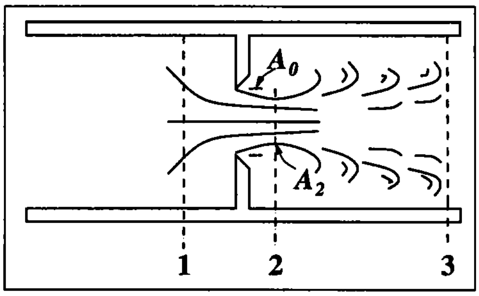

FIG. 2.11 – Turbulent flow through a sharp-edged orifice

Turbulent orifice flow

Figure 2.11 illustrates the turbulent flow through an orifice. Since most orifice flows occur at high Reynolds numbers, turbulent flow (inertia dominated) is more common across orifices. Due to its inertia, the fluid is moving in a curved path at the orifice, and thus the smallest area of the issuing jet is not situated at the geometric restriction but it is ahead of it in the direction of the flow. The point along the jet where the area becomes minimum is called the *vena contracta*. The ratio of the stream area at the *vena contracta* A_2 to the orifice area A_0 is called the contraction coefficient C_c.

$$A_2 = C_c A_0 \tag{2.9}$$

The flow between points 1 and 2 (see Figure 2.11) is streamline, and experience has justified the use of Bernoulli's equation (2.2), which if integrated between points 1 and 2 leads to

$$u_2^2 - u_1^2 = \frac{2}{\rho}(P_1 - P_2) \tag{2.10}$$

where u_i and P_i are the velocity and the pressure at point i. Besides, the continuity equation (2.3) for steady incompressible flow yields

$$Q = A_1 u_1 = A_2 u_2 \tag{2.11}$$

where Q is the volume flow rate. This shows that the jet velocity u_2 is higher than the upstream velocity u_1, hence the fluid undergoes an acceleration when crossing the orifice. This acceleration is indeed the main cause of the pressure drop across the orifice. Combining the above two equations gives

$$u_2 = \left[1 - \left(\frac{A_2}{A_1}\right)^2\right]^{-1/2} \sqrt{\frac{2}{\rho}(P_1 - P_2)} \tag{2.12}$$

Due to the viscous friction the jet velocity is slightly less than found in (2.12) by an empirical factor called the velocity coefficient C_v and is usually around 0.98 and approximated by 1 in most applications. Using the foregoing fact and equations we get

$$
\begin{aligned}
Q &= A_2 u_2 && (2.13)\\
&= \frac{C_v A_2}{\sqrt{1-(A_2/A_1)^2}}\sqrt{\frac{2}{\rho}(P_1-P_2)} && (2.14)\\
&= C_d A_0 \sqrt{\frac{2}{\rho}(P_1-P_2)} && (2.15)
\end{aligned}
$$

where C_d, called the discharge coefficient, is expressed as follows :

$$C_d = \frac{C_v C_c}{\sqrt{1-C_c^2(\frac{A_0}{A_1})^2}} \tag{2.16}$$

Actually, we have $C_d \approx C_c$ since $C_v \approx 1$ and A_0 is by far less than A_1. For sharp-edged annular orifices, Viersma [86] gives $C_d = 0.611$. Finally, analysis of the divergent part (between A_2 and A_3), revealed that there is no energy conversion from kinetic to pressure energy, and consequently $P_3 \approx P_2$.

Laminar orifice flow

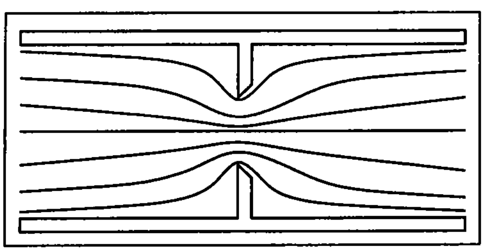

FIG. 2.12 – Laminar flow through a sharp-edged orifice

Figure 2.12 shows an orifice in the laminar flow regime. The pressure drop across the orifice is mainly due to the internal shear forces resulting from fluid viscosity. The Reynolds number for an orifice at laminar flow is defined by

$$\mathcal{R}e = \frac{\rho(Q/A_0)D_h}{\mu} \tag{2.17}$$

where (Q/A_0) represents the jet velocity at the orifice opening. For low Reynold's numbers the equation (2.15) is not valid. However, attempts to extend it to the laminar flow case ended by finding the following relation

$$C_d = \delta\sqrt{\mathcal{R}e} \tag{2.18}$$

for $\mathcal{R}e < 10$. In (2.18) δ is called the laminar flow coefficient, and is calculated as $\delta = 0.2$ for a sharp-edged round orifice. Substituting (2.17) and (2.18) into (2.15) yields

$$Q = \frac{2\delta^2 D_h A_0}{\mu}(P_1 - P_2) \tag{2.19}$$

We note here that the flow rate for a laminar flow across an orifice is directly proportional to the pressure drop across it.

2.3.5 Relation between the laminar and turbulent phases

Both extreme cases are given by (2.19) ($\mathcal{R}e \to 0$) and (2.15) ($\mathcal{R}e \to \infty$), in both cases we can use the flow rate expression of the turbulent phase unless we use the proper expression of C_d :

$$C_d = \begin{cases} \delta\sqrt{\mathcal{R}e} & \text{laminar phase} \\ C_{d\infty} = 0.611 & \text{turbulent phase} \end{cases} \tag{2.20}$$

Hence we define the transient Reynolds number $\mathcal{R}e_t$ as the intersection between both asymptotes $C_d(\mathcal{R}e)$ in order to guarantee the continuity.

$$C_{d\infty} = \delta\sqrt{\mathcal{R}e_t} \Leftrightarrow \sqrt{\mathcal{R}e_t} = \frac{C_{d\infty}}{\delta}$$

$$\mathcal{R}e_t = \left(\frac{0.611}{\delta}\right)^2 \tag{2.21}$$

By using the aforementioned transient Reynolds number, we can distinguish the laminar flow by $\mathcal{R}e < \mathcal{R}e_t$ and the turbulent flow by $\mathcal{R}e > \mathcal{R}e_t$.

2.4 Model of one port inside a spool valve

In this section we define the flow rate expressions describing the hydraulic flow through the valve orifices. It is useful to classify the valve as having either ideal or practical geometry. Ideal geometry implies that the orifice edges are perfectly square with no rounding and that there is no radial clearances between the spool and sleeve, which in turn implies that there is no leakage flow. Although these geometrical perfection are not possible in practice, the vast majority of applications, where spool valve models are used, neglect the leakage flow [62] [74] [70]. Therefore, the flow through an underlapped port (open port) is given by equation (2.15)

$$Q = C_d A_0 \sqrt{\frac{2}{\rho}(P_1 - P_2)}$$

whereas it is considered to be zero for an overlapped port (closed port). Although the ideal model may be satisfactory in some applications, the evident presence of leakage in the real case indicates that at small servovalve spool displacement, leakage flow is significant and cannot be ignored. In several control application such as precise piston positioning or fine force applications; where the servovalve operates within the null region, neglecting leakage flow may severely degrade the performance of the control scheme. In the next sections, we develop an improved spool valve model in which we include expression of the leakage flow. This is an original contribution of this work [20]. We try herein to establish a model that can describe as best the behaviour of a spool valve and can reproduce all the characteristic curves shown in section 2 including its leakage flow. Meanwhile keeping it simple to be handled mathematically for the control design purposes.

2.4.1 Overlapped port

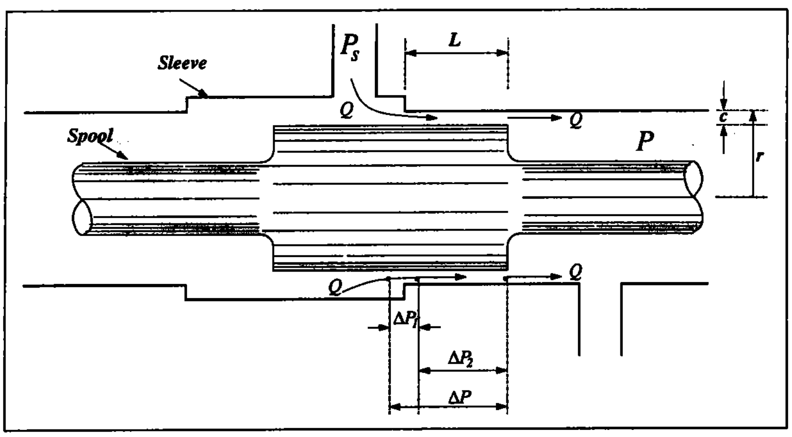

FIG. 2.13 – A spool valve at an overlapped position

Figure 2.13 depicts a spool valve port in an overlapped position. We consider that the fluid admits a pressure drop ΔP_1 corresponding to a laminar flow through a sharp-edged orifice at the entrance of the overlap region. Then a pressure drop of ΔP_2 owed to a laminar flow through a conduit that is created by the overlap between the spool and the sleeve. Hence the volume flow rate Q across the orifice is given by see [52] :

$$Q = \alpha \Delta P_1 \quad \text{with} \quad \alpha = \frac{\pi c^2 (2\pi r)}{32\mu} > 0 \tag{2.22}$$

corresponding to the pressure drop at the entrance of the orifice, and

$$Q = \frac{\alpha_2}{L} \Delta P_2 \quad \text{with} \quad \alpha_2 = \frac{\pi r c^3}{6\mu} > 0 \tag{2.23}$$

resulting from the pressure drop in the conduit. Using the foregoing relations in addition to an overall pressure drop $\Delta P = \Delta P_1 + \Delta P_2$ we get the following volume flow rate expression for an overlapped port :

$$\begin{aligned} Q &= \alpha \Delta P_1 \\ Q &= \alpha(\Delta P - \Delta P_2) \\ Q &= \alpha(\Delta P - \frac{L}{\alpha_2} Q) \\ Q(1 + \frac{\alpha}{\alpha_2} L) &= \alpha \Delta P \\ Q &= \frac{\alpha}{1 + \frac{\alpha}{\alpha_2} L} \Delta P \end{aligned}$$

$$Q_o(L, \Delta P) = \frac{\alpha}{1 + \beta L} \Delta P \quad \text{with } \beta = \frac{\alpha}{\alpha_2} = \frac{3}{8} \frac{\pi}{c} \tag{2.24}$$

Interpretation of equation (2.24) shows that the leakage is larger for larger values of c (clearance dimension) and gets smaller for small values of c, and this matches the real case.

2.4.2 Underlapped port

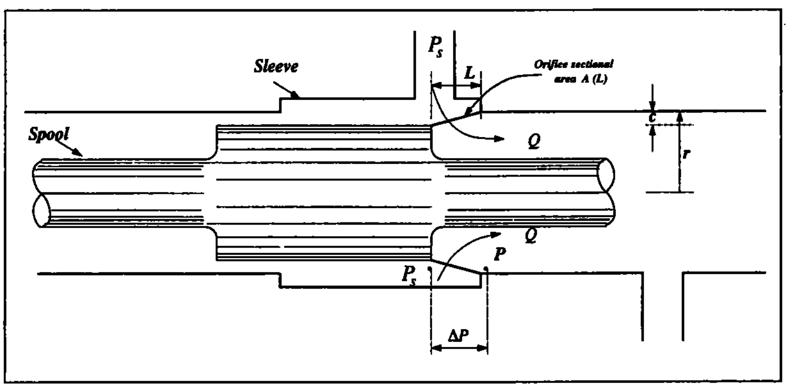

FIG. 2.14 – A spool valve at an underlapped position

Figure 2.14 depicts a spool valve port in an underlapped position. As soon as the underlap is sufficiently large and the pressure drop is relatively important the flow is considered to be turbulent. Thus, from the previous section, the volume flow rate expression takes the following form :

$$Q(L, \Delta P) = A(L) C_{d\infty} \sqrt{\frac{2}{\rho} \Delta P}$$

where $A(L)$ represents the orifice cross-sectional area. In order to guarantee the continuity of the flow rate expression at $L = 0$, the limit $\lim_{L \to 0} Q(L) = \alpha \Delta P$ should be satisfied. To insure this identity we should add the term $\frac{\alpha}{1+\beta L}\Delta P$ to the previous expression and impose $A(0) = 0$. The added term decreases rapidly for an increasing L and guarantees the continuity of the flow rate expression and the transition between the laminar and the turbulent phases. Eventually, the expression that governs the flow rate through an underlapped land-port is found to satisfy the following equation :

$$Q_u(L, \Delta P) = \frac{\alpha}{1+\beta L}\Delta P + A(L)C_{d\infty}\sqrt{\frac{2}{\rho}\Delta P} \quad \text{with } A(0) = 0 \tag{2.25}$$

2.4.3 Transition from overlapped to underlapped ports

The laminar phase characterizing condition $\mathcal{R}e < \mathcal{R}e_t$ is equivalent to :

$$\Delta P < \Delta P_{lim}(L)$$

in which the transient pressure drop $\Delta P_{lim}(L)$ is given by equating (2.15) and (2.19), the flow rate expressions for the turbulent and laminar cases.

$$C_d A_0 \sqrt{\frac{2}{\rho}\Delta P_{lim}(L)} = \frac{2\delta^2 D_h A_0}{\mu}\Delta P_{lim}(L)$$

$$\Delta P_{lim}(L) = \left(\frac{C_{d\infty}}{\delta^2}\frac{\mu}{D_h(L)}\sqrt{\frac{\rho}{2}}\right)^2 \tag{2.26}$$

When neglecting minor losses caused by bends and sharp-edged entrances, in addition to assuming $c \ll r$ the hydraulic diameter is given by

$$D_h(L) = \frac{4A(L)}{S} = \frac{4 \times 2\pi r\sqrt{L^2+c^2}}{2\pi r + 2\pi r} = 2\sqrt{L^2+c^2}$$

for underlap position and becomes

$$D_h = \frac{8\pi r c}{2\pi r + 2\pi r} = 2c$$

for the overlap position. Thus the expression of the transient pressure drop satisfy both underlap and overlap positions if L is brought to null ($L = 0$) in the expression of $D_h(L)$ for the overlap position.

$$\Delta P_{lim}(L) = \left(\frac{C_{d\infty}}{\delta^2}\frac{\mu}{2}\sqrt{\frac{\rho}{2}}\right)^2 \frac{1}{L^2+c^2}$$

Three curves corresponding to $\Delta P_{lim}(L)$ for three different values of c are depicted in Figure 2.15. The parameters values used to obtain these curves are the commonly used values, and they are stated in the following table.

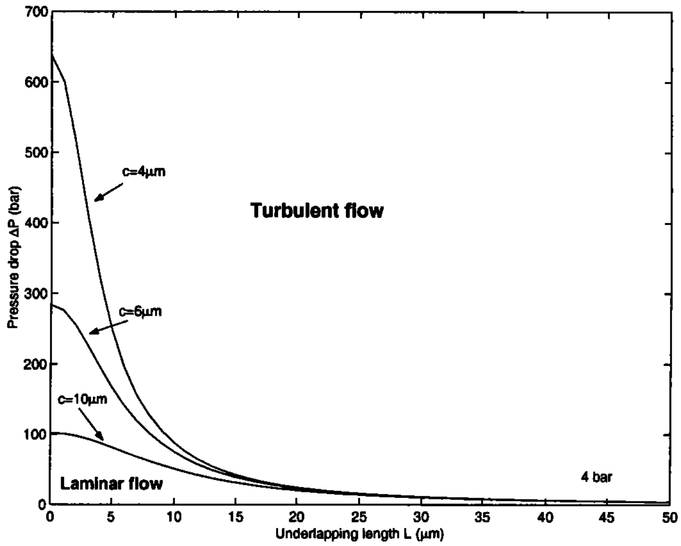

FIG. 2.15 – Laminar-turbulence transition curves

Parameter	Value	unit
$C_{d\infty}$	0.611	
δ	0.1	
μ	$50\ 10^{-6}$	m^2/s
ρ	875	Kg/m^3

Admitting possible variations in the fluid parameters as well as flow parameters in addition to possible changes in the simplifying hypotheses related to the geometry of orifice, we can only get a rough idea from the above curves. Nevertheless, they justify the assumption of laminar flow while the port is in the overlap position and show that the flow quickly turns into turbulent as the port starts to be underlapped.

2.5 Model of a symmetric critically-lapped spool valve

A spool valve is said to be matched and symmetrical if (referring to Figure 2.1) the following two conditions are satisfied :

- the orifice R_{s1} corresponding to an input value i is identical to the orifice R_{1r} for an opposite input $-i$.
- the orifice R_{2r} is identical to the orifice R_{s1} and the orifice R_{s2} is identical to the orifice R_{1r} for any input value i.

Now, we find the relation between the input current and the spool displacement. Let's express the spool dynamics using Newton's second law, i.e.

$$m_s\ddot{x}_s = -b_s\dot{x}_s - 2k_sx_s + K_{fc}i \ , \tag{2.27}$$

where m_s is the valve spool mass, x_s is the spool displacement relative to central (closed) position, b_s is the spool viscous damping coefficient, k_s is the spring constant, K_{fc} is the coil force coefficient, and i is the coil current. We can neglect the term $m_s\ddot{x}_s$ in equation (2.27) by considering that the spool inertial force is much smaller than the force applied by the internal springs of the valve. Accordingly, we may write

$$\dot{x}_s = -\frac{2k_s}{b_s}x_s + \frac{K_{fc}}{b_s}i \ . \tag{2.28}$$

Thus if we consider the static case where the spool is at rest we have

$$\dot{x}_s = 0 \quad \Rightarrow x_s = \frac{K_{fc}}{2k_s}i = K_d i \ .$$

Equations (2.24) and (2.25) show that the flow is proportional to the size of the passage, namely L which is a positive quantity, thus we have $L = K_d|i|$ and this yields

$$Q_o(i, \Delta P) = \frac{\alpha}{1+\gamma|i|}\Delta P \ , \quad \gamma = \beta K_d \ , \tag{2.29}$$

and if we consider $L \gg c$, then

$$\begin{aligned} A(L)C_{d\infty}\sqrt{\frac{2}{\rho}} &= 2\pi r C_{d\infty}\sqrt{\frac{2}{\rho}}\ L \\ A(L)C_{d\infty}\sqrt{\frac{2}{\rho}} &= 2\pi r C_{d\infty}\sqrt{\frac{2}{\rho}}\ K_d|i| \\ A(L)C_{d\infty}\sqrt{\frac{2}{\rho}} &= k|i| \end{aligned}$$

eventually obtaining

$$Q_u(i, \Delta P) = k|i|\sqrt{\Delta P} + \frac{\alpha}{1+\gamma|i|}\Delta P \ , \tag{2.30}$$

k will be denoted as the servovalve sizing factor. We are now ready to give the mathematical model of a symmetrical matched critically lapped spool valve.

Figure 2.16 shows a symmetric critically-lapped spool valve corresponding to different input values. With regard to the flow rates expressed in (2.29) and (2.30) and the symmetry assumption the flow rates $Q_1(i, P_1)$ and $Q_2(i, P_2)$ can be expressed as follows :

$$Q_1 = Q_{s1} - Q_{1r} \quad \text{and} \quad Q_2 = Q_{s2} - Q_{2r}$$

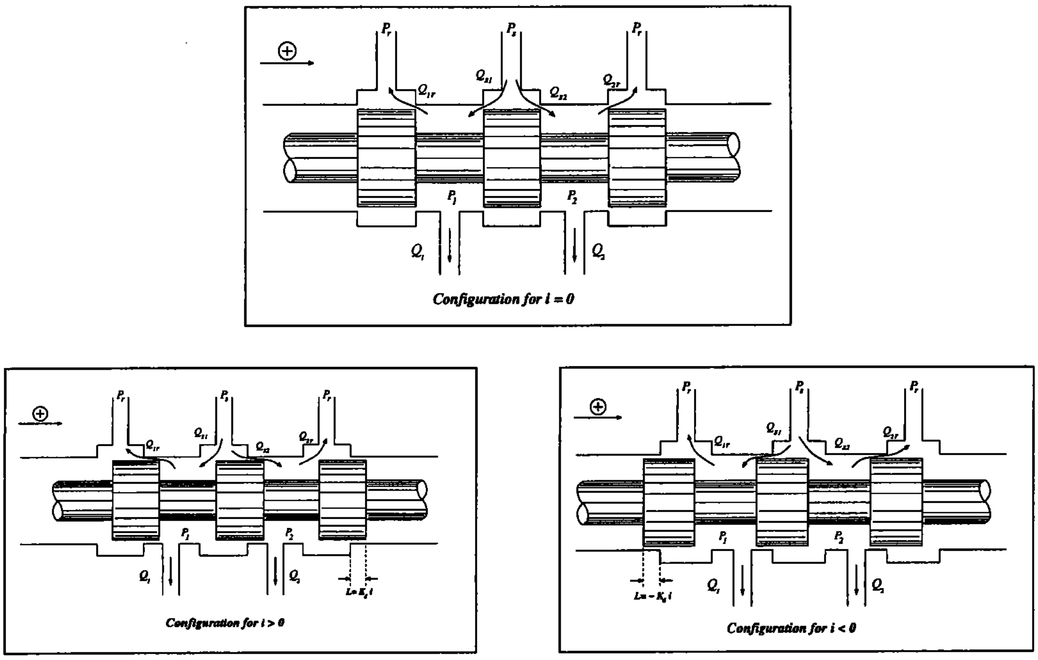

FIG. 2.16 – Critically lapped spool valve in different positions

$$Q_1(i,P_1) = \begin{cases} ki\sqrt{P_s - P_1} + \frac{\alpha}{1+\gamma i}(P_s - P_1) - \frac{\alpha}{1+\gamma i}(P_1 - P_r) & \text{if } i \geq 0 \\ ki\sqrt{P_1 - P_r} + \frac{\alpha}{1-\gamma i}(P_s - P_1) - \frac{\alpha}{1-\gamma i}(P_1 - P_r) & \text{if } i < 0 \end{cases} \tag{2.31}$$

$$Q_2(i,P_2) = \begin{cases} -ki\sqrt{P_2 - P_r} + \frac{\alpha}{1+\gamma i}(P_s - P_2) - \frac{\alpha}{1+\gamma i}(P_2 - P_r) & \text{if } i \geq 0 \\ -ki\sqrt{P_s - P_2} + \frac{\alpha}{1-\gamma i}(P_s - P_2) - \frac{\alpha}{1-\gamma i}(P_2 - P_r) & \text{if } i < 0 \end{cases} \tag{2.32}$$

For the sake of simplicity we considered $P_1, P_2 \in [P_r\ ,\ P_s]$. In other respects, we only need to replace $\sqrt{x}$ by $\sqrt{|x|}\text{sign}(x)$.

2.5.1 Internal leakage and pressure sensitivity model

The pressure sensitivity and the internal leakage flow are the most relevant characterizing features for a servovalve. Whence, obtaining expressions of these characteristics is very crucial in evaluating the mathematical model.

In fact, manufacturers carry out some necessary production tests to insure reasonable conformance to design specifications of the servovalve. Among these tests, we state the pressure sensitivity and internal leakage tests, results of which are provided with the servovalve. The flow curve is another data also provided by the constructor. Therefore, a comparison can be made between these experimental curves and the curves obtained through the model.

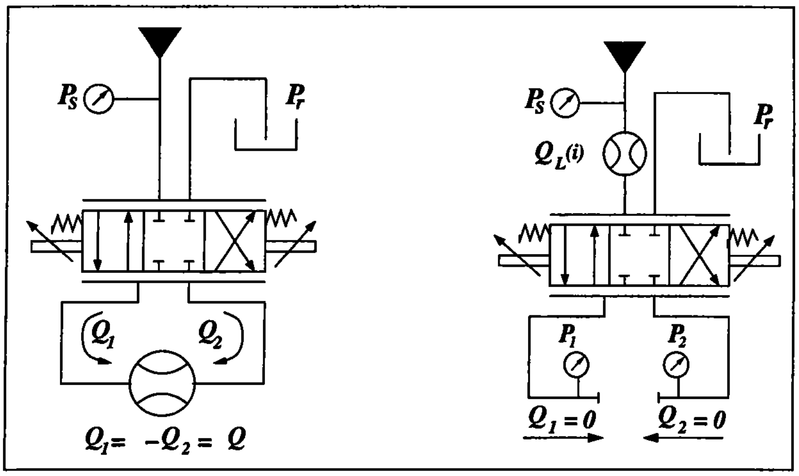

FIG. 2.17 – Setups for characteristics tests.

By using the setup leading to obtain the flow curve, we can write see Figure 2.17-a

$$P_1 = P_2 = P \quad \text{and} \quad Q_1 = -Q_2 = Q \; .$$

Substituting these in (2.31) and (2.32) results in

$$P = \frac{P_s + P_r}{2} \; , \quad Q = ki\sqrt{\frac{P_s - P_r}{2}} \; . \tag{2.33}$$

The pressure sensitivity test measures the change in the load pressure drop ($P_L = P_1 - P_2$), with zero control flow (control ports blocked), as the spool is stroked around the null region [77]. The internal leakage flow test uses the same setup (see Figure 2.17-b) to measure the total supply flow (which is actually a leakage flow since the load flow is zero) as the spool travels a full stroke length [77].

In both tests we have zero load flow that is

$$Q_1 = Q_2 = 0 \; , \tag{2.34}$$

since the servovalve is assumed to be matched and symmetrical and in addition we know that an outgoing flow is equal to the incoming flow, then we can write (see Figure 2.16)

$$Q_{s1} = Q_{1r} \tag{2.35}$$

$$Q_{s2} = Q_{2r} \tag{2.36}$$

substituting (2.34), (2.35) and (2.36) in (2.31) and (2.32) we obtain

$$\text{if } i \geq 0 \; , \quad \begin{cases} ki\sqrt{P_s - P_1} + \frac{\alpha}{1+\gamma i}(P_s - P_1) = \frac{\alpha}{1+\gamma i}(P_1 - P_r) \; , \\ ki\sqrt{P_2 - P_r} + \frac{\alpha}{1+\gamma i}(P_2 - P_r) = \frac{\alpha}{1+\gamma i}(P_s - P_2) \; . \end{cases} \tag{2.37}$$

$$\text{if } i < 0 \,, \quad \begin{cases} -ki\sqrt{P_1 - P_r} + \frac{\alpha}{1-\gamma i}(P_1 - P_r) = \frac{\alpha}{1-\gamma i}(P_s - P_1) \,, \\ -ki\sqrt{P_s - P_2} + \frac{\alpha}{1-\gamma i}(P_s - P_2) = \frac{\alpha}{1-\gamma i}(P_2 - P_r) \,. \end{cases} \tag{2.38}$$

Now, since the total supply flow is actually the internal leakage flow, then

$$Q_L(i) = Q_s(i)$$

but we also have

$$Q_s(i) = Q_{s1} + Q_{s2} \,,$$

therefore if we consider the simplest expressions of the leakage given by the right hand sides of (2.37) and (2.38) we have

$$Q_L(i) = \begin{cases} Q_{1r} + Q_{s2} \,, & \text{if } i \geq 0 \\ Q_{s1} + Q_{2r} \,, & \text{if } i < 0 \end{cases}$$

$$Q_L(i) = \begin{cases} \frac{\alpha}{1+\gamma i}(P_s - P_r + (P_1 - P_2)) \,, & \text{if } i \geq 0 \\ \frac{\alpha}{1-\gamma i}(P_s - P_r - (P_1 - P_2)) \,, & \text{if } i < 0 \end{cases}$$

Equivalently, the internal leakage flow is given in terms of the input current as follows :

$$Q_L(i) = \frac{\alpha}{1+\gamma|i|}\Big(P_s - P_r + \text{sign}(i)\big(P_1(i) - P_2(i)\big)\Big) \,, \tag{2.39}$$

where the expressions of $P_1(i)$ and $P_2(i)$ are the positive solutions of (2.37) and (2.38). We can easily check that

$$P_1(i,\gamma) = \begin{cases} \frac{P_s+P_r}{2} + \frac{-a^2(i)+\sqrt{a^4(i)+2a^2(i)(P_s-P_r)}}{2} & a(i) \stackrel{def}{=} \frac{ki(1+\gamma i)}{2\alpha} & \text{if } i \geq 0 \\ \frac{P_s+P_r}{2} - \frac{-a^2(i)+\sqrt{a^4(i)+2a^2(i)(P_s-P_r)}}{2} & a(i) \stackrel{def}{=} \frac{-ki(1-\gamma i)}{2\alpha} & \text{if } i < 0 \end{cases} \tag{2.40}$$

$$P_2(i,\gamma) = \begin{cases} \frac{P_s+P_r}{2} - \frac{-a^2(i)+\sqrt{a^4(i)+2a^2(i)(P_s-P_r)}}{2} & a(i) \stackrel{def}{=} \frac{ki(1+\gamma i)}{2\alpha} & \text{if } i \geq 0 \\ \frac{P_s+P_r}{2} + \frac{-a^2(i)+\sqrt{a^4(i)+2a^2(i)(P_s-P_r)}}{2} & a(i) \stackrel{def}{=} \frac{-ki(1-\gamma i)}{2\alpha} & \text{if } i < 0 \end{cases} \tag{2.41}$$

Equations (2.33), (2.39), (2.40) and (2.41) will be used to find the model parameters as we will see in the next section.

2.5.2 Determination of model parameters

Among the data provided by the manufacturer we cite, for our need, the rated current, the rated flow, the internal null leakage and the pressure sensitivity curve at a given pressure. Substituting these rated values in equation (2.33) we get

$$k = \frac{Q_R}{i_R\sqrt{\frac{P_s-P_r}{2}}} \,.$$

To find the parameter α we use the internal null leakage value $Q_L(0)$. Should we substitute $i = 0$ in (2.37) and (2.38) we get

$$P_1(0) = \frac{P_s + P_r}{2} \quad \text{and} \quad P_2(0) = \frac{P_s + P_r}{2}$$

thus, (2.39) becomes $Q_L(0) = \alpha(P_s - P_r)$, hence,

$$\alpha = \frac{Q_L(0)}{P_s - P_r} \; .$$

Finally, to determine γ we use the pressure gain and the current value i_0 corresponding to $40\%(P_s - P_r)$ and we solve for γ the equation

$$P_1(i_0, \gamma) - P_2(i_0, \gamma) = 0.4(P_s - P_r) \; . \tag{2.42}$$

The solution of the above equation can be obtained graphically or using numerical techniques.

2.5.3 Model evaluation

The servovalve mathematical model suggested in this work, described by equations (2.31) and (2.32) has been validated using a Moog 760-723A type servovalve with 40 lpm no-load rated flow and 25 mA rated current at 70 bar valve pressure drop. The model parameters are calculated using the foregoing analysis and servovalve data measured at $P_s = 137.9\ bar$. The obtained parameter values are :

parameter	value	unit
k	1.46×10^{-5}	$m^3 s^{-1} A^{-1} Pa^{-1/2}$
α	4.605×10^{-13}	$m^3 s^{-1} Pa$
γ	10615	A^{-1}

These parameters where used to simulate and appraise the leakage flow and the pressure sensitivity of the servovalve for different supply pressures. The obtained parameters were inserted in equation (2.39) and we plotted the estimated leakage curve together with the experimental results[1] in Figure 2.18. Equations (2.40) and (2.41) were used simultaneously to plot an estimation of the pressure sensitivity curve. This is delineated in Figure 2.19 together with the experimental results.

When comparing the estimated curves and the experimental results, we can notice that our model reflects the leakage flow better than any other model in literature. We

[1]The author wants to thank PhD student Bora Eryilmaz (Northeastern University, Boston) for providing the experimental data.[19]

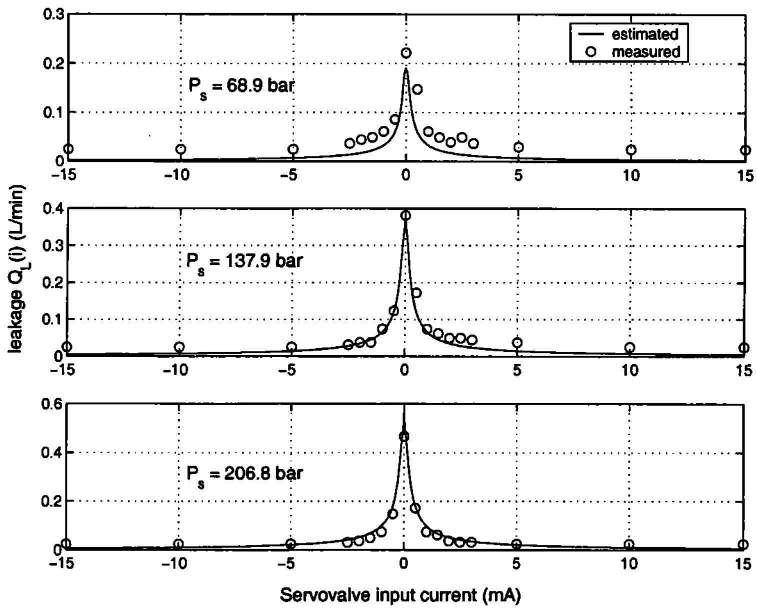

FIG. 2.18 – Measured and estimated internal leakage flow (Q_L)

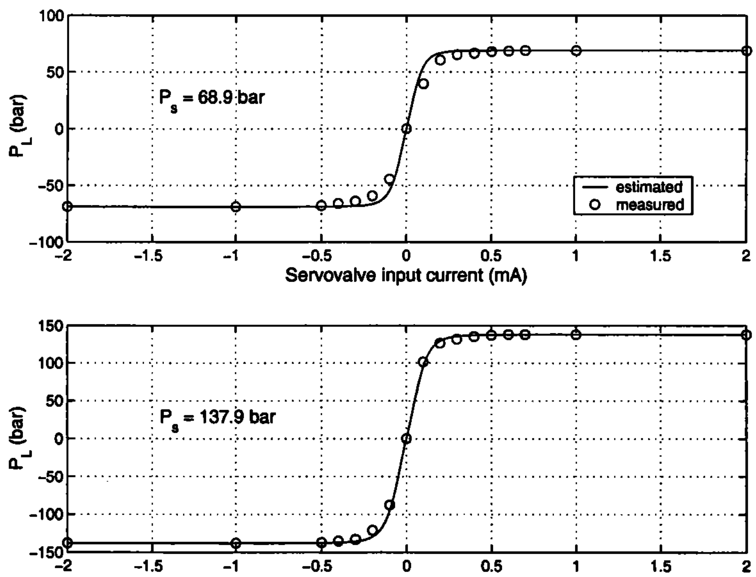

FIG. 2.19 – Measured and estimated pressure sensitivity

can notice that the leakage flow is perfectly estimated within the null region, however, slightly underestimated for high input current. In fact for high input current the flows through the control ports are very important that the leakage flow can be neglected. The leakage flow is more important in the null region wherein it is almost exactly estimated. Nevertheless, we can report some degradation for low supply pressure. We can also notice that using the value of γ in equation (2.24) shows that the clearance size is in the order of several μm, which is quite reasonable. Similarly, Figure 2.19 shows that the pressure sensitivity is also very well estimated, therefore confirming the accuracy of the servovalve model presented in this work.

Although this model was derived for a critical center type of servovalve, we can always extend it to the closed center as well as open center types of symmetrical and matched servovalve. The mathematical model of such servovalves is given in the next sections. However, we do not give experimental validation for these cases.

2.6 Model of a symmetric underlapped spool valve

In Figure 2.20 we show an underlapped spool valve corresponding to different input values. The flow rates expressions of $Q_1(i, P_1)$ and $Q_2(i, P_2)$ are very much similar to those found in (2.31) and (2.32) except from some slight difference due to the gap length L_{un} which is proportional to an input current that we will express as i_{un} and hence the flow rates will be expressed as follows

$$Q_1(i,P_1) = \begin{cases} \bullet\ k(i+i_{un})\sqrt{P_s-P_1} + \dfrac{\alpha}{1+\gamma(i+i_{un})}(P_s-P_1) \\ -\dfrac{\alpha}{1+\gamma(i-i_{un})}(P_1-P_r) & \text{if } i > i_{un} \\ \\ \bullet\ k(i_{un}+i)\sqrt{P_s-P_1} - k(i_{un}-i)\sqrt{P_1-P_r} \\ +\dfrac{\alpha}{1+\gamma(i_{un}+i)}(P_s-P_1) - \dfrac{\alpha}{1+\gamma(i_{un}-i)}(P_1-P_r) & \text{if } |i| \le i_{un} \\ \\ \bullet - k(-i+i_{un})\sqrt{P_1-P_r} - \dfrac{\alpha}{1+\gamma(-i+i_{un})}(P_1-P_r) \\ +\dfrac{\alpha}{1+\gamma(-i-i_{un})}(P_s-P_1) & \text{if } i < -i_{un} \end{cases} \tag{2.43}$$

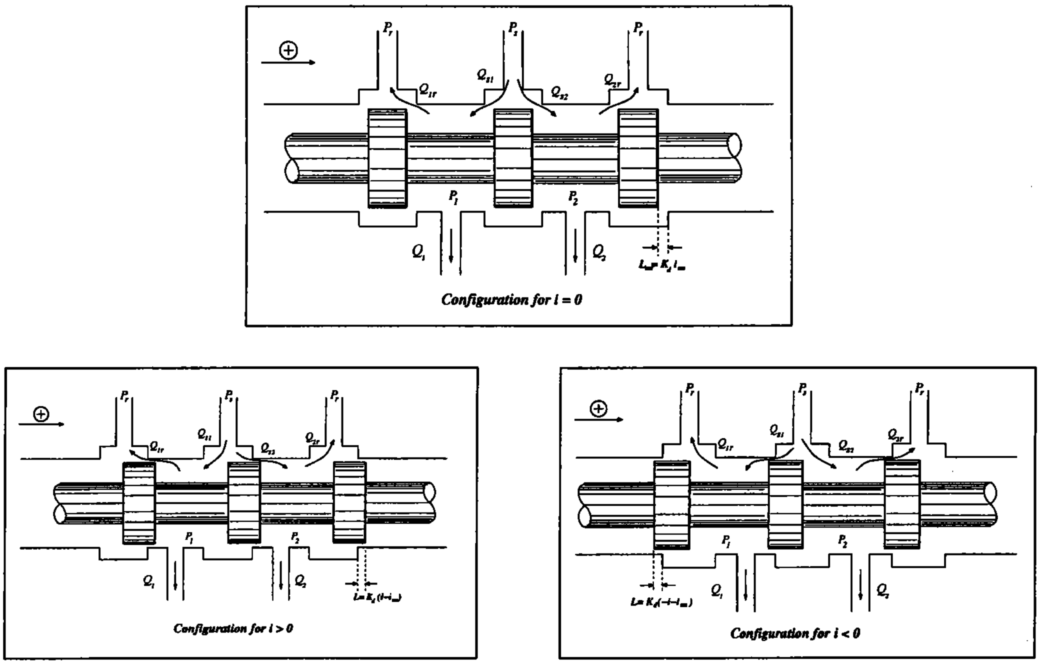

FIG. 2.20 – Underlapped spool valve in different positions

$$Q_2(i,P_2) = \begin{cases} \bullet -k(i+i_{un})\sqrt{P_2-P_r} - \dfrac{\alpha}{1+\gamma(i+i_{un})}(P_2-P_r) \\ +\dfrac{\alpha}{1+\gamma(i-i_{un})}(P_s-P_2) & \text{if } i \geq i_{un} \\ \\ \bullet\ k(i_{un}-i)\sqrt{P_s-P_2} - k(i_{un}+i)\sqrt{P_2-P_r} \\ \dfrac{\alpha}{1+\gamma(i_{un}-i)}(P_s-P_2) - \dfrac{\alpha}{1+\gamma(i_{un}+i)}(P_2-P_r) & \text{if } |i| \leq i_{un} \\ \\ \bullet\ k(-i+i_{un})\sqrt{P_s-P_2} + \dfrac{\alpha}{1-\gamma(-i+i_{un})}(P_s-P_2) \\ -\dfrac{\alpha}{1+\gamma(-i-i_{un})}(P_2-P_r) & \text{if } i < -i_{un} \end{cases} \tag{2.44}$$

2.7 Model of a symmetric overlapped spool valve

In Figure 2.21 an underlapped spool valve corresponding to different input values is shown. The flow rates expressions of $Q_1(i,P_1)$ and $Q_2(i,P_2)$ are very much similar to those found in (2.43) and (2.44). The valve ports are initially overlapped and according to the value of the input control, the flow can be decided to satisfy (2.24) or (2.25). It is indeed clear that an input current of i_{ov} corresponding to the overlap distance L_{ov} should be applied before a significant flow can pass.

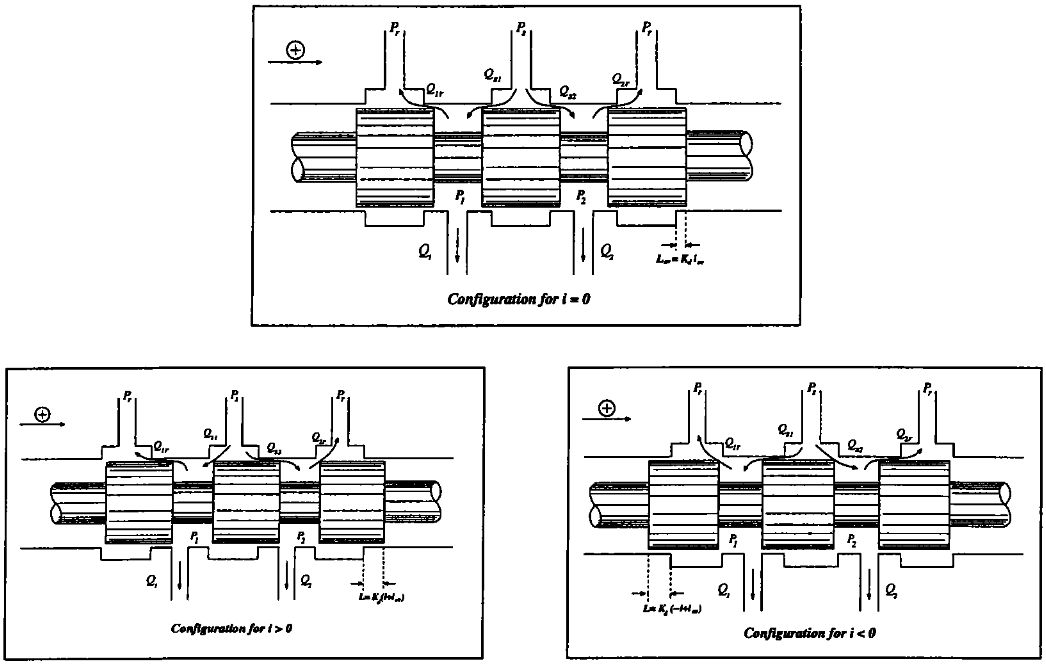

FIG. 2.21 – Overlapped spool valve in different positions

$$Q_1(i,P_1) = \begin{cases} \bullet\ k(i-i_{ov})\sqrt{P_s-P_1} + \dfrac{\alpha}{1+\gamma(i-i_{ov})}(P_s-P_1) \\ -\dfrac{\alpha}{1+\gamma(i+i_{ov})}(P_1-P_r) & \text{if } i > i_{ov} \\ \\ \bullet\ \dfrac{\alpha}{1+\gamma(i_{ov}-i)}(P_s-P_1) - \dfrac{\alpha}{1+\gamma(i_{ov}+i)}(P_1-P_r) & \text{if } |i| \leq i_{ov} \\ \\ \bullet - k(-i-i_{ov})\sqrt{P_1-P_r} - \dfrac{\alpha}{1+\gamma(-i-i_{ov})}(P_1-P_r) \\ +\dfrac{\alpha}{1+\gamma(-i+i_{ov})}(P_s-P_1) & \text{if } i < -i_{ov} \end{cases} \tag{2.45}$$

$$Q_2(i,P_2) = \begin{cases} \bullet - k(i-i_{ov})\sqrt{P_2-P_r} - \dfrac{\alpha}{1+\gamma(i-i_{ov})}(P_2-P_r) \\ +\dfrac{\alpha}{1+\gamma(i+i_{ov})}(P_s-P_2) & \text{if } i \geq i_{ov} \\ \\ \bullet\ \dfrac{\alpha}{1+\gamma(i_{ov}+i)}(P_s-P_2) - \dfrac{\alpha}{1+\gamma(i_{ov}-i)}(P_2-P_r) & \text{if } |i| \leq i_{ov} \\ \\ \bullet\ k(-i-i_{ov})\sqrt{P_s-P_2} + \dfrac{\alpha}{1-\gamma(-i-i_{ov})}(P_s-P_2) \\ -\dfrac{\alpha}{1+\gamma(-i+i_{ov})}(P_2-P_r) & \text{if } i < -i_{ov} \end{cases} \tag{2.46}$$

2.8 Model of a spool valve controlled piston

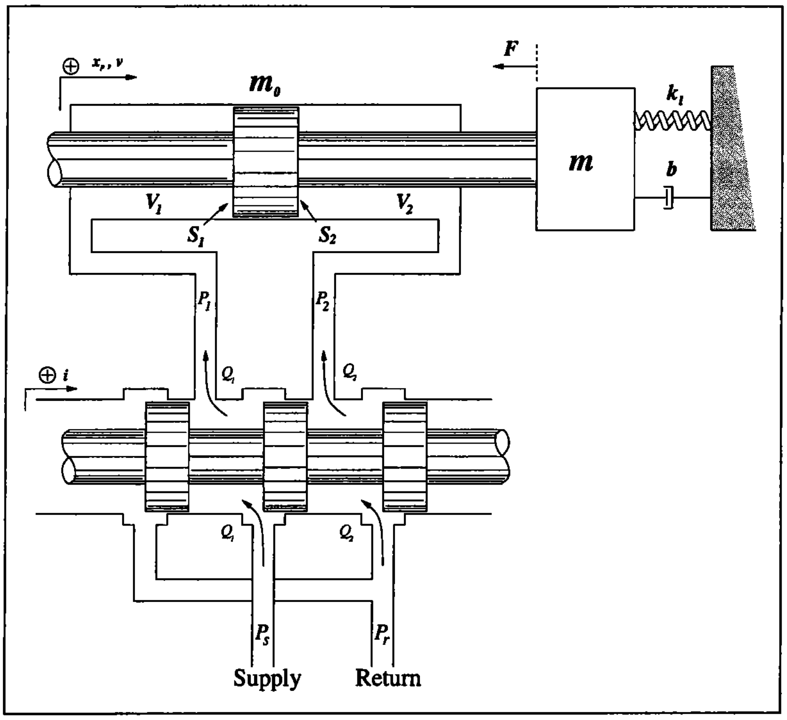

FIG. 2.22 – Valve-piston combination

Nomenclature

V_1	=	volume of forward chamber (includes valve, connecting hose and piston volume), m^3.
V_2	=	volume of return chamber (includes valve, connecting hose and piston volume), m^3.
V_{10}	=	initial volume of forward chamber, m^3.
V_{20}	=	initial volume of return chamber, m^3.
S_1 , S_2	=	piston surface areas of each side, m^2
x_p	=	piston position relative to the middle of the stroke, m
l_p	=	full stroke length of the piston, m
v	=	velocity of piston, m/s
m_0	=	mass of the piston, kg
m	=	mass of the load, kg
k_l	=	load spring gradient, N/m
b	=	viscous damping coefficient, Ns/m

Linear hydraulic actuation devices are usually referred to as pistons. These actuation devices may be controlled by pumps or valves giving two basic systems : pump controlled and valve controlled. In this purview, we will deal with the valve controlled pistons combined with a valve. Our main concern will be to determine the state equations describing the dynamic performance of the overall system, knowledge of which is absolutely essential in the rational design of hydraulic control systems.

The hydraulic system shown in Figure 2.22 consists of a four-way spool valve, supplying a double effect linear cylinder with a double-rodded piston. This piston applies a force on an object modeled by a mass, a spring and a sliding viscous friction. The establishment of a model for this type of systems is based on the pressure evolution inside the chambers of the cylinder, the orifice flow relations and the laws of motion for rigid bodies.

The continuity equation (2.3) can be written

$$\sum \mathcal{M}_{in} - \sum \mathcal{M}_{out} = \frac{d(\rho V)}{dt} = \rho \frac{dV}{dt} + V \frac{d\rho}{dt} \tag{2.47}$$

Moreover, if we assume constant temperature the mass density at a given pressure can be expressed as

$$\rho = \rho_0 + \frac{\rho_0}{B} P$$

where ρ_0 and B are respectively the mass density and the bulk modulus at zero pressure. Now knowing that the mass flow rate can be expressed in terms of the volume flow rate as follows :

$$\mathcal{M} = \rho Q$$

we can combine the preceding equations to yield

$$\sum Q_{in} - \sum Q_{out} = \frac{dV}{dt} + \frac{V}{B}\frac{dP}{dt} \tag{2.48}$$

The last equation is highly useful, the first term on the right side is the flow resulting from the expansion of the control volume and the second term describes the flow resulting from pressure changes.

2.8.1 Asymmetric piston

A servovalve-piston combination is shown schematically in Figure 2.22. The servovalve orifices are assumed matched and symmetrical so that the valve flows are described by (2.31) and (2.32). Applying equation (2.48) to each of the piston chambers yields

$$Q_1 = \frac{dV_1}{dt} + \frac{V_1}{B}\frac{dP_1}{dt} \tag{2.49}$$

$$Q_2 = \frac{dV_2}{dt} + \frac{V_2}{B}\frac{dP_2}{dt} \tag{2.50}$$

We note that the volume of the piston chambers may be written as

$$V_1 = V_{10} + S_1 x_p \tag{2.51}$$
$$V_2 = V_{20} - S_2 x_p \tag{2.52}$$

though the initial chamber volumes are not necessarily equal, it will be assumed that the piston is centered such that these volumes are equal, that is

$$V_{10} = V_{20} = V_0$$

the interest of this assumption is solely to reduce the number of parameters and simplify the analysis of the overall system.

The final equation arises by applying Newton's second law to the forces acting on the piston. The resulting force equation is

$$(m + m_0)\frac{dv}{dt} = S_1 P_1 - S_2 P_2 - bv - k_l(x_p - x_{p0}) \tag{2.53}$$

where x_{p_0} is the initial spring expansion.

All the previous equations may be gathered to obtain a set of ordinary nonlinear differential equations that represent the state equations describing the dynamics of the hydraulic systems shown in figure (2.22).

$$\frac{dP_1}{dt} = \frac{B}{V_0 + Sx_p}(Q_1(i, P_1) - S_1 v)\ , \tag{2.54a}$$
$$\frac{dP_2}{dt} = \frac{B}{V_0 - Sx_p}(Q_2(i, P_2) + S_2 v)\ , \tag{2.54b}$$
$$\frac{dv}{dt} = \frac{1}{m + m_0}\Big(S_1 P_1 - S_2 P_2 - bv - k_l(x_p - x_{p0})\Big)\ , \tag{2.54c}$$
$$\frac{dx_p}{dt} = v\ . \tag{2.54d}$$

with

$$Q_1(i, P_1) = \begin{cases} ki\sqrt{P_s - P_1} + \frac{\alpha}{1+\gamma i}(P_s - P_1) - \frac{\alpha}{1+\gamma i}(P_1 - P_r) & \text{if } i \geq 0 \\ ki\sqrt{P_1 - P_r} + \frac{\alpha}{1-\gamma i}(P_s - P_1) - \frac{\alpha}{1-\gamma i}(P_1 - P_r) & \text{if } i < 0 \end{cases} \tag{2.55}$$

$$Q_2(i, P_2) = \begin{cases} -ki\sqrt{P_2 - P_r} + \frac{\alpha}{1+\gamma i}(P_s - P_2) - \frac{\alpha}{1+\gamma i}(P_2 - P_r) & \text{if } i \geq 0 \\ -ki\sqrt{P_s - P_2} + \frac{\alpha}{1-\gamma i}(P_s - P_2) - \frac{\alpha}{1-\gamma i}(P_2 - P_r) & \text{if } i < 0 \end{cases} \tag{2.56}$$

2.8.2 Symmetric piston

The foregoing model can be used for an asymmetric model (i.e. $S_1 \neq S_2$) as well as for a symmetric piston (i.e. $S_1 = S_2 = S$). For the latter case, however, further simplifications can be brought. Consider equation (2.53) and let $m_t = m + m_0$ then we have

$$m_t \frac{dv}{dt} = S(P_1 - P_2) - bv - k_l(x_p - x_{p0})$$

define

$$P_L \overset{def}{=} P_1 - P_2 \tag{2.57}$$

and

$$Q_L \overset{def}{=} \frac{Q_1 - Q_2}{2} \tag{2.58}$$

then using equations (2.49), (2.50), (2.51) and (2.52) yields

$$Q_L = S\frac{dx_p}{dt} + \frac{V_0}{2B}\frac{d}{dt}(P_1 - P_2) + \frac{Sx_p}{2B}\frac{d}{dt}(P_1 + P_2)$$

Assuming again a matched and symmetrical valve then for a given input control $i(t)$ we always have equal volume flow passing through (geometrically) identical ports; that is (referring to Figure 2.16)

$$Q_{s1} = -Q_{2r} \quad ; \quad Q_{s1} = -Q_{2r}$$

Taking the case of $i \geq 0$ for instance we obtain the following equalities

$$ki\sqrt{P_s - P_1} + \frac{\alpha}{1+\gamma i}(P_s - P_1) = ki\sqrt{P_2 - P_r} + \frac{\alpha}{1+\gamma i}(P_2 - P_r)$$

$$\frac{\alpha}{1+\gamma i}(P_1 - P_r) = \frac{\alpha}{1+\gamma i}(P_s - P_2)$$

if we refer to the simplest of the two above equations and thinking that $\frac{\alpha}{1+\gamma i} > 0$ we get

$$P_1 + P_2 = P_s + P_r \tag{2.59}$$

whence

$$Q_L = Sv + \frac{V_0}{2B}\frac{dP_L}{dt} \tag{2.60}$$

and (2.59) together with (2.57) leads to

$$P_1 = \frac{P_s + P_r + P_L}{2} \quad ; \quad P_2 = \frac{P_s + P_r - P_L}{2} \tag{2.61}$$

Next, we can define $V_t \overset{def}{=} 2V_0$, where V_t denotes the total volume of the cylinder to get

$$Q_L = Sv + \frac{V_t}{4B}\frac{dP_L}{dt} \tag{2.62}$$

Moreover, we can use equations (2.31) and (2.32) to express Q_L as follows

$$Q_L = \begin{cases} \frac{ki}{2}\left(\sqrt{P_s - P_1} + \sqrt{P_2 - P_r}\right) - \frac{\alpha}{1+\gamma i}P_L & \text{if } i \geq 0 \\ \frac{ki}{2}\left(\sqrt{P_1 - P_r} + \sqrt{P_s - P_2}\right) - \frac{\alpha}{1+\gamma i}P_L & \text{if } i < 0 \end{cases} \tag{2.63}$$

in which we will substitute the values of P_1 and P_2 found in (2.61) to obtain

$$Q_L = ki\sqrt{\frac{P_s - P_r - \text{sign}(i)P_L}{2}} - \frac{\alpha}{1+\gamma|i|}P_L \tag{2.64}$$

and therefore, the overall system model can be written

$$\frac{dP_L}{dt} = \frac{4B}{V_t}\left(ki\sqrt{\frac{P_s - P_r - \text{sign}(i)P_L}{2}} - \frac{\alpha}{1+\gamma|i|}P_L - Sv\right), \tag{2.65a}$$

$$\frac{dv}{dt} = \frac{1}{m_t}\Big(SP_L - bv - k_l(x_p - x_{p0})\Big), \tag{2.65b}$$

$$\frac{dx_p}{dt} = v. \tag{2.65c}$$

2.9 Summary

In this chapter we have attempted to establish a model of a steady state spool valve. In the outset we have introduced the spool valve then described it and presented its different characterizing features.

The flow fundamentals of liquid have been given next in order to comprehend the motion of fluid inside the valve. As a general rule, only those equations that describe intentionally inserted hydraulic resistances are used in a dynamic analysis. Therefore the formulas most often used are those describing the flow through orifices.

In the introduction of section 4 we mentioned that the model usually used for a valve neglect leakages, thus does not reflect the behaviour of a practical valve, but that of an ideal one. In sections 4 and 5 we have developed a spool valve model that considers the leakage and reflects better the behaviour of a real valve. Actually, a more detailed model exists in literature [17] but it is so complex that makes the control analysis a tough burden.

Our spool valve model was then used to derive a model for a valve piston combination, a mechanical setup that is widely used in practice. This combination together with its model will constitute the main system for our control and observability analysis in the coming chapters.

Chapitre 3

Nonlinear stabilization via state feedback

Stability theory plays an important role in systems theory. Stability is addressed from several points of view depending on the problem in question. In this chapter we are concerned with stability of equilibrium points and its application to output tracking. In general, stability of the equilibrium points is characterized in the sense of Lyapunov. In this theory, an equilibrium point is stable if all solutions starting at nearby points stay nearby; otherwise it is unstable. Furthermore, it is asymptotically stable if all solutions starting at nearby points tend to the equilibrium point as time elapses. An extension of this theory has been developed in LaSalle's invariance principle. Definitions and theorems describing this theory will be stated in the next section.

3.1 Stability of nonlinear dynamic systems

Throughout this section we will consider the following non-autonomous system

$$\dot{x}(t) = f(t, x(t)) \ , \quad t \geq 0 \tag{3.1}$$

where $x(t) \in \mathbb{R}^n$ and $f : \mathbb{R}^+ \times \mathbb{R}^n \to \mathbb{R}^n$ is continuous. It is assumed that (3.1) has a unique solution corresponding to each initial condition. We will further assume that the origin constitutes the unique equilibrium point and that $f(t, 0) = 0$, $\forall t \geq t_0$. In what follows, $x(t, t_0, x_0)$ denotes the solution of (3.1) corresponding to the initial condition $x(t_0) = x_0$ evaluated at time t.

Lyapunov theory of stability investigates the behaviour of the solution $x(t, t_0, x_0)$ when $x_0 \neq 0$ but situated in its neighborhood. The following definitions and theorems is a brief summary of Lyapunov theory, for detailed study the reader is referred to the books of Hahn [34] and Vidyasagar [85].

Definition 3.1 *The origin of (3.1) is stable (in the sense of Lyapunov) if, for each* $\epsilon > 0$ *and each* $t_0 \in \mathbb{R}^+$ *there exists* $\delta = \delta(\epsilon, t_0)$ *such that*

$$\|x_0\| < \delta(\epsilon, t_0) \Rightarrow \|x(t, t_0, x_0)\| < \epsilon \ , \quad \forall t \geq t_0 \tag{3.2}$$

The origin is unstable if it is not stable. □

Definition 3.2 *The origin of (3.1) is attractive if for each* $t_0 \in \mathbb{R}^+$ *there is an* $\eta(t_0) > 0$ *such that*

$$\|x_0\| < \eta(t_0) \Rightarrow x(t, t_0, x_0) \to 0 \text{ as } t \to \infty \tag{3.3}$$

□

If in definitions 3.1, 3.2 we can find constants $\delta(\epsilon)$ and η independent off t_0 then the origin is said to be uniformly stable respectively uniformly attractive.

Definition 3.3 *The origin of (3.1) is (uniformly) asymptotically stable if it is (uniformly) stable and (uniformly) attractive.* □

Asymptotic stability guaranties that trajectories initiated close to the origin , eventually tends to it in the future. Another stronger notion of stability that defines the speed of convergence is the following

Definition 3.4 *The origin of system (3.1) is exponentially stable if there exist constants* r , a , $b > 0$ *such that*

$$\|x(t, t_0, x_0)\| \leq a e^{-b(t-t_0)} \ , \quad \forall t \geq t_0 \quad \forall x_0 \in B_r \tag{3.4}$$

where B_r *is a ball of radius* r *centered at the origin.* □

All the forgoing properties were defined locally in a neighborhood of the origin. However, if these properties still pertain for all initial state, that is B_r is extended to $\mathbb{R}^n$, we can state the following definitions

Definition 3.5 *The origin of (3.1) is globally uniformly asymptotically stable (GUAS) if*

(i) it is uniformly stable

(ii) for each $M > 0$ *arbitrarily large and* $\epsilon > 0$ *arbitrarily small, there exists a finite* $T = T(M, \epsilon) < \infty$ *such that*

$$\|x_0\| < M \Rightarrow \|x(t, t_0, x_0)\| < \epsilon \ , \quad \forall t \geq T(M, \epsilon) \tag{3.5}$$

□

Definition 3.6 *The origin of (3.1) is globally exponentially stable (GES) if there exist constants a, $b > 0$ such that*

$$\|x(t, t_0, x_0)\| \leq a e^{-b(t-t_0)} , \quad \forall t \geq t_0 \quad \forall x_0 \in \mathbb{R}^n \tag{3.6}$$

□

The problem with the above properties in stability analysis is that they require an explicit knowledge of the solution $x(t, t_0, x_0)$ of (3.1). Unfortunately, in general finding an explicit expression for a solution of a nonlinear differential equation represents a challenge itself. For these reasons Lyapunov direct methods are considered to be valuable. Definitions of the so-called functions of class $\mathcal{K}$ and class $\mathcal{L}$ are necessary prior to stating theorems of Lyapunov's direct method.

Definition 3.7 *A function $\phi : \mathbb{R}^+ \to \mathbb{R}^+$ is said to belong to class $\mathcal{K}$ ($\phi \in \mathcal{K}$) if it is continuous, strictly increasing, and $\phi(0) = 0$.* □

Definition 3.8 *A function $\sigma : \mathbb{R}^+ \to \mathbb{R}^+$ is said to belong to class $\mathcal{L}$ ($\sigma \in \mathcal{L}$) if it is continuous, strictly decreasing, $\sigma(0) < \infty$, and $\sigma(r) \to 0$ as $r \to \infty$.* □

Let us now recast the various stability definitions in terms of class $\mathcal{K}$ and class $\mathcal{L}$ functions

Definition 3.9 *The origin of (3.1) is stable if and only if for each $t_0 \in \mathbb{R}^+$ there exist a number $d(t_0) > 0$ and a function $\phi_{t_0} \in \mathcal{K}$ such that*

$$\|x(t, t_0, x_0)\| \leq \phi_{t_0}(\|x_0\|) , \quad \forall x_0 \in B_{d(t_0)} \tag{3.7}$$

□

Definition 3.10 *The origin of (3.1) is attractive if and only if for each $t_0 \in \mathbb{R}^+$ there exist a number $r(t_0) > 0$ and a function $\sigma_{t_0} \in \mathcal{L}$ such that*

$$\|x(t, t_0, x_0)\| \leq \sigma_{t_0}(t - t_0) , \quad \forall t \geq t_0 \quad \forall x_0 \in B_{r(t_0)} \tag{3.8}$$

□

Again the uniform stability (attractivity) can be deduced if we can find a positive constant $d > 0$ ($r > 0$) and a function $\phi \in \mathcal{K}$ ($\sigma \in \mathcal{L}$) independent off the initial time t_0 such that the inequalities (3.7) respectively (3.8) hold.

Using the preceding stability definitions and the definition of class $\mathcal{K}$ functions, the following theorems can be proved (see [85]). We will denote by Lyapunov function candidate or shortly Lyapunov function any continuously differentiable function ($\mathcal{C}^1$ function)

$V(t,x)$ satisfying for all $t \in \mathbb{R}^+$

$$\begin{cases} V(t,0) = 0 \\ V(t,x) > 0 \quad \forall x \neq 0 \end{cases}$$

Theorem 3.1 *The origin of system (3.1) is (globally) stable if there exist a Lyapunov function $V(t,x)$ and functions $\alpha \in \mathcal{K}$ such that $\forall x \in B_r$, $r > 0$ ($\forall x \in \mathbb{R}^n$) we have*

(i) $\alpha(\|x\|) \leq V(t,x)$

(ii) $\dot{V}(t,x) = \frac{\partial V(t,x)}{\partial x} f(t,x(t)) + \frac{\partial V(t,x)}{\partial t} \leq 0$ □

Theorem 3.2 *The origin of system (3.1) is (globally) uniformly asymptotically stable if there exist a Lyapunov function $V(t,x)$ and functions $\alpha_i \in \mathcal{K}$ ($i = 1,2,3$) such that $\forall x \in B_r$, $r > 0$ ($\forall x \in \mathbb{R}^n$) we have*

(i) $\alpha_1(\|x\|) \leq V(t,x) \leq \alpha_2(\|x\|)$

(ii) $\dot{V}(t,x) \leq -\alpha_3(\|x\|)$ □

Theorem 3.3 *The origin of system (3.1) is (globally) exponentially stable if there exists a Lyapunov function $V(t,x)$ and positive constants $a_i > 0$ ($i = 1,2,3$) and $p > 0$ such that $\forall x \in B_r$, $r > 0$ ($\forall x \in \mathbb{R}^n$) we have*

(i) $a_1\|x\|^p \leq V(t,x) \leq a_2\|x\|^p$

(ii) $\dot{V}(t,x) \leq -a_3\|x\|^p$ □

Conversely we have

Theorem 3.4 *Suppose that $f(t,0) = 0$ and that f is C^k ($k \geq 1$) and Lipschitz with respect to x uniformly in t. Suppose further that the origin of (3.1) is uniformly asymptotically stable in the neighborhood of the origin (B_r). Under these conditions there exist a C^k Lyapunov function $V(t,x)$ and functions $\alpha_i \in \mathcal{K}$ ($i = 1,2,3$) such that $\forall x \in B_r$*

(i) $\alpha_1(\|x\|) \leq V(t,x) \leq \alpha_2(\|x\|)$

(ii) $\dot{V}(t,x) \leq -\alpha_3(\|x\|)$

(iii) $\sup_{x \in B_r} \left\| \frac{\partial V(t,x)}{\partial x} \right\| < \infty$ □

Theorem 3.5 *Suppose that $f(t,0) = 0$ and that f is C^k ($k \geq 1$) and Lipschitz with respect to x uniformly in t. Suppose further that the origin of (3.1) is exponentially stable in the neighborhood of the origin (B_r). Under these conditions there exist a C^k Lyapunov function $V(t,x)$ and constants $a_i > 0$ ($i = 1,2,3$) such that the following hold $\forall x \in B_r$*

(i) $a_1\|x\|^2 \leq V(t,x) \leq a_2\|x\|^2$

(ii) $\dot{V}(t,x) \leq -a_3\|x\|^2$

(iii) $\left\| \frac{\partial V(t,x)}{\partial x} \right\| < a_4\|x\|$ □

As an extension to these theorems and especially Theorem 3.1 LaSalle has developed further results

Theorem 3.6 *Let Ω be a compact (closed and bounded) set with the property that every solution of (3.1) which starts in Ω remains for all future time in Ω. Let $V : \Omega \to \mathbb{R}$ be a C^1 function such that $\dot{V}(x) \leq 0$ in Ω. Let E be the set of all points in Ω where $\dot{V}(x) = 0$. Let M be the largest invariant set in E. Then every solution starting in Ω approaches M as $t \to \infty$.* □

Corallary 3.1 *Consider system (3.1) with its origin as an equilibrium point. Let V be a C^1 function defined on a neighborhood of the origin $U \subseteq \mathbb{R}^n$ such that $\dot{V}(x) \leq 0$ in $U \subseteq \mathbb{R}^n$. Let $S = \{x \in U \subseteq \mathbb{R}^n | \dot{V}(x) = 0\}$, and suppose that no solution can stay forever in S, other than the trivial solution. Then the origin is asymptotically stable. It is globally asymptotically stable if $U = \mathbb{R}^n$ and in addition V is radially unbounded.* □

The above corollary shows formally that if in a domain about the origin we can find a Lyapunov function whose derivative along the trajectories of the system is negative semidefinite, and if we can establish that no system trajectory can stay forever at points where $\dot{V}(x) = 0$ except at the origin, then the origin is asymptotically stable.

3.2 Stabilization via state feedback

The problem of controlling a dynamical system has been addressed from two directions, namely the open loop and the closed loop control. Applications have shown that closed loop control is more accurate whenever stabilization is reached.

In closed loop technique, the control law is designed using the state variables. Thus we can describe the feedback stabilization problem for a nonlinear dynamic system

$$\dot{x} = f(x, u) \tag{3.9}$$

to be the problem of designing a feedback control law

$$u = \Gamma(x) \tag{3.10}$$

such that the origin $x = 0$ is an asymptotically stable equilibrium point of the closed-loop system

$$\dot{x} = f(x, \Gamma(x)) \tag{3.11}$$

In a typical control problem, additional constraint other than asymptotic stability might be required. Therefrom several stabilizing techniques replying to different requirements has been designed. To name a few, we state the tangential linearization of the nonlinear dynamical system around the origin, therefore one can use the linear theory results to design a stabilizing controller. An other approach to the synthesis of a feedback control law is the so-called exact linearization. It consists in finding a nonlinear diffeomorphism that transforms the nonlinear system into a linear one see [38] [9]. Away from the linearization techniques, a third method consists in designing a stabilizing control law directly from the nonlinear model without any kind of linearization. The method concerns nonlinear systems, non-affine in the control, with dissipative drift see Jurdjevic and Quinn [39], Gauthier and Bonard [29], Byrnes *et. al.* Outbib and Sallet [58], Wei Lin [43] [44] and Outbib and Richard [57]. The common feature in all the previous approaches is that the nonlinear system is supposed to be perfectly known. However in general, mathematical models which describe real systems contain uncertain elements due to modelling error and parameter variation to name a few. Sometimes these uncertainties yield to degrading the performance of the stabilizing scheme or even to instabilities in some other times. Therefore, a new approach to design robust stabilizing controller is required. Sliding mode approach is one that was adapted by many researchers see for instance Utkin [83], Slotine [68], Ramirez [66], Spurgeon [45].

3.2.1 Linearization

The most direct way to design a stabilizing controller for the nonlinear dynamical system, is to appeal to the neat results available from linear state feedback control theory. Consider the system

$$\dot{x} = f(x, u) \tag{3.12}$$

where $f(0,0) = 0$ and $f(x,u)$ is continuously differentiable in a domain $\mathcal{X} \times \mathcal{U} \subset \mathbb{R}^n \times \mathbb{R}^p$ that contains the origin ($x = 0,\ u = 0$). The aim is to design a state feedback control $u = \Gamma(x)$ to stabilize the system. Linearization of (3.12) about the origin results in the linear system

$$\dot{x} = Ax + Bu$$

where

$$A = \frac{\partial f}{\partial x}(x,u)\bigg|_{(x,u)=(0,0)} \qquad B = \frac{\partial f}{\partial u}(x,u)\bigg|_{(x,u)=(0,0)}$$

Assume the pair (A, B) is controllable, or at least stabilizable. Design a matrix K to assign the eigenvalues of $A+BK$ to desired locations in the open left-half complex plane. Now apply the linear state feedback control $u = Kx$ to the nonlinear system (3.12). The closed-loop system is

$$\dot{x} = f(x, Kx)$$

Clearly the origin is an equilibrium point of the closed-loop system. The linearization of this system about the origin $x = 0$ is given by

$$\begin{aligned}\dot{x} &= \left[\frac{\partial f}{\partial x}(x, Kx) + \frac{\partial f}{\partial u}(x, Kx)K\right]_{x=0} x \\ &= (A + BK)x\end{aligned}$$

Since $A + BK$ is Hurwitz stable, it follows from Theorem 3.7 that the origin is an asymptotically stable equilibrium point of the closed-loop system.

Theorem 3.7 *Let $x = 0$ be an equilibrium point for the nonlinear system $\dot{x} = f(x)$, where $f : U \to \mathbb{R}^n$ is continuously differentiable and U is a neighborhood of the origin. Let*

$$A = \frac{\partial f}{\partial x}(x)\bigg|_{x=0}$$

then,

(i) The origin is asymptotically stable if all eigen values of A have strictly negative real parts.

(ii) The origin is unstable if at least one of the eigenvalues of A has strictly positive real part. □

Proof : See [41, page 130].

Clearly, this approach is local; that is, it can only guarantee asymptotic stability of the origin, but it cannot, in general prescribe a region of attraction nor can it achieve global asymptotic stability.

3.2.2 Exact linearization

There has been a great deal of excitement in recent years over the development of a rather complete theory for explicitly linearizing the input-output map of nonlinear dynamic systems using state feedback. The idea of cancelling the nonlinearities is an attractive one, not only does it reduce the design problem to a linear one, but it also produces a linear closed-loop system.

In presenting this approach we will consider the case of single-input single-output nonlinear dynamic systems described by the following equations on $\mathbb{R}^n$

$$\dot{x} = f(x) + g(x)u \tag{3.13a}$$

$$y = h(x) \tag{3.13b}$$

In what follows $L_f h(x)$ denotes the Lie derivative of the function $h(x)$ with respect to the vector field f. High order Lie derivative can be defined recursively as

$$L_f^0 h(x) = h(x) \ , \quad L_f^k h(x) = L_f\big(L_f^{k-1} h(x)\big) \ , k > 1 \ .$$

We first give the following definition and results. (The reader is referred to [38] for more details)

Definition 3.11 *System (3.13) is said to have relative degree r at a point x_0 if*
(i) $L_g L_f^k h(x) = 0$ for all x in a neighborhood of x_0 and all $k < r-1$
(ii) $L_g L_f^{r-1} h(x_0) \neq 0$ □

Definition 3.12 *The system (3.13) is said to have strong relative degree r in an open set $U \in \mathbb{R}^n$ if it has relative degree r at every point $x_0 \in U$.* □

Lemma 3.1 *if system (3.13) has relative degree r, then the row vectors*

$$dh(x_0),\ dL_f h(x_0), \ldots, dL_f^{r-1} h(x_0)$$

are linearly independent. □

Proposition 3.1 *Suppose the system (3.13) has strong relative degree r in U, and $r \leq n$. Set*

$$\begin{array}{rcccc} z_1 & = & \phi_1(x) & = & h(x) \\ z_2 & = & \phi_2(x) & = & L_f h(x) \\ \vdots & = & \vdots & = & \vdots \\ z_r & = & \phi_r(x) & = & L_f^{r-1} h(x) \ . \end{array}$$

If the relative degree r is strictly less than n, it is always possible to find $n-r$ more functions $\phi_{r+1}(x), \ldots, \phi_n(x)$ such that the mapping

$$z = \Phi(x) = \begin{pmatrix} \phi_1(x) \\ \vdots \\ \phi_n(x) \end{pmatrix}$$

has a jacobian matrix which is nonsingular at every $x_0 \in U$ and therefore qualifies as a local coordinates transformation in U. Moreover, it is always possible to choose $\phi_{r+1}(x), \ldots, \phi_n(x)$ in such a way that $L_g \phi_i(x) = 0$ for all $r+1 \leq i \leq n$ and all $x \in U$. □

In this section we will assume that (3.13) has strong relative degree r, hence using the local coordinate transformation defined in Proposition 3.1, the state-space description of system (3.13) will be as follows

$$\begin{aligned}
\dot{z}_i &= z_{i+1}\,, \quad 1 \le i \le r-1 && (3.14a)\\
\dot{z}_r &= L_f^r h(\Phi^{-1}(z)) + L_g L_f^{r-1} h(\Phi^{-1}(z))u && (3.14b)\\
\dot{z}_j &= q_j(z)\,, \quad r+1 \le j \le n && (3.14c)\\
y &= z_1 && (3.14d)
\end{aligned}$$

Although from proposition 3.1 these functions may be chosen such that they are independent of the control u, in general this is a very hard task since finding such functions amounts to solve a system of $n-r$ nonlinear partial differential equations.

A more convenient description of the system represented by (3.14) is as follows. Set

$$\xi = \begin{pmatrix} z_1 \\ z_2 \\ \dots \\ z_r \end{pmatrix}, \quad \eta = \begin{pmatrix} z_{r+1} \\ z_{r+2} \\ \dots \\ z_n \end{pmatrix},$$

and recall that, in particular,

$$\xi = \begin{pmatrix} h(x) \\ L_f h(x) \\ \vdots \\ L_f^{r-1} h(x) \end{pmatrix}.$$

Moreover , let the matrices $A \in \mathbb{R}^{r\times r}$, $B \in \mathbb{R}^{r\times 1}$ and $C \in \mathbb{R}^{1\times r}$ as follows

$$A = \begin{pmatrix} 0 & 1 & 0 & \dots & 0 \\ 0 & 0 & 1 & \dots & 0 \\ \vdots & \vdots & \vdots & \ddots & \vdots \\ 0 & 0 & 0 & \dots & 1 \\ 0 & 0 & 0 & \dots & 0 \end{pmatrix}, B = \begin{pmatrix} 0 \\ 0 \\ \vdots \\ 0 \\ 1 \end{pmatrix},$$

$$C = \begin{pmatrix} 1 & 0 & 0 & \dots & 0 & 0 \end{pmatrix}$$

and let $q(\xi,\eta)$ be equal to

$$q(\xi,\eta) = \begin{pmatrix} q_{r+1}(z) \\ q_{r+2}(z) \\ \dots \\ q_n(z) \end{pmatrix}.$$

Define

$$\begin{aligned}
a(\xi,\eta) &= L_g L_f^{r-1} h(\Phi^{-1}(z))\\
b(\xi,\eta) &= L_f^r h(\Phi^{-1}(z))
\end{aligned}$$

Eventually, the transformed system (3.14) can be written in the following form

$$\dot{\xi} = A\xi + B\Big(b(\xi,\eta) + a(\xi,\eta)u\Big) \tag{3.15a}$$
$$\dot{\eta} = q(\xi,\eta) \tag{3.15b}$$
$$y = C\xi \tag{3.15c}$$

Now since $a(\xi,\eta)$ is bounded away from zero, from the definition of the relative degree of system (3.13), then its inverse is well defined and so is the control law derived using (3.14) by

$$u = \frac{1}{a(\xi,\eta)}\Big(- b(\xi,\eta) + \nu\Big)\ . \tag{3.16}$$

This feedback law yields a closed-loop system that is described by equations of the form

$$\dot{\xi} = A\xi + B\nu \tag{3.17a}$$
$$\dot{\eta} = q(\xi,\eta) \tag{3.17b}$$
$$y = C\xi\ . \tag{3.17c}$$

This system clearly appears decomposed into a linear subsystem, of dimension r, which is the only one responsible for the input-output behaviour, and a possibly nonlinear subsystem, of dimension $n-r$, whose behaviour does not affect the output. It is also worth noting that the linear part is a controllable and observable r dimensional system, and that here, ν is a new control to be designed to meet control specifications. One can choose ν so that the linear part described by (3.17a) is exponentially stable. However, this does not always guarantee the stability of the subsystem described by (3.17b), see [73].

Let us consider the dynamics described by

$$\dot{\eta} = q(0,\eta) \tag{3.18}$$

which are referred to as the zero dynamics corresponding to system (3.13) (this terminology is due to Byrnes and Isidori [8])

Definition 3.13 *The system described by (3.13) is said to be a (hyperbolically) minimum-phase nonlinear system if its corresponding zero dynamics are (exponentially) asymptotically stable.* □

The aim in most applications is output tracking. That is, it is desired that the output $y(t)$ be equal to a prescribed signal $y_d(t)$. We observe that $y(t) = y_d(t)$ implies that

$$z_i(t) = y_d^{(i-1)}(t) \quad \forall\, t \quad \text{and} \quad 1 \leq i \leq r$$

where $y_d^{(i-1)}(t) = \left(\frac{d}{dt}\right)^{i-1} y_d(t)$.

Set

$$\xi_d = \begin{pmatrix} y_d \\ y_d^{(1)} \\ \vdots \\ y_d^{(r-1)} \end{pmatrix} .$$

and define $e(t) = \xi(t) - \xi_d(t)$. Our aim is to choose a suitable feedback control law to make the resulting dynamics of $e(t)$ at least asymptotically stable. Choose

$$\begin{aligned} \nu &= y_d^{(r)} - \sum_{i=1}^{r} c_{i-1}\big(z_i - y_d^{(i-1)}\big) \\ &= y_d^{(r)} - \sum_{i=1}^{r} c_{i-1}\big(L_f^{i-1}h(x) - y_d^{(i-1)}\big) \\ &= y_d^{(r)} + K\big(\xi - \xi_d\big) \\ &= y_d^{(r)} + Ke \end{aligned} \tag{3.19}$$

where $K = \big(-c_0 \quad -c_1 \quad -c_2 \ldots -c_{r-1}\big)$. Imposing a feedback control law u defined by (3.16) and (3.19)

$$u = \frac{1}{a(\xi,\eta)}\Big(-b(\xi,\eta) + y_d^{(r)} + Ke\Big) . \tag{3.20}$$

yields to

$$\dot{e} = (A + BK)e \tag{3.21a}$$

$$\dot{\eta} = q(e + \xi_d, \eta) \tag{3.21b}$$

with

$$A + BK = \begin{pmatrix} 0 & 1 & 0 & \ldots & 0 \\ 0 & 0 & 1 & \ldots & 0 \\ \vdots & \vdots & \vdots & \ddots & \vdots \\ 0 & 0 & 0 & \ldots & 1 \\ -c_0 & -c_1 & -c_2 & \ldots & -c_{r-1} \end{pmatrix} .$$

In particular, the matrix $A + BK$ has a characteristic polynomial

$$p(s) = s^r + c_{r-1}s^{r-1} + \ldots + c_1 r + c_0 .$$

From this form of the closed-loop system (3.21), we can deduce the following properties.

Proposition 3.2 *Suppose that system (3.13) is minimum-phase, $\xi_d = 0$, and that the polynomial $p(s)$ is Hurwitz stable (*i.e. *all its roots have negative real parts). Then the feedback control law defined by (3.20) locally asymptotically stabilizes the equilibrium $(\xi,\eta) = (0,0)$.*

Proof : See [38, page 175].

Proposition 3.3 *Suppose that system (3.13) is hyperbolically minimum-phase, and the polynomial $p(s)$ is Hurwitz stable. Then there exists a positive constant c^* and an open set $\Omega \subset \Phi(U)$, such that if $\|\xi_d\| < c*$, then, for all initial conditions in Ω, asymptotic output tracking is achieved with the trajectories remaining in the set $\Phi(U)$ for all times.* □

Proof : See [5].

3.2.3 Sliding mode control

This section investigates sliding mode control, also called variable structure control, see Utkin [83], Slotine [69]. In this approach the gain in each feedback path switches between two values according to a rule that depends on the value of the state at each instant. The purpose of the switching control law is to drive the nonlinear system state trajectory onto a prescribed surface in the state space and to maintain the state trajectory on the surface for all subsequent time. This surface is called the sliding surface (sliding manifold), since once the trajectory is on the surface, it slide along it. Therefore, the first crucial point of the sliding mode control design is to properly choose the sliding surface so that the system, when confined to the surface, has desired dynamics, such as stability of the origin or tracking. The second critical point is to choose the necessary control that will drive the state trajectory to the sliding surface and maintain it on the surface upon interception.

Let us consider for instance the system defined by

$$\dot{x} = f(x) + g(x)u \tag{3.22a}$$
$$y = h(x) \tag{3.22b}$$

having a strong relative degree r in an open set $U \in \mathbb{R}^n$. It has been shown in the previous section that there exist a local coordinate transformation such that system (3.22) is represented as

$$\dot{\xi} = A\xi + B\Big(b(\xi,\eta) + a(\xi,\eta)u\Big) \tag{3.23a}$$
$$\dot{\eta} = q(\xi,\eta) \tag{3.23b}$$
$$y = C\xi \tag{3.23c}$$

The problem of output tracking consists in determining the appropriate control law that forces the output function $y(t)$ to be equal to a prescribed signal $y_d(t)$. It is easy to see that $y(t) = y_d(t)$ implies that

$$z_i(t) = y_d^{(i-1)}(t) \quad \forall\, t \quad \text{and} \quad 1 \le i \le r$$

Therefore, the aim to obtain

$$e_y(t) = y(t) - y_d(t) = 0$$

is similar to the aim to have

$$e(t) = \xi(t) - \xi_d(t) = 0 \ .$$

It is also obvious that to have exact tracking, then $\xi(0)$ must be such that

$$\xi_d(0) = \xi(0) \ . \tag{3.24}$$

Define

$$S = \left(\frac{d}{dt} + \lambda\right)^{r-1} e_1 \qquad \lambda > 0 \ . \tag{3.25}$$

Given initial condition (3.24), the problem of output tracking $\xi(t) = \xi_d(t) \Leftrightarrow e(t) = 0$ is also equivalent to remaining on the surface $S = 0$ for all $t > 0$; indeed, $S = 0$ represents a linear differential equation whose unique solution is $e(t) = 0$, given initial condition (3.24). Therefore, the tracking problem $y(t) = y_d(t)$ is reduced to keeping the scalar quantity S at zero.

Keeping the scalar S at zero can be achieved by choosing a control law for (3.23) such that outside of $S(t) = 0$ we have

$$S\dot{S} < 0 \ . \tag{3.26}$$

This is called the sliding condition, and it is a necessary condition to keep the surface $S = 0$ an invariant one. A suitable choice to satisfy (3.26) is

$$\dot{S} = -w \ \mathrm{sign}(S) \ , \quad w > 0 \ . \tag{3.27}$$

$S(t)$ verifying (3.26) is called a sliding surface, and if the system behaviour is confined to the sliding surface, we say that the system is at sliding mode. Furthermore, satisfying (3.26) guarantees that if the initial condition does not satisfy (3.24) the surface will nonetheless be reached in a finite time.

$$t_r \le \frac{|S(t=0)|}{w} \ , \tag{3.28}$$

indeed integrating (3.27) gives

$$S(t) = \begin{cases} -wt + S(t=0) & \text{if } S(t=0) > 0 \text{ and } t < t_r \\ wt + S(t=0) & \text{if } S(t=0) < 0 \text{ and } t < t_r \end{cases}$$

whence we can deduce (3.28).

To find the feedback control we use (3.25) and (3.27)

$$\begin{aligned}
\dot{S} &= \left(\frac{d}{dt}+\lambda\right)^{r-1}\dot{e}_1 \\
\dot{S} &= \left(\frac{d}{dt}+\lambda\right)^{r-1} e_2 \\
-w\ \text{sign}(S) &= \left(\frac{d}{dt}+\lambda\right)^{r-1} e_2 \\
-w\ \text{sign}(S) &= b(\xi,\eta)+a(\xi,\eta)u-\dot{\xi}_d+\sum_{k=1}^{r-1}\binom{k}{r-1}\lambda^k e_{r-k+1}
\end{aligned}$$

where

$$\binom{k}{r-1}=\frac{(r-1)!}{(r-1-k)!k!}\ .$$

Therefore, a feedback control law can be chosen as

$$u=\frac{1}{a(\xi,\eta)}\Big(-b(\xi,\eta)+\dot{\xi}_d-w\ \text{sign}(S)-a_{r-1}e_r-a_{r-2}e_{r-1}-\ldots-a_1e_2\Big) \tag{3.29}$$

where

$$a_k=\binom{r-k}{r-1}\lambda^{r-k}\ ,\quad k=1,\ldots,r-1\ .$$

By construction, the control law defined by (3.29) will force the states ξ to be equal to ξ_d for all $t>t_r$. Thus, the state η will be governed by the dynamics

$$\dot{\eta}=q(\xi_d,\eta)\ ,\quad \forall\, t>t_r\ .$$

Therefore, if the system (3.22) is (hyperbolically) minimum-phase, the results of Proposition 3.2 and 3.3 hold.

3.2.4 Feedback stabilization : A passive approach

Consider a smooth (C^∞) affine control system in $\mathbb{R}^n$

$$\dot{x}=f(x)+g(x)u \tag{3.30}$$

and assume without loss of generality that the origin $x=0$ is a stable equilibrium point of the autonomous dynamics

$$\dot{x}=f(x)$$

a sufficient condition to deduce the stability of the origin of the above autonomous system is the existence of a smooth function V defined on a neighborhood of the origin $U\subseteq\mathbb{R}^n$ satisfying

(i) $V(0) = 0$ and $V(x) > 0$ for $x \neq 0$

(ii) $L_f V(x) \leq 0 \quad \forall x \in U \subseteq \mathbb{R}^n$

We introduce the distribution D_1

$$D_1 = \text{span}\Big\{g,\ ad_f g, \ldots, ad_f^{n-1} g\Big\}$$

$ad_f g(x)$ denotes the Lie bracket of the vector fields f and g, and a set associated with D_1 defined by

$$S_1 = \Big\{x \in U \subseteq \mathbb{R}^n | L_f^k L_\varrho v(x) = 0 \ \forall \varrho \in D_1;\ k = 0, 1, \ldots\Big\}$$

Theorem 3.8 *Suppose that the smooth affine control system (3.30) has stable drift at the origin and let V be an associated smooth Lyapunov function. If on some neighborhood U of the origin we have $S_1 = \{0\}$, then the system (3.30) is smoothly stabilizable by the feedback control law $u(x) = -L_g V(x)$. Moreover, stabilization is global provided that V is uniformly bounded and $U = \mathbb{R}^n$.* □

Proof : See [42]

Consider now a single input nonlinear dynamic system which is not affine in the control

$$\dot{x} = f(x, u) \tag{3.31}$$

where f is a smooth vector field and the uncontrolled dynamic system

$$\dot{x} = f(x, 0) = f_0(x)$$

is Lyapunov stable *i.e.* there exist a smooth Lyapunov function satisfying

(i) $V(0) = 0$ and $V(x) > 0$ for $x \neq 0$

(ii) $L_{f_0} V(x) \leq 0 \quad \forall x \in U \subseteq \mathbb{R}^n$

Due to the smoothness property of f system (3.31) can be written as

$$\dot{x} = f(x, 0) + g(x, u)u$$

since it suffices to observe that

$$f(x, u) - f(x, 0) = \int_0^1 \frac{\partial f(x, su)}{\partial s} ds = \int_0^1 \frac{\partial f(x, \omega)}{\partial \omega}\bigg|_{\omega = su} u \, ds$$

Set $g_0(x) = g(x, 0)$ and define the distribution D_2 as

$$D_2 = \text{span}\Big\{ad_{f_0}^k g_0 : 0 \leq k \leq n-1\Big\}$$

and two sets S_2 and Ω_2 by

$$S_2 = \Big\{x \in U \subseteq \mathbb{R}^n : L_{f_0}^k L_\varrho V(x) = 0\ , \forall \varrho \in D_2\ ; k = 0, 1, 2, \ldots\Big\}$$

$$\Omega_2 = \Big\{x \in U \subseteq \mathbb{R}^n : L_{f_0}^k V(x) = 0\ , k = 1, 2, \ldots\Big\}$$

Theorem 3.9 *Consider system (3.31) having a stable drift at the origin. If $S_2 \cap \Omega_2 = \{0\}$ then (3.31) is locally asymptotically stabilizable at the origin by a smooth state feedback. in particular*

$$u(x) = -L_{g(x,u)}V(x) \ . \tag{3.32}$$

If furthermore, V is proper, $S_2 \cap \Omega_2 = \{0\}$ $\forall x \in \mathbb{R}^n$ and $u(x)$ is well-defined on $\mathbb{R}^n$ then (3.31) is globally stabilizable by (3.32). □

Proof : See [43].

Another interesting class of nonlinear systems has been investigated by Outbib and Richard [57], with application to stabilizing electropneumatic systems. Consider the class of nonlinear systems defined by

$$\dot{x} = f(x) + g(x)\varphi(x,u)u \tag{3.33}$$

having the origin as an equilibrium point, and where $\varphi(.,.)$ is a scalar function. Assume that the following hypotheses are pertaining to system (3.33)

($\mathcal{H}1$) There is a smooth Lyapunov function V, proper and such that $L_fV(x) \leq 0$ on $\mathbb{R}^n$

($\mathcal{H}2$) There exist r and h two C^1 scalar functions such that
- (i) $r(x) > 0$ on $\mathbb{R}^n$
- (ii) $xh(x) > 0$ for $x \neq 0$ and $h(0) = 0$
- (iii) $\varphi\Big(x, -r(x)h\big(L_gV(x)\big)\Big) > 0$

($\mathcal{H}3$) The set

$$S_3 = \Big\{x \in \mathbb{R}^n : L_f^kL_gV(x) = 0 \ , k = 0,1,2,\dots\Big\} = \{0\}$$

Then we have the following result :

Theorem 3.10 *Consider system (3.33) verifying ($\mathcal{H}1$), ($\mathcal{H}2$) and ($\mathcal{H}3$) then the feedback control law defined by*

$$u(x) = -r(x)h\big(L_gV(x)\big) \tag{3.34}$$

asymptotically stabilizes system (3.33) at the origin. □

Proof : Consider the closed-loop system defined by (3.33) and (3.34) as

$$\dot{x} = f(x) - g(x)\varphi\Big(x, -r(x)h\big(L_gV(x)\big)\Big)r(x)h\big(L_gV(x)\big) \ . \tag{3.35}$$

The derivative of V along the trajectories of (3.35) is given by

$$\dot{V} = L_fV(x) - \varphi\Big(x, -r(x)h\big(L_gV(x)\big)\Big).r(x).L_gV(x)h\big(L_gV(x)\big)$$

using (i) and (ii) of ($\mathcal{H}2$) it follows that $\dot{V}(x) \leq 0$. Whence (3.35) is stable at the origin.

Set $\Omega_3 = \{x \in \mathbb{R}^n | \dot{V}(x) = 0\}$, then from LaSalle's invariance Theorem 3.6 all solutions tend to $M \subset \Omega_3$ the largest invariant set by the closed loop dynamics. By using condition (iii) we can conclude that $M = \{0\}$ (see [58]). Eventually, yielding that the origin is asymptotically stable.

3.3 Design of force controller for an electrohydraulic system

Hydraulic systems are potential choices for modern industries due to their stiffness and high payload capabilities. Their application scope ranges from precision control systems such as robotics, to heavy-duty manipulators such as forging presses and civil engineering plants. The relatively high force-to-weight ratio of electrohydraulic systems in addition to their fast and smooth response had made them widely solicited in many industrial domains.

Although hydraulic systems offer many advantages, they unfortunately pose many problems in controller design due to their model complexities. In fact, the nonlinear characteristics of a hydraulic system, especially those resulting from servovalve flow-pressure relations in addition to the inevitable model uncertainties made the design of feedback controllers a challenging task.

In wide range of applications where electrohydraulic manipulators are involved, the output force is required to follow a specific given reference. This necessitates the design of a feedback control law. This problem was treated by many researchers and it revealed to be a difficult one. In solving this problem, different control methods have been used, such as PID controllers [3], adaptive controllers [2] and quantitative feedback theory [55].

In this chapter, we will use the electrohydraulic manipulator model developed in chapter 2 to design feedback force controllers using the input-output linearization technique [21]. We also design a feedback control law using the sliding mode method [23], where we give a simple method on how to choose a sliding surface for a class of nonlinear systems. We show the robustness of the sliding method with respect to parameter changes.

Parameter	value	unit
	fluid	
B	2.2×10^9	Pa
P_s	300×10^5	Pa
P_r	1×10^5	Pa
	piston	
m_0	50	kg
S	1.5×10^{-3}	m^2
V_t	1×10^{-3}	m^3
	load	
m	20	kg
b	590	kg/s
k_l	125000	N/m
	servovalve	
k	5.12×10^{-5}	$m^3 s^{-1} A^{-1} Pa^{-1/2}$
α	4.1816×10^{-12}	$m^3 s^{-1} Pa^{-1}$
γ	8571	s^{-1}

TAB. 3.1 – Numerical values used for simulations.

3.3.1 Input-output linearization feedback control

Consider the hydraulic manipulator presented in chapter 2 with $x_1 = P_L$, $x_2 = v$, $x_3 = x_p$ and without loss of generality we will assume that $x_{p0} = 0$, then we have

$$\dot{x}_1 = \frac{4B}{V_t}\Big(ku\sqrt{\frac{P_s - P_r - \text{sign}(u)x_1}{2}} - \frac{\alpha}{1+\gamma|u|}x_1 - Sx_2\Big) \tag{3.36a}$$

$$\dot{x}_2 = \frac{1}{m_t}(Sx_1 - bx_2 - k_l x_3) \tag{3.36b}$$

$$\dot{x}_3 = x_2 \tag{3.36c}$$

where we should have $P_r - P_s < x_1 < P_s - P_r$ and $-\frac{l_p}{2} < x_3 < \frac{l_p}{2}$. Clearly this is not a system that is affine in the control. However, if we let $\gamma = 0$, the above system becomes affine in the control, but it will not reflect the leakage flow correctly. In this case the hydraulic manipulator is modeled by the following dynamic system

$$\dot{x}_1 = \frac{4B}{V_t}\Big(ku\sqrt{\frac{P_s - P_r - \text{sign}(u)x_1}{2}} - \alpha x_1 - Sx_2\Big) \tag{3.37a}$$

$$\dot{x}_2 = \frac{1}{m_t}(Sx_1 - bx_2 - k_l x_3) \tag{3.37b}$$

$$\dot{x}_3 = x_2 \tag{3.37c}$$

Thus we can write (3.37) in the form

$$\dot{x} = f(x) + \begin{cases} g^+(x)u & \text{if} \quad u \geq 0 \\ g^-(x)u & \text{if} \quad u < 0 \end{cases}$$

with

$$f(x) = \begin{pmatrix} -\frac{4B}{V_t}(\alpha x_1 + Sx_2) \\ \frac{1}{m_t}(Sx_1 - bx_2 - k_l x_3) \\ x_2 \end{pmatrix}$$

$$g^+(x) = \begin{pmatrix} \frac{4B}{V_t}k\sqrt{\frac{P_s - P_r - x_1}{2}} \\ 0 \\ 0 \end{pmatrix} \qquad g^-(x) = \begin{pmatrix} \frac{4B}{V_t}k\sqrt{\frac{P_s - P_r + x_1}{2}} \\ 0 \\ 0 \end{pmatrix}$$

Let the output to be controlled be the force measured at the contact point between the piston and the load, namely

$$h(x) = F$$

we want the output force to track a desired force F_d. In order to explicit the expression of F as a function of the states we use Newton's second law of motion for the piston dynamics

$$SP_L - F = m_0 \frac{dv}{dt} \quad \Leftrightarrow \quad \frac{dv}{dt} = \frac{1}{m_0}(SP_L - F) \; .$$

Substituting in equation (3.37b) yields

$$\begin{aligned} \frac{1}{m_0}(SP_L - F) &= \frac{1}{m_t}(SP_L - bv - k_l x_p) \\ \frac{1}{m_0}F &= \frac{1}{m_0}SP_L - \frac{1}{m + m_0}SP_L + \frac{1}{m + m_0}bv + \frac{1}{m + m_0}k_l x_p \\ F &= \frac{m}{m + m_0}SP_L + \frac{m_0}{m + m_0}(bv + k_l x_p) \end{aligned}$$

thus

$$y = h(x) = \frac{m}{m + m_0}Sx_1 + \frac{m_0}{m + m_0}(bx_2 + k_l x_3) \; . \tag{3.38}$$

We can easily check that

$$L_{g^+}h(x) = \frac{m}{m + m_0}S\frac{4B}{V_t}k\sqrt{\frac{P_s - P_r - x_1}{2}} > 0 \quad \forall\, x_1 \in]P_r - P_s, P_s - P_r[\; , \tag{3.39}$$

$$L_{g^-}h(x) = \frac{m}{m + m_0}S\frac{4B}{V_t}k\sqrt{\frac{P_s - P_r + x_1}{2}} > 0 \quad \forall\, x_1 \in]P_r - P_s, P_s - P_r[\; , \tag{3.40}$$

thus system (3.37) has a strong relative degree equal to 1 in the domain of operation of the hydraulic system.

If we consider the coordinate transformation

$$\begin{pmatrix} z_1 \\ z_2 \\ z_3 \end{pmatrix} = \Phi(x) = \begin{pmatrix} h(x) \\ x_2 \\ x_3 \end{pmatrix} = \begin{pmatrix} \frac{m}{m+m_0} Sx_1 + \frac{m_0}{m+m_0}(bx_2 + k_l x_3) \\ x_2 \\ x_3 \end{pmatrix},$$

then using (3.38) we have

$$Sx_1 = \frac{m+m_0}{m} h(x) - \frac{m_0}{m} bx_2 - \frac{m_0}{m} k_l x_3$$

hence (3.37b) becomes

$$\begin{aligned} \dot{x}_2 &= \frac{1}{m+m_0}(Sx_1 - bx_2 - k_l x_3) \\ &= \frac{1}{m+m_0}\Big(\frac{m+m_0}{m} h(x) - \frac{m_0}{m} bx_2 - \frac{m_0}{m} k_l x_3 - bx_2 - k_l x_3\Big) \\ &= \frac{1}{m+m_0}\Big(\frac{m+m_0}{m} h(x) - \frac{m+m_0}{m} bx_2 - \frac{m+m_0}{m} k_l x_3\Big) \\ &= \frac{1}{m}\big(h(x) - bx_2 - k_l x_3\big) \,. \end{aligned}$$

Therefore, by using the coordinates transformation $z = \Phi(x)$, the system is described by the following equations

$$\begin{aligned} \dot{z}_1 &= L_f h\big(\Phi^{-1}(z)\big) + L_g h\big(\Phi^{-1}(z)\big) u \\ \dot{z}_2 &= \frac{1}{m}(z_1 - bz_2 - k_l z_3) \\ \dot{z}_3 &= z_2 \end{aligned}$$

Calculating the control law

If we require the output force to track a prescribed reference force F_d then according to (3.16), and since we know that

$$L_{g^+} h(x) > 0 \quad \text{and} \quad L_{g^-} h(x) > 0 \,,$$

it follows that

$$\text{sign}(u) = \text{sign}\big(N(x)\big)$$

where,

$$N(x) = -L_f h(x) - c_0\big(h(x) - F_d\big) + \dot{F}_d$$

eventually, we obtain

$$u(x) = \begin{cases} \dfrac{N(x)}{L_{g^+} h(x)} & \text{if} \quad N(x) \geq 0 \\ \dfrac{N(x)}{L_{g^-} h(x)} & \text{if} \quad N(x) < 0 \end{cases}$$

where

$$L_f h(x) = \frac{m}{m_t}\frac{4BS}{V_t}(-\alpha x_1 - Sx_2) + \frac{bm_0}{m_t^2}(Sx_1 - bx_2 - k_l x_3) + \frac{m_0}{m} k_l x_2$$

and $L_{g^+}h(x)$ and $L_{g^-}h(x)$ as described in (3.39) and (3.40).

Investigating the zero dynamics

The zero dynamics are a two-dimensional linear system, particularly

$$\begin{bmatrix} \dot{z}_2 \\ \dot{z}_3 \end{bmatrix} = \begin{bmatrix} -\frac{b}{m} & -\frac{k_l}{m} \\ 1 & 0 \end{bmatrix} \begin{bmatrix} z_2 \\ z_3 \end{bmatrix}$$

and are exponentially stable for the selected particular values. (See Table 3.1). Therefore, the hydraulic system in question is hyperbolically minimum-phase and the result of proposition 3.3 holds. Indeed, if we let $e_1 = z_1 - F_d$ we can verify that the closed loop system can be written as

$$\begin{aligned} \dot{e}_1 &= -c_0 e_1 \ , && (3.41a) \\ \dot{z}_2 &= \frac{1}{m}(e_1 + F_d - bz_2 - k_l z_3) \ , && (3.41b) \\ \dot{z}_3 &= z_2 \ . && (3.41c) \end{aligned}$$

Since $e_1 = 0$ is an exponentially stable equilibrium of (3.41a), then tracking is exponentially achieved if z_2 and z_3 behave within the practical operating domain, namely $-\frac{l_p}{2} < z_3 < \frac{l_p}{2}$. In fact when $e_1 = 0$, z_2 and z_3 are governed by the following dynamics (substituting $e_1 = 0$ in (3.41b) and (3.41c)).

$$\begin{bmatrix} \dot{z}_2 \\ \dot{z}_3 \end{bmatrix} = \begin{bmatrix} -\frac{b}{m} & -\frac{k_l}{m} \\ 1 & 0 \end{bmatrix} \begin{bmatrix} z_2 \\ z_3 \end{bmatrix} + \begin{bmatrix} \frac{1}{m} \\ 0 \end{bmatrix} F_d \qquad (3.42)$$

which is in the form

$$\dot{\eta} = A\eta + BF_d$$

Let $F_d(t)$ be bounded, that is there exists $F_{\max}$ such that

$$\|F_d(t)\| \leq F_{\max} \quad \forall\, t > 0 \ ,$$

we know that A is Hurwitz stable, then there exist $M > 0$ and $\mu > 0$ such that

$$\|\exp(At)\| \leq M \exp(-\mu t) \quad \forall\, t > 0 \ .$$

The solution of (3.42) can be expressed as follows

$$\eta(t) = \exp(At)\eta(0) + \int_0^t \exp\big(A(t-\tau)\big) BF_d(\tau) d\tau$$

taking norms

$$
\begin{aligned}
\|\eta(t)\| &\leq \|\exp(At)\|.\|\eta(0)\| + \int_0^t \|\exp\big(A(t-\tau)\big)\|.\|B\|F_{\max}d\tau \\
&\leq M\exp(-\mu t)\|\eta(0)\| + \|B\|F_{\max}M\exp(-\mu t)\int_0^t \exp(\mu\tau)d\tau \\
&\leq M\exp(-\mu t)\|\eta(0)\| + \|B\|F_{\max}M\exp(-\mu t)\frac{1}{\mu}\big(\exp(\mu t)-1\big) \\
&\leq M\exp(-\mu t)\|\eta(0)\| + \|B\|F_{\max}\frac{M}{\mu} - \|B\|F_{\max}\frac{M}{\mu}\exp(-\mu t) \\
&\leq M\Big(\|\eta(0)\| - \|B\|F_{\max}\frac{1}{\mu}\Big)\exp(-\mu t) + \|B\|F_{\max}\frac{M}{\mu}
\end{aligned}
$$

whence, it can be seen that for a suitable choice of $F_{\max}$ and the initial condition $\eta(0)$ (*i.e.* $z_2(0)$ and $z_3(0)$), then tracking will be achieved exponentially fast and the trajectories $z_2(t)$ and $z_3(t)$ will tend to be bounded within a ball of radius $\frac{1}{m}F_{\max}\frac{M}{\mu}$, as $t \to \infty$.

Using the practical values shown in Table 3.1, we have simulated system 3.37, with a tracking coefficient $c_0 = 50$. We first wanted the output force to follow a step force changing abruptly from zero to $10000N$, Figures 3.1 and 3.2 show the behaviour of the states and the output force of the system.

Next we show that the tracking is also achieved for a time varying force, for the purpose we used an exponentially decaying sinusoidal force, having amplitude $10000N$, frequency $5Hz$ and decaying constant $7s^{-1}$. Similarly to the previous case the system was initiated at the origin. The results of the second simulations are shown in Figures 3.3 and 3.4.

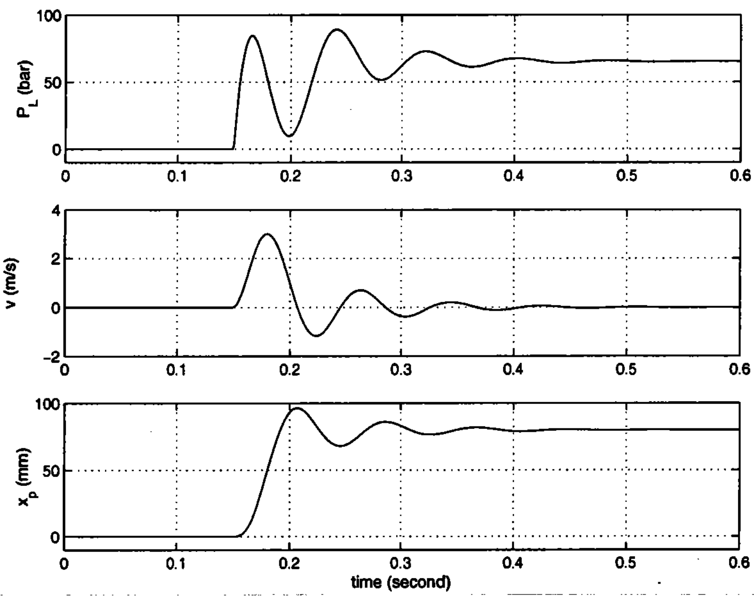

FIG. 3.1 – State behaviour of the system. (tracking constant force)

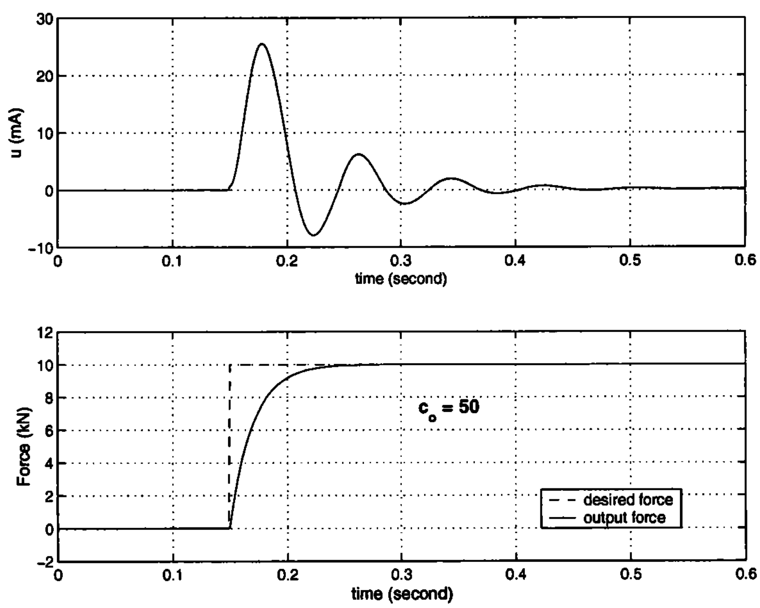

FIG. 3.2 – Force behaviour and needed control law. (tracking constant force)

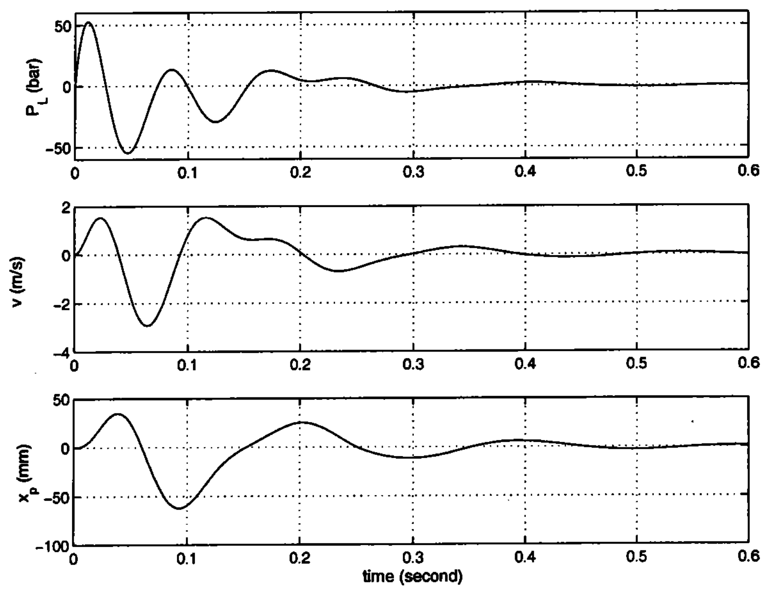

FIG. 3.3 – State behaviour of the system. (tracking time-varying force)

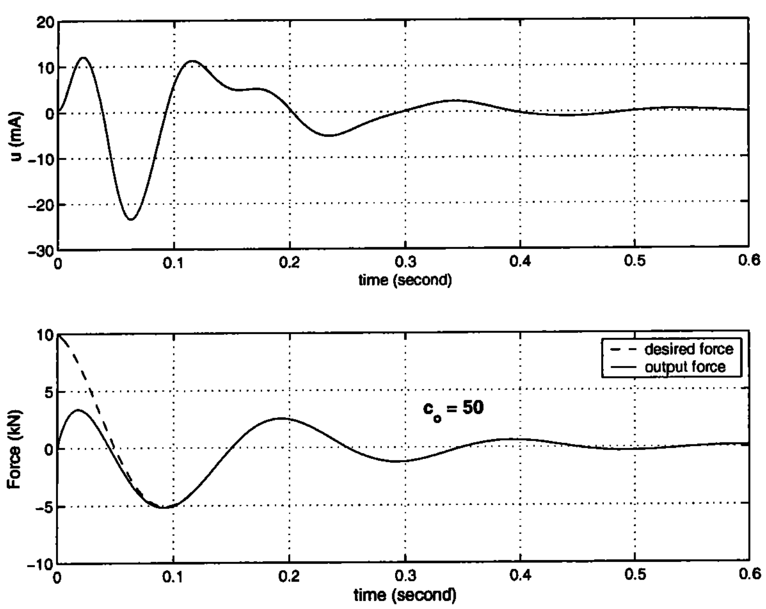

FIG. 3.4 – Force behaviour and needed control law. (tracking time-varying force)

3.3.2 Sliding mode control

In the previous section we have developed a feedback control law for the hydraulic system using input-output linearization method. Therein, we have assumed that the system model is perfectly known. However, in most cases parameters are known within a range of uncertainty. For instance, the spring k_l is used to model the environment stiffness, as a matter of fact the value of k_l cannot be exactly known. We can see in Figure 3.5 that the linearizing feedback control law fails to track the force in the presence of system uncertainties, namely Δk_l and Δm.

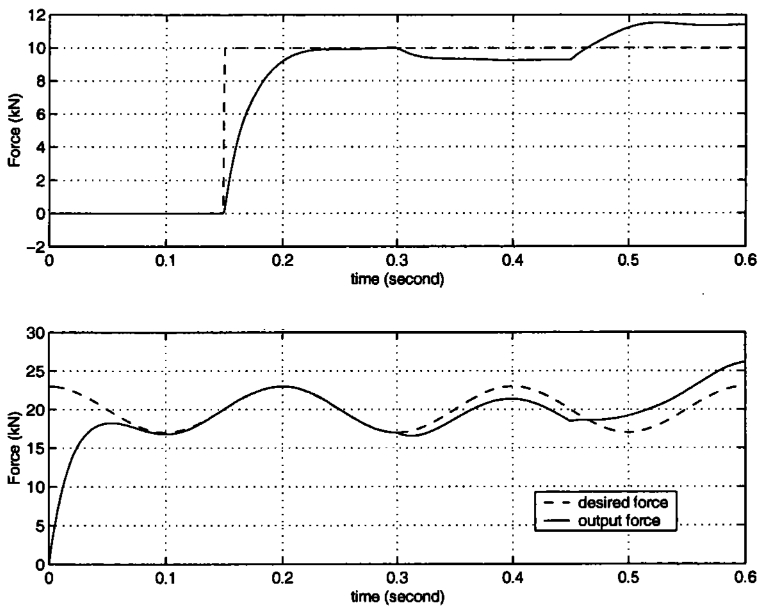

FIG. 3.5 – State behaviour of the system with linearizing feedback control, undergoing parameter uncertainties.

These simulation were carried with $\Delta k_l = +50000 N/m$ in the time interval $0.3 \leq t < 0.45$ and $\Delta k_l = -50000 N/m$ in the time interval $0.45 \leq t < 0.6$ and $\Delta m = 10 kg$ that is with an uncertainty of $\pm 40\%$ and $+50\%$ on the parameters. In general applications, it is normally preferable to obtain the desired output despite of parameter uncertainties. One reliable way to design a robust control is the sliding mode method. Next we develop a new simple way to design sliding surfaces for a rather general class of dynamic systems. Then we design the feedback control law needed for the output tracking.

Constructing discontinuity surface

We consider the following nonlinear dynamical system :

$$\dot{x} = f(x) + g(x)u, \quad x \in \mathbb{R}^n, \quad u \in \mathbb{R} . \tag{3.43}$$

Where f and g are smooth vector fields, and u is an input to the system. Suppose that there exists a stabilizing feedback $\gamma(x)$ such that the autonomous system

$$\dot{x} = f(x) + g(x).\gamma(x) \ , \tag{3.44}$$

is uniformly asymptotically stable. According to Theorem 3.4 , there exist a $\mathcal{C}^\infty$ Lyapunov function $V(x)$ and functions $\alpha_i \in \mathcal{K}$ $(i = 1, 2, 3)$ such that

(i) $\alpha_1(\|x\|) \leq V(x) \leq \alpha_2(\|x\|)$
(ii) $\dot{V}(x) \leq -\alpha_3(\|x\|)$
(iii) $\sup\limits_{x}\left\|\frac{\partial V(x)}{\partial x}\right\| < \infty$

Now if we choose a nonlinear sliding surface of the form,

$$\sigma(x) = L_g V(x) = 0 \ , \tag{3.45}$$

then the following equality :

$$\dot{V}(x) = L_f V(x) + L_g V(x).\gamma(x) = L_f V(x) \leq -\alpha_3(\|x\|) \tag{3.46}$$

holds on the sliding surface $\sigma(x) = 0$.

Remark 3.1 *We can say that on the sliding surface the autonomous system $\dot{x} = f(x)$ is asymptotically stable, and admits $V(x)$ as a Lyapunov function. Furthermore, (3.46) implies that any uncertainties in the system parameters that are used to calculate the feedback law $\gamma(x)$ will not affect the behaviour of the system (3.44) if the states are restricted to the sliding surface.*

In order to restrict the states to the sliding surface we should choose a feedback control that leads to the attractivity of the surface, necessary condition to which is $\sigma\dot{\sigma} < 0$. One way, is to choose

$$\dot{\sigma} = -W\text{sign}(\sigma), \quad W > 0 \ , \tag{3.47}$$

so that $\sigma\dot{\sigma} = -W|\sigma| < 0$. Knowing that

$$\dot{\sigma} = \frac{\partial \sigma}{\partial x} f(x) + \frac{\partial \sigma}{\partial x} g(x).u \ , \tag{3.48}$$

and combining with (3.47) we get

$$u(x) = \frac{-\frac{\partial \sigma}{\partial x} f(x) - W sign(\sigma)}{\frac{\partial \sigma}{\partial x} g(x)} \ . \tag{3.49}$$

Applying this type of feedback control, the states will be attracted to the surface $\sigma(x) = 0$, then they will slide along $\sigma(x) = 0$ to the equilibrium point.

Remark 3.2 *Note that the system is controlled to restrict the states behaviour to the sliding surface. Once the states are confined to the sliding surface, the system is not controlled but the trajectories only slide to the equilibrium point. This inherently means that the equilibrium point should belong to the sliding surface.*

Output tracking using sliding mode

We consider now the system (3.43) with the following output

$$y = h(x) \ , \tag{3.50}$$

We want $y(t)$ to equal a desired output value $y_d(t)$. To this aim we consider the coordinate transformation $z = \Phi(x)$ transforming (3.43) into (3.23), we recall

$$\begin{aligned} \dot{\xi} &= A\xi + B\Big(b(\xi,\eta) + a(\xi,\eta)u\Big) \\ \dot{\eta} &= q(\xi,\eta) \\ y &= C\xi \end{aligned}$$

which we can write in general as

$$\dot{z} = f_L(z) + g_L(z).u \ . \tag{3.51}$$

It has been shown in previous sections that a stabilizing control law exists for this type of systems which results in a closed-loop system of the form

$$\dot{e} = A_c e \tag{3.52a}$$

$$\dot{\eta} = q(e + \xi_d, \eta) \tag{3.52b}$$

If we assume that (3.51) is minimum-phase and we take into account the following theorem

Theorem 3.11 *(Seibert and Suarez [65]) we consider system (3.53).*

$$\dot{x}_1 = g_1(x_1) \ , \tag{3.53a}$$

$$\dot{x}_2 = g_2(x_1, x_2) \ , \tag{3.53b}$$

Under the assumption that g_1 and g_2 are Lipschitz, if $x_1 = 0$ is asymptotically stable (AS) for (3.53a) and $x_2 = 0$ is AS for $\dot{x}_2 = g_2(0, x_2)$ then $(x_1, x_2) = (0,0)$ is AS for (3.53). □

Then it is sufficient to stabilize the subsystem defined by (3.52a), in order to stabilize (3.52). Since (3.52a) is a linear system, it is easy to find a Lyapunov function $V_L(z)$ corresponding to it. Next we construct a sliding surface

$$\sigma_L = L_{g_L} V_L(z) \ .$$

Hence using (3.49) we obtain an expression for the feedback control law

$$u(z) = \frac{-\frac{\partial \sigma_L}{\partial z} f_L(z) - W sign(\sigma_L)}{\frac{\partial \sigma_L}{\partial z} g_L(z)} . \tag{3.54}$$

$u(z)$ will force (3.51) trajectories to slide on the surface σ_L until they reach equilibrium, and since the equilibrium point of (3.52a) is its origin, then at steady state we obviously get $e = 0 \Leftrightarrow y(t) = y_d(t)$. Furthermore, since by assumption that system (3.51) is minimum-phase, then by Theorem 3.11 the overall system is asymptotically stable.

Robust force tracking using the hydraulic manipulator

We consider system

$$\begin{aligned}
\dot{x}_1 &= \frac{4B}{V_t}\left(ku\sqrt{\frac{P_s - P_r - \text{sign}(u)x_1}{2}} - \alpha x_1 - Sx_2\right) \\
\dot{x}_2 &= \frac{1}{m_t}(Sx_1 - bx_2 - k_l x_3) \\
\dot{x}_3 &= x_2
\end{aligned}$$

from the previous section we have seen that it can be transformed into

$$\begin{aligned}
\dot{z}_1 &= L_f h(\Phi^{-1}(z)) + L_g h(\Phi^{-1}(z))u && (3.55a) \\
\dot{z}_2 &= \frac{1}{m}(z_1 - bz_2 - k_l z_3) && (3.55b) \\
\dot{z}_3 &= z_2 && (3.55c)
\end{aligned}$$

and there exists a feedback control law such that the closed-loop system is

$$\begin{aligned}
\dot{e}_1 &= -c_o e_1 \\
\dot{z}_2 &= \frac{1}{m}(e_1 + F_d - bz_2 - k_l z_3) \\
\dot{z}_3 &= z_2
\end{aligned}$$

where $e_1 = z_1 - F_d$. A Lyapunov function for the first equation is trivially found $V_L(e_1) = \frac{1}{2}e_1^2$ and leads to :

$$\begin{aligned}
\sigma_L(z) &= L_{g_L} V_L(e_1) \\
&= e_1\, g_L(z) \\
&= e_1\, a(\xi, \eta)
\end{aligned}$$

but

$$a(\xi, \eta) = L_g h(\Phi^{-1}(z))$$

thus

$$\sigma_L(z) = e_1 \; L_g h\big(\Phi^{-1}(z)\big)$$

Moreover, $L_g h(x)$ is always positive for the practical values of pressures, therefore

$$\sigma_L(z) = 0 \Leftrightarrow e_1 = 0 \; .$$

Whence, we can simply take

$$\begin{aligned} \sigma_L &= e_1 \\ \sigma_L &= z_1 - F_d \\ \sigma_L &= h(x) - F_d \\ \sigma_L &= F - F_d = 0 \end{aligned} \tag{3.56}$$

as a sliding surface. Now, using (3.56) and (3.55) we obtain the following equalities

$$\frac{\partial \sigma}{\partial z} f_L(z) = L_f h(x) \; , \quad \frac{\partial \sigma}{\partial t} = 0 \; , \quad \frac{\partial \sigma}{\partial z} g_L(z) = L_g h(x) \; . \tag{3.57}$$

Thus using (3.54) we have

$$u(x) = \frac{-L_f h(x) - W \mathrm{sign}(F - F_d)}{L_g h(x)} \; . \tag{3.58}$$

Figures 3.6 and 3.7 show the state behaviour of the system and the resultant output, when applying the control law (3.58) to track a constant force. Figures 3.8 and 3.9 show the state behaviour of the system and the resultant output, when applying the control law (3.58) to track a time-varying force. It is clear that the output obtained from applying a sliding mode control is exactly equal to the desired output for all different uncertainties. We recall $\Delta k_l = +50000 N/m$ in the time interval $0.3 \le t < 0.45$ and $\Delta k_l = -50000 N/m$ in the time interval $0.45 \le t < 0.6$ and $\Delta m = 10 kg$ that is with an uncertainty of $\pm 40\%$ and $+50\%$ on the parameters.

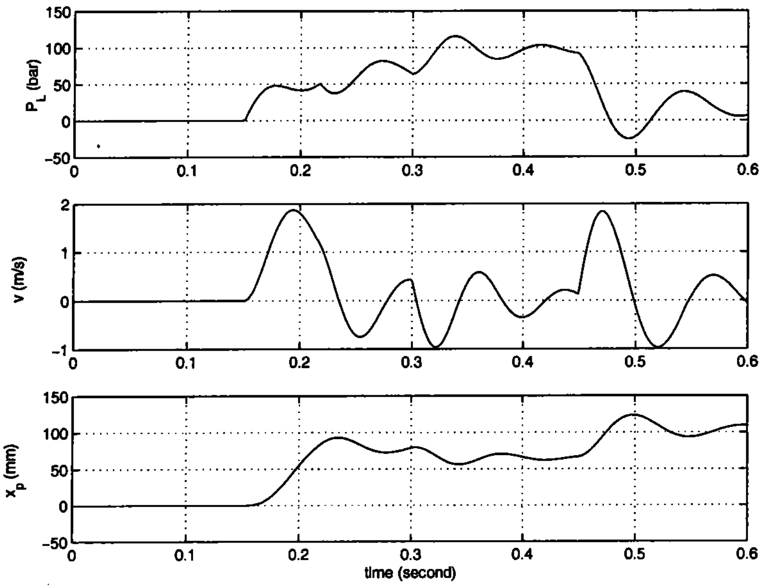

FIG. 3.6 – State behaviour of the system. (tracking constant force)

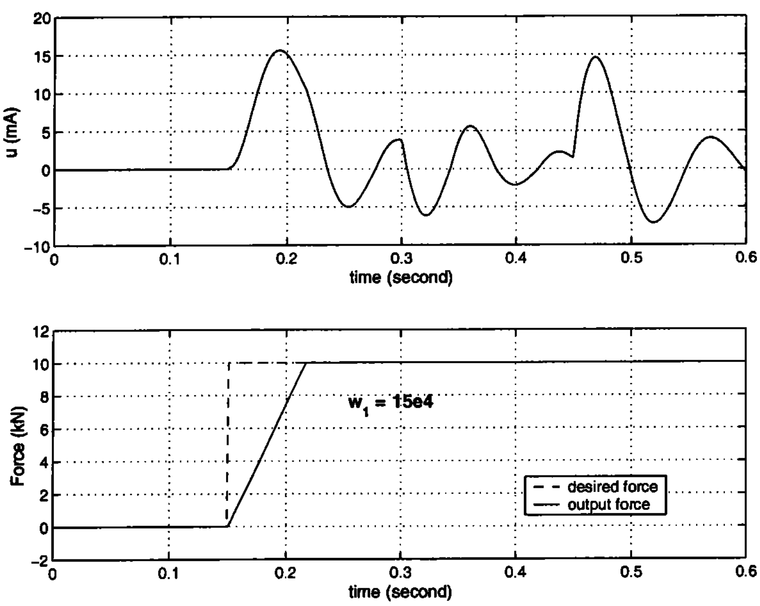

FIG. 3.7 – Force behaviour and needed control law. (tracking constant force)

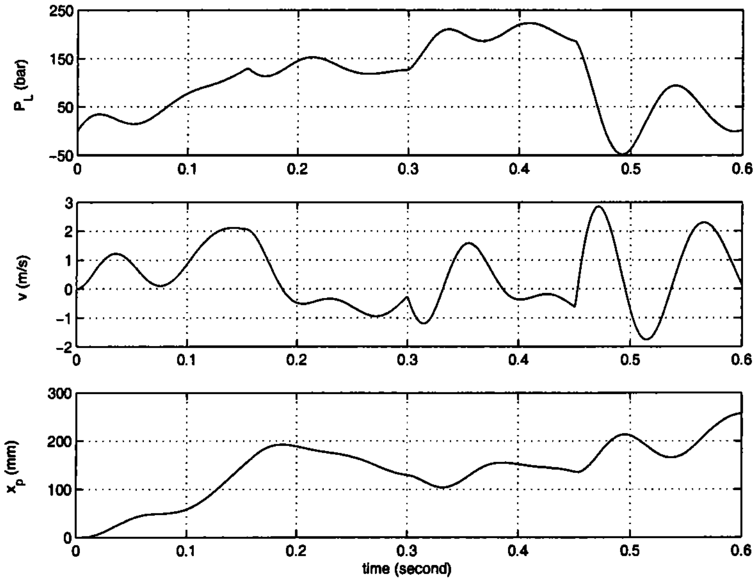

FIG. 3.8 – State behaviour of the system. (tracking time-varying force)

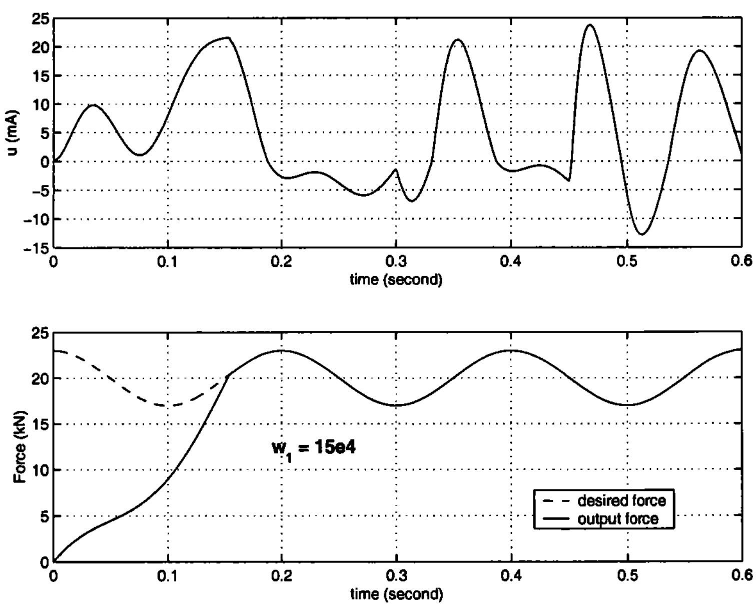

FIG. 3.9 – Force behaviour and needed control law. (tracking time-varying force)

3.3.3 Feedback stabilization using passive approach

Using the results developed by Wei Lin in [43], we consider the hydraulic manipulator model described by

$$\begin{aligned}
\dot{x}_1 &= \frac{4B}{V_t}\Big(ku\sqrt{\frac{P_s - P_r - \mathrm{sign}(u)x_1}{2}} - \frac{\alpha}{1+\gamma|u|}x_1 - Sx_2\Big) \\
\dot{x}_2 &= \frac{1}{m_t}(Sx_1 - bx_2 - k_l x_3) \\
\dot{x}_3 &= x_2
\end{aligned}$$

This model can be written in the form

$$\dot{x} = f(x,u) = f(x,0) + g(x,u)u$$

where

$$f(x,0) = f_0(x) = \begin{pmatrix} \frac{4B}{V_t}(-\alpha x_1 - Sx_2) \\ \frac{1}{m_t}(Sx_1 - bx_2 - k_l x_3) \\ x_2 \end{pmatrix}$$

$$g(x,u) = \begin{pmatrix} \frac{4B}{V_t}\Big(k\sqrt{\frac{P_s-P_r-\mathrm{sign}(u)x_1}{2}} + \alpha\gamma\frac{\mathrm{sign}(u)}{1+\gamma|u|}x_1\Big) \\ 0 \\ 0 \end{pmatrix}.$$

As a Lyapunov function to the autonomous system $\dot{x} = f_0(x)$ we suggest

$$V(x) = \frac{1}{2P_s}\Big(\frac{V_t}{4B}x_1^2 + m_t x_2^2 + k_l x_3^2\Big)$$

taking the derivative of $V(x)$ with respect to time, along the trajectories of the autonomous system $\dot{x} = f_0(x)$ yields

$$\begin{aligned}
\dot{V}(x) &= \frac{\partial V(x)}{\partial x} f_0(x) \\
&= \frac{1}{P_s}\Big(\frac{V_t}{4B}x_1\dot{x}_1 + m_t x_2\dot{x}_2 + k_l x_3\dot{x}_3\Big) \\
&= \frac{1}{P_s}(-\alpha x_1^2 - Sx_2x_1 + Sx_1x_2 - bx_2^2 - k_l x_2 x_3 + k_l x_3 x_2) \\
&= -\frac{1}{P_s}(\alpha x_1^2 + bx_2^2)
\end{aligned}$$

Let us define two sets S_2 and Ω_2 by

$$S_2 = \Big\{x \in U \subseteq \mathbb{R}^n : L_{f_0}^k L_\varrho V(x) = 0\ , \forall \varrho = ad_{f_0}^k g(x,0)\ ; k = 0,1,2,\dots\Big\}$$

$$\Omega_2 = \left\{ x \in U \subseteq \mathbb{R}^n : L_{f_0}^k V(x) = 0 \,, k = 1, 2, \dots \right\}$$

We can verify that

$$L_{f_0} V(x) = \frac{\partial V(x)}{\partial x} f_0(x) = -\frac{1}{P_s}(\alpha x_1^2 + b x_2^2)$$

is zero for all $x \in \Omega_{21}$

$$\Omega_{21} = \{ x \in U \subseteq \mathbb{R}^n : x_1 = 0 \; x_2 = 0 \}$$

And also

$$\begin{aligned} L_{f_0}^2 V(x) &= \frac{\partial L_{f_0} V(x)}{\partial x_1} \frac{4B}{V_t}(-\alpha x_1 - S x_2) + \frac{\partial L_{f_0} V(x)}{\partial x_2} \frac{1}{m_t}(S x_1 - b x_2 - k_l x_3) \\ &= \frac{2}{P_s} \alpha x_1 \frac{4B}{V_t}(\alpha x_1 + S x_2) - \frac{2}{P_s} b x_2 \frac{1}{m_t}(S x_1 - b x_2 - k_l x_3) \\ &= \frac{1}{P_s}\left(\frac{8B\alpha^2}{V_t} x_1^2 + \left(\frac{8BS\alpha}{V_t} - \frac{2bS}{m_t} \right) x_1 x_2 + \frac{2b^2}{m_t} x_2^2 + \frac{2bk_l}{m_t} x_2 x_3 \right) \end{aligned}$$

is equal to zero for all $x \in \Omega_{21}$. Next, we verify that

$$\begin{aligned} \frac{\partial L_{f_0}^2 V(x)}{\partial x_1} &= \frac{1}{P_s}\left(\frac{16B\alpha^2}{V_t} x_1 + \left(\frac{8BS\alpha}{V_t} - \frac{2bS}{m_t} \right) x_2 \right) \\ \frac{\partial L_{f_0}^2 V(x)}{\partial x_2} &= \frac{1}{P_s}\left(\left(\frac{8BS\alpha}{V_t} - \frac{2bS}{m_t} \right) x_1 + \frac{4b^2}{m_t} x_2 + \frac{2bk_l}{m_t} x_3 \right) \\ \frac{\partial L_{f_0}^2 V(x)}{\partial x_3} &= \frac{1}{P_s} \frac{2bk_l}{m_t} x_2 \end{aligned}$$

thus we have

$$\begin{aligned} L_{f_0}^3 V(x) &= \frac{\partial L_{f_0}^2 V(x)}{\partial x_1} \frac{4B}{V_t}(-\alpha x_1 - S x_2) + \frac{\partial L_{f_0}^2 V(x)}{\partial x_2} \frac{1}{m_t}(S x_1 - b x_2 - k_l x_3) \\ &\quad + \frac{\partial L_{f_0}^2 V(x)}{\partial x_3} x_2 \end{aligned}$$

$$L_{f_0}^3 V(x) = x^T \mathbf{M} x \tag{3.59}$$

where

$$\mathbf{M} = \begin{bmatrix} \frac{8BS^2\alpha}{P_s V_t m_t} - \frac{2bS^2}{P_s m_t^2} - \frac{64B^2\alpha^3}{P_s V_t^2} & 0 & 0 \\ -6\frac{S(16\alpha^2 B^2 m_t^2 - b^2 V_t^2)}{P_s V_t^2 m_t^2} & -\frac{8BS}{P_s V_t}\left(\frac{4BS\alpha}{V_t} - \frac{bS}{m_t} \right) - \frac{2b}{P_s m_t}\left(\frac{2b^2}{m_t} - k_l \right) & 0 \\ \frac{4Sbk_l}{P_s m_t^2} - \frac{8B\alpha}{P_s V_t m_t} & -6\frac{b^2 k_l}{P_s m_t^2} & -2\frac{bk_l^2}{P_s m_t^2} \end{bmatrix}$$

since $\mathbf{M}$ is a nonsingular matrix, then $L^3_{f_0}V(x) = 0$ requires $x = 0$. Therefore $\Omega_2 = \{0\}$, hence $\Omega_2 \cap S_2 = \{0\}$, thus according to Theorem 3.9 we can construct a stabilizing feedback control law having the following expression

$$\begin{aligned} u(x) &= -L_{g(x,u)}V(x) \\ u(x) &= -\frac{x_1}{P_s}\left(k\sqrt{\frac{P_s - P_r - \text{sign}(u)x_1}{2}} + \text{sign}(u)\gamma\frac{\alpha}{1+\gamma|u|}x_1\right) \end{aligned}$$

We can check that $u(0) = 0$. However, when $x \neq 0$ we need to distinguish two cases according to the sign of $u(x)$. Before going any further we can also expect, from application viewpoint, that $u(x)$ should be positive if x_1(*i.e.* P_L) is negative and vice versa. Splitting the expression of $u(x)$ into two cases yields :

case 1 : $u \geq 0$

$$\begin{aligned} u &= -\left(k\frac{x_1}{P_s}\sqrt{\frac{P_s - P_r - x_1}{2}}\right) - \left(\frac{\gamma}{P_s}\frac{\alpha}{1+\gamma u}x_1^2\right) \\ (1+\gamma u)u &= -(1+\gamma u)\left(k\frac{x_1}{P_s}\sqrt{\frac{P_s - P_r - x_1}{2}}\right) - \frac{\gamma}{P_s}\alpha x_1^2 \end{aligned}$$

$$\gamma u^2 + \left(1 + \gamma k\frac{x_1}{P_s}\sqrt{\frac{P_s - P_r - x_1}{2}}\right)u + k\frac{x_1}{P_s}\sqrt{\frac{P_s - P_r - x_1}{2}} + \frac{\gamma}{P_s}\alpha x_1^2 = 0$$

the largest of the two solutions of the above equation is

$$u(x) = \frac{-\left(1 + \gamma k\frac{x_1}{P_s}\sqrt{\frac{P_s - P_r - x_1}{2}}\right) + \sqrt{\left(1 - \gamma k\frac{x_1}{P_s}\sqrt{\frac{P_s - P_r - x_1}{2}}\right)^2 - 4\frac{\gamma^2}{P_s}\alpha x_1^2}}{2\gamma}$$

We can see that for $x_1 \leq 0$, we have $u(x) \geq 0$ as expected.

case 2 : $u < 0$

$$\begin{aligned} u &= -\left(k\frac{x_1}{P_s}\sqrt{\frac{P_s - P_r + x_1}{2}}\right) + \left(\frac{\gamma}{P_s}\frac{\alpha}{1-\gamma u}x_1^2\right) \\ (1-\gamma u)u &= -(1-\gamma u)\left(k\frac{x_1}{P_s}\sqrt{\frac{P_s - P_r + x_1}{2}}\right) + \frac{\gamma}{P_s}\alpha x_1^2 \end{aligned}$$

$$\gamma u^2 - \left(1 - \gamma k\frac{x_1}{P_s}\sqrt{\frac{P_s - P_r + x_1}{2}}\right)u - k\frac{x_1}{P_s}\sqrt{\frac{P_s - P_r + x_1}{2}} + \frac{\gamma}{P_s}\alpha x_1^2 = 0$$

the smallest of the two solutions of the above equation is

$$u(x) = \frac{\left(1 - \gamma k \frac{x_1}{P_s}\sqrt{\frac{P_s - P_r + x_1}{2}}\right) - \sqrt{\left(1 + \gamma k \frac{x_1}{P_s}\sqrt{\frac{P_s - P_r + x_1}{2}}\right)^2 - 4\frac{\gamma^2}{P_s}\alpha x_1^2}}{2\gamma}$$

Similarly, we can check that $u(x) \leq 0$ for positive values of x_1.

Figure 3.10 shows the plot of $u(x)$ versus x_1 corresponding to both cases. The results of the application of such feedback control law to the hydraulic manipulator is given in Figure 3.11. It is shown that the system is stabilized to the origin.

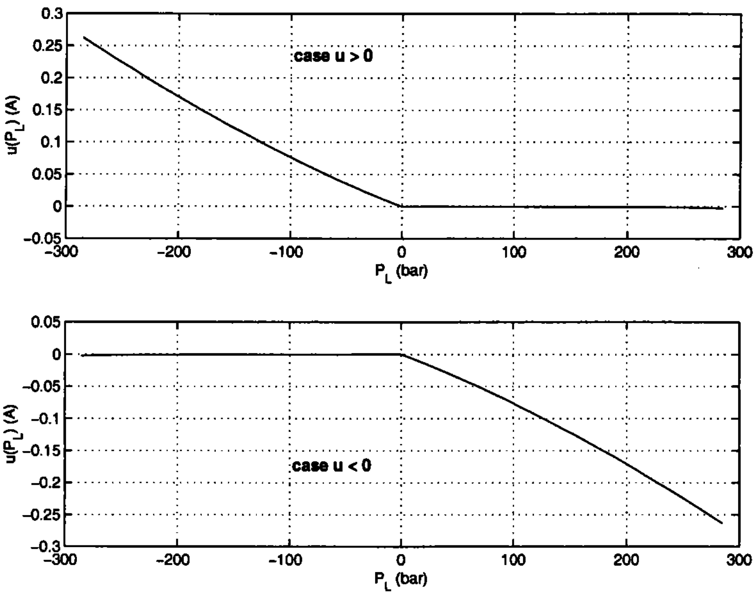

FIG. 3.10 – $u(x)$ versus x_1.

3.4 Summary

In this chapter we have presented different stabilization methods applied to the nonlinear dynamic systems. We have then applied these methods to the hydraulic manipulator with the aim of output tracking. More specifically, we wanted the output force resulting from the interaction of the hydraulic manipulator with the environment to follow a prescribed reference force. Our contribution is resumed in presenting a simple way to choose sliding surfaces that lead to robust stabilization.

The application of the input-output linearization method as well as the sliding mode method were to a modified model of the hydraulic manipulator, which in fact does not

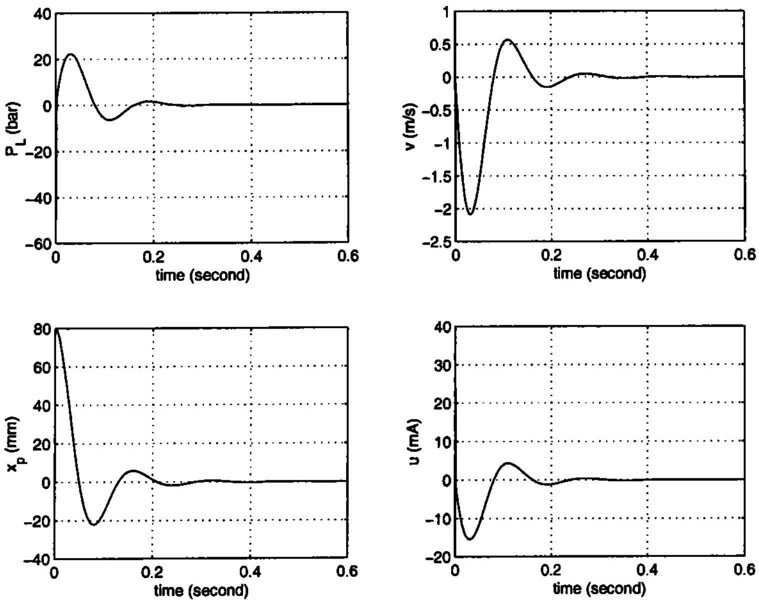

FIG. 3.11 – State behaviour and needed control law.

reflect the correct leakage flow. Recently, we have thought of including the dynamics of the spool namely

$$\dot{x}_s = -\frac{2k_s}{b_s}x_s + \frac{K_{fc}}{b_s}u \,.$$

in the model. Certainly this will increase the complexity of the model, and rise the number of state variables from three to four. However, by substituting u in the first equation of the model by its corresponding value as a function of x_s (see chapter 2 section 4), we obtain a four dimensional nonlinear system which is affine in the control. Stabilization of this type of model is being studied.

On the other hand, in the application of the passive approach we have only considered stabilization to the origin and did not simulate output tracking. This is because we could not find an obvious Lyapunov function to the system, if the pressure state variable was substituted by the force as a state variable. Further research is also being done in this direction.

Chapitre 4

Nonlinear observers design : state-of-the-art

Since the emergence of state space methods in control strategies, research has shown that state feedback gives more degrees of freedom to the designer than the output feedback can do. This is clearly evident, since the output is merely an algebraic combination of the state variables and possibly the independent time variable. A common feature of this control scheme is the premise that the system state vector is available for the feedback control purposes.

While in some cases this can be achieved by direct measurements, in general either the additional complexity required to perform a reliable measurement or the very nature of this system becomes a hindrance to such approach. Therefore, the fact that the states availability assumption is not satisfied necessitate either a radical revision of the state space method, at the loss of its favorable properties, or the reconstruction of the missing state variables.

Adopting the latter approach, the state reconstruction problem is founded on the design of a new auxiliary system called "state observer" or "state estimator" which gives an estimate of the true states using only the direct measurable variables of the system, namely the output and the input.

Once designed, an observer will not be solely used for the control objectives [6] [11] [35] [53] but besides one can use the observer states for monitoring hard-to-measure variables of the system, system diagnostics [1] and fault detection [33] [37] [16].

Although the theory of observer design for linear systems is a well developed field thanks to Luenberger [46] [47] see also [40] [56], its counterpart for nonlinear systems is still a very active domain, and challenging many researchers. Almost all of the existing theory in this field is based on hypotheses that should be satisfied by the nonlinear system in question, hence, to our knowledge, there is no general expression for observing general nonlinear systems.

A first systematic contribution to the theory of observers of nonlinear systems was offered by Thau [76]. This method is based on considering an observable linear system where to its dynamics was added a Lipschitzian nonlinear function. Therefore, a Luenberger-like observer is designed and sufficient conditions for asymptotic stability of the error dynamics can be derived. This method was then extended by Tsinias [80] and Ciccarella *et. al.* [12].

Later on Krener, Isidori and Respondek [92] [30] have considered the linearization method using output injection and nonlinear change of coordinates, thus a Luenberger-like observer can be constructed for such systems. Zeitz has also developed observer for nonlinear systems in this sense [92].

A nice contribution to the observation of a class of nonlinear systems affine in the control, the so-called bilinear systems was presented by Williamson [90]. This work was next improved by Sallet *et. al.* [10].

A different approach based on high-gain approximate cancellation of the nonlinearity has been introduced by Tornambè [79], and was thereafter improved by J.P. Gauthier *et. al.* [32] [30]. Another different type of observers has been introduced by Utkin [83] for the class of linear systems. This was extended by Slotine *et. al.* [67] and Edwards and Spurgeon [15] to the case of nonlinear systems. Sliding observers are based on the theory of variable structure systems, and were known for their robustness especially in the presence of unknown inputs.

Another kind of observers that can be used in the case of nonlinear systems with unknown parameters is the adaptive observer presented by Marino and Tomei [51] [50]. They consider systems that can be transformed to a certain canonical form. Adaptive observers help to identify the unknown parameters simultaneously with the system states.

In this chapter we will give some brief study of some of the foregoing observers, a kind of bibliographic basis before introducing our own contribution to the theory of nonlinear observer design.

4.1 Observability and observer notions

Let Σ denotes an arbitrary complete time-invariant system with outputs, having a state space $\mathcal{X}$ and input value space $\mathcal{U}$. An observer $\hat{\Sigma}$ for Σ is an auxiliary system that produces an estimate of the current state of Σ based on past observations. At any instant, the inputs to $\hat{\Sigma}$ are the current inputs and outputs of Σ, and the estimates are obtained as a function of its state which are supposed to be accessible by construction.

Definition 4.1 *(Sontag [71]) An observer for Σ consists of a system $\hat{\Sigma}$ having state space $\mathcal{Z}$ and input value space $\mathcal{U} \times \mathcal{Y}$ together with a map*

$$\Phi : \mathcal{Z} \times \mathcal{U} \times \mathcal{Y} \to \mathcal{X}$$

so that the following property holds : For each $x_0 \in \mathcal{X}$, each $z_0 \in \mathcal{Z}$ and $u \in \mathcal{U}^+$, ($\mathcal{U}^+$ is the set of controls $u(t) = 0$ if $t < 0$), we let $x(t, x_0, u(t))$ (hereafter denoted by $x(t)$) be the path resulting from initial state x_0 and control $u(t)$, for all $t \geq 0$, and we let $y(t) = h(x(t))$ the output of Σ, we also let $z(t, z_0, (u(t), y(t)))$ (hereafter denoted by $z(t)$) be the path resulting from initial state z_0 and control $(u(t), y(t))$ for the system $\hat{\Sigma}$, and finally we write

$$\hat{x}(t) = \Phi(z(t), u(t), y(t)).$$

Then it is required that, for every x_0, z_0 and every $u(t)$,

$$d(x(t), \hat{x}(t)) \to 0 \quad as \quad t \to \infty$$

(global convergence of estimate) as well as that for each $\epsilon > 0$ there be some $\delta > 0$ so that for every x_0, z_0, $u(t)$

$$d(x_0, \Phi(z_0)) < \delta \quad \Rightarrow \quad d(x(t), \hat{x}(t)) < \epsilon \quad for\ all\ t \geq 0.$$

(close initial estimate results in small future errors) $\square$

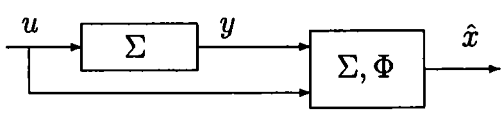

FIG. 4.1 – General observer scheme

That is, given a dynamical system described by

$$\dot{x} = f(x, y) \tag{4.1a}$$
$$y = h(x) \tag{4.1b}$$

where $x \in \mathbb{R}^n$, $u \in \mathbb{R}^m$, $y \in \mathbb{R}^p$ and $f : \mathbb{R}^n \times \mathbb{R}^m \to \mathbb{R}^n$ is a smooth vector field. An observer can be written as

$$\dot{z} = \hat{f}(z, u, y) \tag{4.2a}$$
$$\hat{x} = \Phi(z, u, y) \tag{4.2b}$$

where $z \in \mathbb{R}^q$, $\hat{x} \in \mathbb{R}^n$, $\hat{f} : \mathbb{R}^q \times \mathbb{R}^m \times \mathbb{R}^p \to \mathbb{R}^q$ and $\Phi : \mathbb{R}^q \times \mathbb{R}^m \times \mathbb{R}^p \to \mathbb{R}^n$ are smooth vector fields, and $q \geq n$. In general $\hat{f}$ and Φ are determined using a *priori* knowledge about the system vector field f. In this case, with $\dim(\hat{x}) = \dim(x)$ the observer is said to be full-order. If $\dim(\hat{x}) < \dim(x)$ the observer is said to be reduced-order.

Before constructing an observer, an important question rises : Under which conditions is the construction of an observer possible ? Several definitions that we will state here are prerequisite to answer this question.

Definition 4.2 *(Vidyasagar [85]) Consider system (4.1). Two states x_0 and x_1 are said to be* ***distinguishable*** *if there exists an input function $u(.)$ such that $y(., x_0, u) \neq y(., x_1, u)$ where $y(., x_i, u)$ $i = 1, 2$ is the output function of system (4.1) corresponding to the input function $u(.)$ and the initial condition $x(0) = x_i$.* □

Definition 4.3 *System (4.1) is said to be* ***locally observable*** *at $x_0 \in \mathbb{R}^n$ if there exists a neighborhood $\mathcal{X}$ of x_0 such that every $x \in \mathcal{X}$ other than x_0 is distinguishable from x_0. Finally, the system is said to be locally observable if it is locally observable at each $x_0 \in \mathbb{R}^n$. If the neighborhood extends to all the state space then we have* ***global observability****.* □

Note that two states may be indistinguishable for some set of inputs, but the existence of at least on distinguishing input is enough to guarantee local observability.

4.1.1 Observers for linear systems

In the case of linear systems, the analysis is simple since the notions of local and global observability are the same. Furthermore, if a linear system is observable for an input function, so it is for any input function.

Let's consider the linear time invariant system described by

$$\dot{x} = Ax + Bu \;, \tag{4.3a}$$
$$y = Cx \;, \tag{4.3b}$$

where $A \in \mathbb{R}^{n \times n}$, $B \in \mathbb{R}^{n \times m}$ and $C \in \mathbb{R}^{p \times n}$

Theorem 4.1 *For the system (4.3) the following are equivalent,* *(i) The pair (C, A) is observable (*i.e. *(4.3) is observable).*

(ii) The following rank condition is satisfied

$$rank \begin{pmatrix} C \\ CA \\ \vdots \\ CA^{n-1} \end{pmatrix} = n.$$

(iii) For any polynomial $p(\lambda) = \lambda^n + a_1\lambda^{n-1} + \ldots + a_{n-1}\lambda + a_n$ $a_i \in \mathbb{R}$; $i = 1, 2, \ldots, n$, there exists a constant matrix $L \in \mathbb{R}^{n\times p}$ such that $det\big(\lambda I - A + LC\big) = p(\lambda)$. □

proof : See [40].

From the theorem we can immediately notice that the observability of the system does not depend on the input u. Indeed, a full-order observer for the linear system defined by (4.3) has the generic form

$$\dot{\hat{x}} = \hat{A}\hat{x} + \hat{B}u + Ly \; .$$

the observer design consists in choosing the appropriate matrices $\hat{A}$, $\hat{B}$ and L so that $\hat{x}$ converges to x. To determine these matrices, let

$$e = x - \hat{x} \; ,$$

be the estimation error, then

$$\begin{aligned} e &= Ax + Bu - \hat{A}(x - e) - \hat{B}u - LCx \; , \\ &= \hat{A}e + \big(-\hat{A} + A - LC\big)x + (B - \hat{B})u \; . \end{aligned}$$

Should we choose

$$\hat{A} = A - LC \; , \quad \hat{B} = B \; ,$$

then the error is independent of the state x and input u

$$\dot{e} = \hat{A}e$$

and it converges to zero if $\hat{A}$ is Hurwitz stable. Since A, B and C are defined by the plant, then the only design parameter is L. Therefor the observer can be written as

$$\dot{\hat{x}} = A\hat{x} + Bu + L(y - C\hat{x}) \; , \tag{4.4a}$$

$$\hat{y} = C\hat{x} \; . \tag{4.4b}$$

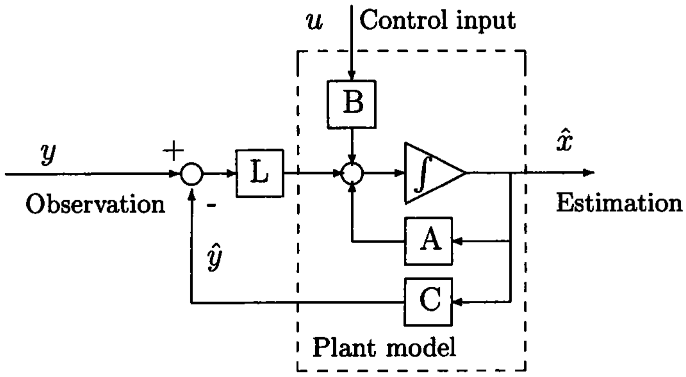

FIG. 4.2 – Full-order observer for linear systems

4.1.2 Generalization to nonlinear systems

The concept of an observer carries over to nonlinear systems. However, for a nonlinear system, the structure of the observer is not nearly as obvious as it is for a linear system. In fact, the notion of observability for nonlinear systems is rather subtle. First, the distinguishability of any two states depends, in general, on the input function. There may exist some input function that yields the same output function for two different initial states although they might be distinguishable. Another important peculiarity is that in general, observability may only be satisfied locally see [91] [36]

An observer for a plant described by the following dynamical system

$$\dot{x} = f(x,u) , \tag{4.5a}$$
$$y = h(x) , \tag{4.5b}$$

can be obtained by simply imitating the procedure used in the linear case, namely to construct a model of the original system and force it with the output error feedback. The equation of the observer thus becomes

$$\dot{\hat{x}} = f(\hat{x},u) + \eta\Big(y - g(\hat{x},u)\Big) ,$$

where $\eta(.)$ is a suitably chosen function.

Analogous to the observability matrix rank condition in the linear case, we can express the $(n-1)$ time derivatives of the output as

$$h(x),\ L_f h(x),\ L_f^2 h(x), \ldots, L_f^{n-1} h(x)$$

and then define an observability matrix $\mathcal{O}(x)$ as

$$\mathcal{O}(x) \stackrel{def}{=} \frac{d}{dx}\begin{bmatrix} h(x) \\ L_f h(x) \\ \vdots \\ L_f^{n-1}h(x) \end{bmatrix} = \frac{d\Phi}{dx}$$

Theorem 4.2 *(Vidyasagar [85])* ***Sufficient condition for local observability*** *Consider the system (4.5) and let $x_0 \in \mathbb{R}^n$ be given. If $\mathcal{O}(x_0)$ has rank n, then the system is locally observable at x_0.* □

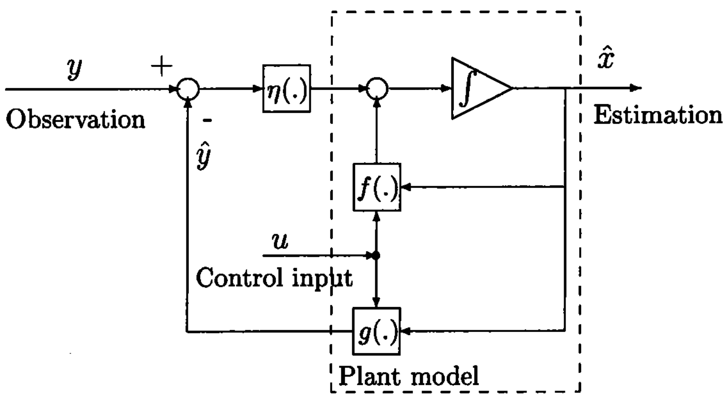

FIG. 4.3 – Structure of nonlinear observer.

4.2 Linearization method

The class of nonlinear systems considered are of the form :

$$\dot{x} = Ax + f(x,u) , \tag{4.6a}$$
$$y = Cx , \tag{4.6b}$$

If the condition *rank* $\mathcal{O}(x_0) = n$ is satisfied, then the system is locally observable at x_0. Moreover this condition is also sufficient for the existence of a local nonlinear diffeomorphic coordinate transformation $z = T(x)$, such that, in the new coordinates the autonomous system

$$\begin{aligned} \dot{x} &= f(x) , \\ y &= h(x) \end{aligned}$$

can be written in the following form

$$\begin{aligned} \dot{z} &= Az + \varphi(z) , \\ y &= Cz , \end{aligned}$$

$$A = \begin{pmatrix} 0 & 1 & 0 & \dots & 0 \\ 0 & 0 & 1 & \dots & 0 \\ \vdots & \vdots & \vdots & \ddots & \vdots \\ 0 & 0 & 0 & \dots & 1 \\ 0 & 0 & 0 & \dots & 0 \end{pmatrix}, \varphi(z) = \begin{pmatrix} 0 \\ 0 \\ \vdots \\ 0 \\ \varphi_n(z) \end{pmatrix} .$$

Clearly (C, A) observable pair. If we can find a local coordinate transformation such that further we have $\varphi(z) = g(y)$ then obviously the auxiliary system

$$\begin{aligned} \dot{\hat{z}} &= A\hat{z} + g(y) + L(y - \hat{y}) \ , \\ \hat{y} &= C\hat{z} \ , \end{aligned}$$

with L properly chosen, is an exponential observer for the autonomous system. For an in-depth discussion about this so called observer linearization problem see [38][32][30].

If for some complexity reasons the coordinate transformation $z = T(x)$ cannot be determined, another analysis can be done if we assume that $f(.,.)$ is smooth vector field satisfying the following Lipschitz condition

$$\|f(x, u) - f(\hat{x}, u)\| \leq \gamma_1 \|x - \hat{x}\| \ .$$

The observer will be assumed to be of the form (Thau [76])

$$\dot{\hat{x}} = A\hat{x} + f(\hat{x}, u) + L(y - C\hat{x}) \tag{4.7}$$

The estimation error dynamics are then seen to be given by

$$\dot{e} = (A - LC)e + \Big(f(x, u) - f(\hat{x}, u)\Big) \ , \quad \text{where} \ \ e = x - \hat{x}. \tag{4.8}$$

Theorem 4.3 *(Thau [76]) If a gain matrix L can be chosen such that*

$$\gamma_1 < \frac{\lambda_{\min}(Q)}{2\lambda_{\max}(P)} \ , \tag{4.9}$$

where Q and P are constant positive definite matrices satisfying the Lyapunov function

$$(A - LC)^T P + P(A - LC) = -Q \ , \tag{4.10}$$

then (4.7) yields to asymptotically stable estimates for (4.6). □

Actually, a sufficient condition for (4.9) to hold is to assume the pair (C, A) is observable, hence we can choose a gain matrix L such that $A_c = A - LC$ is a stable matrix. Then for a symmetric and positive definite matrix Q, there exists a symmetric and positive definite matrix P such that (4.10) is satisfied. To check the stability of (4.8) we use the

Lyapunov function $V = e^T Pe$. We note that for any symmetric positive definite matrix P, the following holds for all vector ν of appropriate dimension

$$\lambda_{\min}(P)\|\nu\|^2 \le \nu^T P\nu \le \lambda_{\max}(P)\|\nu\|^2 \, . \tag{4.11}$$

By taking the time derivative of V along the trajectories of (4.8), we have

$$\begin{aligned}
\dot V &= e^T P\dot e + \dot e^T Pe \\
&= e^T(A_c^T P + PA_c)e + 2e^T P\Big(f(x,u) - f(\hat x,u)\Big) \\
&\le -e^T Qe + 2\|P\|.\|f(x,u) - f(\hat x,u)\|.\|e\| \\
&\le -e^T Qe + 2\gamma_1\lambda_{\max}(P)\|e\|^2 \\
&\le -\Big(\lambda_{\min}(Q) - 2\gamma_1\lambda_{\max}(P)\Big)\|e\|^2 \\
&\le -\left(\frac{\lambda_{\min}(Q)}{2\lambda_{\max}(P)} - \gamma_1\right)2V \, .
\end{aligned}$$

Hence we can have an exponentially decaying bound on the Lyapunov function.

$$V(t) \le V(0)\exp(-2\alpha t)$$

where $\alpha = \frac{\lambda_{\min}(Q)}{2\lambda_{\max}(P)} - \gamma_1$. Using (4.11) we have

$$\|e(t)\|^2 \le \frac{V(t)}{\lambda_{\min}(P)} \le \frac{V(0)\exp(-2\alpha t)}{\lambda_{\min}(P)} \le \frac{\lambda_{\max}(P)}{\lambda_{\min}(P)}\exp(-2\alpha t)\|e(0)\|^2 \, ,$$

equivalently

$$\|e(t)\| \le \sqrt{\frac{\lambda_{\max}(P)}{\lambda_{\min}(P)}}\exp(-\alpha t)\|e(0)\| \, .$$

Whence the error system is exponentially stable if (4.9) is satisfied. Therefore, the observer states converge exponentially fast to the system states.

Remark 4.1 *We shall note here that the matrices P and Q are determined by the choice of the gain matrix L in the observer, and that L is the only degree of freedom in this design approach. We shall also add that it has been shown in [60] that the ratio in (4.9) is maximized when $Q = I$.*

There is an alternative way to see the same result. Let's first state the following lemma [41]

Lemma 4.1 ***(Bellman-Gronwall)*** *Let $\sigma(.)$, $\phi(.)$ and $k(.)$ be real valued piecewise continuous functions on $\mathbb{R}^+$. If $\sigma(.)$ satisfies*

$$\sigma(t) \le \phi(t) + \int_0^t k(\tau)\sigma(\tau)d\tau \, , \quad \forall\, t \ge 0$$

then,

$$\sigma(t) \leq \phi(t) + \int_0^t \phi(\tau)k(\tau)\exp\Big(\int_\tau^t k(s)ds\Big)d\tau\ , \quad \forall\, t > 0\ .$$

□

Now we can express the solution of (4.8) as follows

$$e(t) = \exp(A_c t)e(0) + \int_0^t \exp\big(A_c(t-\tau)\big)\Big(f(x,u) - f(\hat{x},u)\Big)d\tau\ .$$

Since A_c is stable, the following holds for some $M > 0$ and $\alpha > 0$;

$$\|\exp(A_c t)\| \leq M\exp(-\alpha t)\ .$$

thus

$$\|e(t)\| \leq M\exp(-\alpha t)\|e(0)\| + \int_0^t M\exp(-\alpha(t-\tau))\|f(x,u) - f(\hat{x},u)\|d\tau\ .$$

using the Lipschitz condition

$$\|e(t)\exp(\alpha t)\| \leq M\|e(0)\| + \int_0^t M\gamma_1\|e(\tau)\exp(\alpha\tau)\|d\tau\ .$$

Finally, using Lemma 4.1 we obtain

$$\|e(t)\| \leq M\exp(-(\alpha - M\gamma_1)t)\|e(0)\|\ .$$

Therefore, if

$$\frac{\alpha}{M} > \gamma_1\ , \tag{4.12}$$

then the estimation error decays to zero exponentially fast.

Remark 4.2 *We should know that the ratio in (4.9) or in (4.12) cannot be increased abundantly by choosing L that produces eigenvalues with very negative real parts. Indeed, a peaking phenomenon occurs, then some states peak to very large values, before they rapidly decay to zero. Hence leading to a large value of M. Eventually, a trade-off should be used when choosing L to maximize the bounds in (4.9) or (4.12)*

From the previous remarks we conclude that the choice of the observer gain L is crucial to this observer design method. For that purpose Raghavan [61] developed a constructive technique to design such a gain.

Theorem 4.4 *Suppose there exits an $\epsilon > 0$ such that the following Algebraic Riccati Equation (ARE) has a symmetric, positive definite solution P,*

$$AP + PA^T + P\big(I - \frac{1}{\epsilon}C^TC\big)P + \gamma_1^2 I + \epsilon I = 0\ . \tag{4.13}$$

Then, the observer gain L given by

$$L = \frac{1}{2\epsilon} P C^T \tag{4.14}$$

stabilizes the error dynamics given in (4.8) for all nonlinearities f with Lipschitz constant γ_1. *Conversely if the error dynamics can be stabilized by some choice of L, then there exists an* $\epsilon > 0$ *such that the ARE admits a unique symmetric positive definite solution.* □

A solution for (4.13) can be obtained by initiating a positive ϵ then iterating till the solution converges. However, if the algorithm can converge for some observable pairs (C, A), it unfortunately fails for some other pairs. Moreover it does not give insights under what conditions of (C, A) the convergence is ensured.

4.3 High-gain observers

The high-gain observer approach based on "high-gain" approximate cancellation of the nonlinearities was presented by Tornambè [79]. It consists in finding a state diffeomorphism that can separate the system into two subsystems, one is linear with respect to the states and the second contains the system nonlinearities. The observer is then designed on the basis of the linear system, and under mild conditions, one can thereafter use a sufficiently large observer gain to overcome the system nonlinearities. Gauthier *et al.* [32] contribution to the theory of nonlinear high-gain observers is considered as one of the best performing in the last decade. Its simple structure makes it very appreciable in the application domain whenever the necessary hypotheses are satisfied.

In this section we briefly introduce the observer construction method presented in [32]. Consider the single-output autonomous system

$$\dot{x} = f(x) \,, \tag{4.15a}$$
$$y = h(x) \,. \tag{4.15b}$$

We assume that (4.15) is observable on a subset $\Omega \in \mathbb{R}^n$. It is easy to verify that under observability assumption the coordinate transformation $z = T(x)$

$$\begin{aligned} T(x) \ &: \mathbb{R}^n \to \mathbb{R}^n \\ &x \to \Big(h(x), L_f h(x), \ldots, L_f^{n-1} h(x)\Big)^T \end{aligned}$$

is almost everywhere regular.

Now if (4.15) satisfies the following assumption

$(\mathcal{H}1)$ $T(x)$ is a diffeomorphism from Ω onto $T(\Omega)$.

Then it can be written as

$$\dot{x} = \begin{bmatrix} \dot{x}_1 \\ \dot{x}_2 \\ \vdots \\ \dot{x}_{n-1} \\ \dot{x}_n \end{bmatrix} = \begin{bmatrix} x_2 \\ x_3 \\ \vdots \\ x_n \\ \varphi(x) \end{bmatrix} = F(x) \ , \quad y = x_1 \ . \tag{4.16}$$

If we also add the following hypotheses

$(\mathcal{H}2)$ φ can be extended from Ω to $\mathbb{R}^n$ by C^∞ function, globally Lipschitz on $\mathbb{R}^n$,

then we can give the following interesting definition

Definition 4.4 *When $(\mathcal{H}1)$ and $(\mathcal{H}2)$ hold we say that (4.15) is uniformly observable on Ω or (4.16) is uniformly observable on $\mathbb{R}^n$* □

Next we state the first result of [32] concerning the autonomous systems.

Theorem 4.5 *Consider the system*

$$\dot{\hat{x}} = F(\hat{x}) + S_\infty^{-1}C^T(y - C\hat{x}) \ , \quad \hat{x} \in \mathbb{R}^n \tag{4.17}$$

where $C = [1, 0, \ldots, 0]$ and S_∞ is the solution of

$$0 = -\theta S_\infty - A^T S_\infty - S_\infty A + C^T C \tag{4.18}$$

for θ large enough, with A the anti-shift matrix.

System (4.17) is an observer of (4.16) on $\mathbb{R}^n$ with

$$\|x(t) - \hat{x}(t)\| \leq K e^{-\frac{\theta t}{3}} \|x_0 - \hat{x}_0\|$$

□

Remark 4.3 *We notice that in fact the above observer is similar to the observer presented in the previous section if we consider $L = S_\infty^{-1}C^T$. However this constitute an intelligent way to find an observer gain for this particular type of nonlinear systems.*

To extend the following result to the controlled system, namely to the SISO system described on $\mathbb{R}^n$ by

$$\dot{x} = f(x) + g(x)u \ , \tag{4.19a}$$
$$y = h(x) \ , \tag{4.19b}$$

the following hypotheses should be added

($\mathcal{H}3$) the drift system

$$\begin{aligned} \dot{x} &= f(x) \\ y &= h(x) \end{aligned}$$

is uniformly observable in the sense of definition 4.4.

($\mathcal{H}4$) (4.19) is observable for any input [31] i.e. on any finite time interval $[0, T]$ for any measurable bounded input $u(t)$ defined on $[0, T]$ the initial state is uniquely determined on the basis of the output $y(t)$ and the input $u(t)$.

Definition 4.5 *When (4.19) satisfies ($\mathcal{H}3$) and ($\mathcal{H}4$) we say that (4.19) is uniformly observable for any input.* □

Following this definition a preliminary result was proved in [32].

Theorem 4.6 *(4.19) is uniformly observable for any input if and only if (4.19) is diffeomorphic to a system of the form*

$$\begin{aligned} x &= \begin{bmatrix} \dot{x}_1 \\ \dot{x}_2 \\ \vdots \\ \dot{x}_{n-1} \\ \dot{x}_n \end{bmatrix} = \begin{bmatrix} x_2 \\ x_3 \\ \vdots \\ x_n \\ \varphi(x) \end{bmatrix} + \begin{bmatrix} g_1(x_1) \\ g_2(x_1, x_2) \\ \vdots \\ g_{n-1}(x_1, \dots, x_{n-1}) \\ g_n(x_1, \dots, x_n) \end{bmatrix} u = F(x) + G(x)u \ , && \text{(4.20a)} \\ y &= x_1 = Cx \ . && \text{(4.20b)} \end{aligned}$$

□

($\mathcal{H}5$) let $\underline{x}_i$ stands for $(x_1, \dots, x_i)^T$ we require that each of the maps g_i in (4.20a) satisfy

$$\begin{aligned} g_i : \mathbb{R}^i &\to \mathbb{R} \\ \underline{x}_i &\to g_i(\underline{x}_i) \end{aligned}$$

is globally Lipschitz.

Theorem 4.7 *Assume that (4.20) is uniformly observable for any input and assume ($\mathcal{H}5$) is satisfied. Consider the system*

$$\dot{\hat{x}} = F(\hat{x}) + G(\hat{x})u + S_\infty^{-1} C^T (y - C\hat{x}) \ , \tag{4.21}$$

in which S_∞ is as defined by (4.18). Then for inputs u uniformly bounded by some $u_0 \geq 0$, the system described by (4.21) is an observer for (4.20) on $\mathbb{R}^n$ for θ large enough. And

$$\|x(t) - \hat{x}(t)\| \leq K(\theta) e^{-\frac{\theta t}{3}} \|x_0 - \hat{x}_0\|$$

□

Remark 4.4 *The most interesting result of the above theorems is that for any Lipschitz nonlinearity, no matter how large the Lipschitz constant is, as far as it is finite, we can find θ such that the observers, presented previously in this section, converge. It is also worth mentioning that this result follows from ($\mathcal{H}5$) which is very crucial to the proof of Theorem 4.7 see [32] for further details on the proof.*

The forgoing analysis essentially requires the existence of globally defined and globally lipschitzian change of coordinates. The difficulty to find such a map is considered as a drawback of the above approach. Hammami [35] has shown that the above observer design can be extended to nonlinear systems on $\mathbb{R}^n$ that can be transformed to the following form

$$\dot{x} = Ax + Bu + f(x,u) \quad ; \; u \in \mathbb{R}^m, \tag{4.22a}$$

$$y = Cx \quad ; \; y \in \mathbb{R}^p, \tag{4.22b}$$

where A, B and C are any constant matrices of appropriate dimensions and the nonlinear vector field $f = (f_1, f_2, \ldots, f_n)^T$ (T stands for the transpose) is Lipschitz and smooth, with $f(0,0) = 0$. This form is quite general and less restrictive than the form required by Gauthier *et. al.*, and in fact it is satisfied by several nonlinear systems and applications.

We next consider the following system

$$\dot{\hat{x}} = A\hat{x} + Bu + f(\hat{x},u) + S^{-1}C^T(y - C\hat{x}) \tag{4.23a}$$

$$0 = -\theta S - A^T S - SA + C^T C \tag{4.23b}$$

where θ is large enough so that a positive definite solution S can be obtained by solving (4.23b).

Proposition 4.1 *If the system defined by (4.23) satisfies the following hypotheses*

($\mathcal{H}1$) *there exists a positive constant γ_1 such that*

$$\|f(x,u) - f(\hat{x},u)\| \leq \gamma_1 \|x - \hat{x}\|$$

$\forall (x,\hat{x}) \in \mathbb{R}^{n \times n}$ *and* $\forall u \in \mathbb{R}^m$

($\mathcal{H}2$) *the pair (C, A) is observable*

($\mathcal{H}3$) *we can chose $\theta > 0$ such that*

$$\gamma_1 < \frac{\theta}{2} \frac{\lambda_{\min}(S)}{\lambda_{\max}(S)} \tag{4.24}$$

$\lambda_{\min}(.)$ and $\lambda_{\max}(.)$ denote the smallest and largest eigenvalues of the matrix $(.)$. Then the system defined by (4.23) is an observer for the system described by (4.22). □

Proof : If we express equation (4.23b) in the form of a Lyapunov equation

$$\Big(-A^T - \frac{\theta}{2}I\Big)S + S\Big(-\frac{\theta}{2}I - A\Big) = -C^TC$$

then the matrix $A_\theta = -\frac{\theta}{2}I - A$ is Hurwitz stable if

$$\theta > -2\ \min\{\mathcal{R}e(\lambda) | \lambda \in spec(A)\} \tag{4.25}$$

where $spec(A)$ is the spectrum of A. For that condition $S(\theta)$ is positive definite.

Let's define $e = x - \hat{x}$ and consider the system of errors

$$\dot{e} = (A - S^{-1}C^TC)e + f(x,u) - f(\hat{x},u)$$

together with the Lyapunov function $V(e) = e^TSe$

$$\dot{V}(e) = 2e^TSAe - 2e^TC^TCe + 2e^TS\Big(f(x,u) - f(\hat{x},u)\Big)$$

using equation (4.23b)

$$\begin{aligned}
\dot{V}(e) &= -\theta e^TSe - e^TC^TCe + 2e^TS\Big(f(x,u) - f(\hat{x},u)\Big) \\
&\le -\theta e^TSe + 2\gamma_1\lambda_{\max}(S)\|e\|^2 \\
&\le -\Big(\theta\ \lambda_{\min}(S) - 2\gamma_1\lambda_{\max}(S)\Big)\|e\|^2
\end{aligned}$$

hence if $(\mathcal{H}3)$ is satisfied then

$$\dot{V}(e) \le -\xi\|e\|^2$$

$$\text{with} \quad \xi = \theta\ \lambda_{\min}(S) - 2\gamma_1\lambda_{\max}(S) > 0$$

Therefore, the origin $e = 0$ is globally exponentially stable.

Remark 4.5 *Equation (4.24) represents an upper bound on the Lipschitz constant γ_1, but since S depends on θ this bound cannot be increased abundantly but there exists $\bar{\theta}$ for which it is maximized. Therefore, if the nonlinearity is very stiff that the $(\mathcal{H}3)$ cannot be satisfied for any θ, the observer will fail to converge if the system has to operate in the stiff region. In fact this was not the case for the previous observer where we can cover all finite Lipschitz constants. We can deduce that this is the trade off of the generalization.*

4.4 Sliding observers

Sliding mode technique has been the focus of a growing literature since the work done by Utkin [82]. Sliding surfaces have been first used for the development of feedback controllers [13] [68]. Next researchers have tried to exploit their excellent robustness and performance properties to design linear and nonlinear sliding observers [83] [14] [67] [7]. The fundamental difference between a sliding mode observer and other observer approaches is that in other approaches the observer reconstructs the original state vector asymptotically, however, in sliding mode approach a suitable discontinuous output injection is used to guarantee finite time convergence by a deliberate induction of an attractive hyperplane. Robustness, insensitivity properties and simplicity of design make sliding observers a powerful approach. Analysis and comparison of several types of observers can be found in [78] [87] showing that the sliding mode observer is a good approach from the point of view of robustness, ease of design and overall evaluation.

In here we will give a brief idea on nonlinear sliding observers. To begin with, let's consider the following illustrating example of the Van der Pol oscillator

$$\dot{x}_1 = x_2 \tag{4.26a}$$
$$\dot{x}_2 = -x_1 + (1 - x_1^2)x_2 \tag{4.26b}$$
$$y = x_1 \tag{4.26c}$$

We propose the following sliding observer

$$\dot{\hat{x}}_1 = \hat{x}_2 + w_1 \operatorname{sign}(\xi_1 - \hat{x}_1) \tag{4.27a}$$
$$\dot{\hat{x}}_2 = -\xi_1 + (1 - \xi_1^2)\xi_2 + w_2 \operatorname{sign}(\xi_2 - \hat{x}_2) \tag{4.27b}$$
$$\xi_1 = x_1 \tag{4.27c}$$
$$\xi_2 = \hat{x}_2 + w_1 \operatorname{sign}(\xi_1 - \hat{x}_1) \tag{4.27d}$$

where the outputs of the observer (estimations of x_1 and x_2) will be $\hat{x}_1$ and ξ_2. Now we need to choose the observer gain w_1 and w_2 so that $\hat{x}_1$ and ξ_2 converge in finite time to x_1 and x_2 respectively.

From (4.26) and (4.27) the reconstruction error ($e = x - \hat{x}$) dynamics are :

$$\dot{e}_1 = e_2 - w_1 \operatorname{sign}(e_1) \tag{4.28a}$$
$$\dot{e}_2 = (1 - \xi_1^2)(x_2 - \xi_2) - w_2 \operatorname{sign}(\xi_2 - \hat{x}_2) \tag{4.28b}$$

Choose the sliding surface $\sigma_1 \ : \ e_1 = 0$, a necessary condition for the attractivity of the sliding surface σ_1 is to have $e_1\dot{e}_1 < 0$ for this aim a suitable choice is to have

$$\dot{e}_1 = -\delta_1 \operatorname{sign}(e_1) \ , \quad \delta_1 > 0 \ . \tag{4.29}$$

This choice, not only does it guarantee attractivity, but also it leads to a finite reaching time t_r^1, *i.e.* the states of system (4.28) will be confined to the sliding surface $e_1 = 0$ for all $t > t_r^1$, where t_r^1 can be obtained by integrating (4.29)

$$e_1(t) = \begin{cases} -\delta_1 t + e_1(0) & \text{if } e_1(0) > 0 \text{ and } t < t_r^1 \\ \delta_1 t + e_1(0) & \text{if } e_1(0) < 0 \text{ and } t < t_r^1 \end{cases}$$

wherefrom, we can deduce that the sliding surface $e_1 = 0$ will be reached in time t_r^1

$$t_r^1 = \frac{|e_1(0)|}{\delta_1}$$

From (4.28a) and (4.29), we have

$$\begin{aligned} \dot{e}_1 &= -\delta_1 \operatorname{sign}(e_1) \\ e_2 - w_1 \operatorname{sign}(e_1) &= -\delta_1 \operatorname{sign}(e_1) \\ -\big(w_1 - e_2 \operatorname{sign}(e_1)\big) \operatorname{sign}(e_1) &= -\delta_1 \operatorname{sign}(e_1) \\ w_1 - e_2 \operatorname{sign}(e_1) &= \delta_1 \ . \end{aligned}$$

Condition $\delta_1 > 0$, implies that w_1 should be chosen such that

$$w_1 > |e_2|_{\max} \ , \tag{4.30}$$

with $|e_2|_{\max}$ is the maximum value of e_2 for all $t \in [0, \infty]$ and we will also use $|e_2|_{\max}^{t_r^1}$ to denote the maximum value of e_2 for all $t \in [0, t_r^1]$.

Now, if w_1 is chosen to satisfy (4.30), then we will have $e_1 = 0$ for all $t > t_r^1$, consequently $\hat{x}_1$ will converge to x_1 in finite time namely t_r^1.

Moreover, since e_1 is constant namely $e_1 = 0$ for all $t \geq t_r^1$ it follows that $\dot{e}_1 = 0$ for all $t \geq t_r^1$ which leads from (4.28a) to

$$\begin{aligned} 0 &= e_2 - w_1 \operatorname{sign}(e_1) \\ 0 &= x_2 - \hat{x}_2 - w_1 \operatorname{sign}(e_1) \\ x_2 &= \hat{x}_2 + w_1 \operatorname{sign}(e_1) \ . \end{aligned}$$

Therefore, using (4.27d), the observer output ξ_2 is equal to the state x_2 for all $t \geq t_r^1$.

Up to this point, it is clear that for a suitable choice of w_1 the observer (4.27) correctly reproduces the state vector of system (4.26). However, the existence of w_1 depends on the boundedness of $e_2(t)$.

In fact, if $e_2(t)$ does not diverge to infinity in finite time $t_{div} < t_r^1$, then since $\xi_2 = x_2$ for all $t > t_r^1$, (4.28b) becomes

$$\dot{e}_2 = -w_2 \operatorname{sign}(e_2) \ , \quad \forall\, t > t_r^1$$

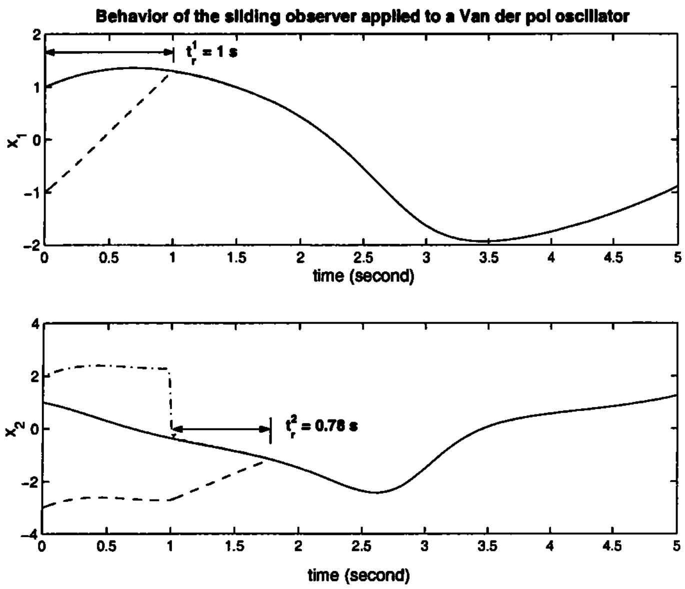

FIG. 4.4 – x(—), $\hat{x}$(- - -), ξ(-.-.-.) $x_1(0) = 1$, $x_2(0) = 1$, $\hat{x}_1(0) = -1$, $\hat{x}_2(0) = -3$ $w_1 = 5$ and $w_2 = 3$

which leads to $e_2 = 0$ in finite time t_r if $w_2 > 0$, particularly

$$t_r = t_r^1 + t_r^2$$

where t_r is the time when the manifold $e = 0$ is reached and t_r^2 denotes the time after which $\sigma_2 \ : e_2 = 0$ is reached, relative to reaching surface σ_1.

$$t_r^2 = \frac{|e_2(t_r^1)|}{w_2} \leq \frac{|e_2|_{\max}^{t_r^1}}{w_2} ,$$

it is then clear that t_r^2 is finite and as a result t_r is also finite. We can clearly see that ξ_2 converge at the same time as x_1 after $t_r^1 = 1s$, whereas x_2 converges later after $t_r = t_r^1 + t_r^2 = 1.78s$.

Let's now consider the general autonomous single output nonlinear system

$$\dot{x} = f(x) , \tag{4.31a}$$
$$y = h(x) . \tag{4.31b}$$

transformable into the system

$$\dot{x} = \begin{bmatrix} \dot{x}_1 \\ \dot{x}_2 \\ \vdots \\ \dot{x}_{n-1} \\ \dot{x}_n \end{bmatrix} = \begin{bmatrix} x_2 \\ x_3 \\ \vdots \\ x_n \\ \varphi(x) \end{bmatrix} = F(x) , \quad y = x_1 . \tag{4.32}$$

A sliding observer for this system is the following dynamical system

$$\begin{bmatrix} \dot{\hat{x}}_1 \\ \dot{\hat{x}}_2 \\ \vdots \\ \dot{\hat{x}}_{n-1} \\ \dot{\hat{x}}_n \end{bmatrix} = \begin{bmatrix} \hat{x}_2 \\ \hat{x}_3 \\ \vdots \\ \hat{x}_n \\ \varphi(\xi) \end{bmatrix} + \begin{bmatrix} w_1 \operatorname{sign}(\xi_1 - \hat{x}_1) \\ w_2 \operatorname{sign}(\xi_2 - \hat{x}_2) \\ \vdots \\ w_{n-1} \operatorname{sign}(\xi_{n-1} - \hat{x}_{n-1}) \\ w_n \operatorname{sign}(\xi_n - \hat{x}_n) \end{bmatrix} . \tag{4.33}$$

where

$$\xi_1 = x_1 = y \quad \text{and} \quad \xi_{i+1} = \hat{x}_{i+1} + w_i \operatorname{sign}(\xi_i - \hat{x}_i) \quad \text{for } i = 1, \ldots, n-1 \tag{4.34}$$

Defining $e_i = x_i - \hat{x}_i$ and subtracting (4.33) from (4.32) gives the dynamical reconstruction error system. Since $\xi_1 = x_1$ we have

$$\begin{bmatrix} \dot{e}_1 \\ \dot{e}_2 \\ \vdots \\ \dot{e}_{n-1} \\ \dot{e}_n \end{bmatrix} = \begin{bmatrix} e_2 \\ e_3 \\ \vdots \\ e_n \\ \varphi(x) - \varphi(\xi) \end{bmatrix} - \begin{bmatrix} w_1 \operatorname{sign}(e_1) \\ w_2 \operatorname{sign}(\xi_2 - \hat{x}_2) \\ \vdots \\ w_{n-1} \operatorname{sign}(\xi_{n-1} - \hat{x}_{n-1}) \\ w_n \operatorname{sign}(\xi_n - \hat{x}_n) \end{bmatrix} . \tag{4.35}$$

Choosing the sliding surface $\sigma_1 \ : \ e_1 = 0$, the ideal sliding mode occurs if there exist a finite time t_r^1 such that $e_1 = 0$ for all $t \geq t_r^1$, where t_r^1 is the time when the sliding surface $\sigma_1 \ : \ e_1 = 0$ is reached. The reaching condition of the sliding mode is $\dot{e}_1 e_1 < 0$, on the other hand

$$\begin{aligned} \dot{e}_1 e_1 &= e_1 e_2 - w_1 e_1 \operatorname{sign}(e_1) \\ &= |e_1|(e_2 \operatorname{sign}(e_1) - w_1) . \end{aligned}$$

Thus, a sufficient condition for the existence of the sliding modes is that

$$w_1 > |e_2|_{\max} .$$

Since at sliding mode $e_1 = 0$ for all $t \geq t_r^1$ then we also have $\dot{e}_1 = 0$ in fact this is also a necessary condition for sliding modes to occur. According to the equivalent control method, the system in sliding mode behaves as if $\operatorname{sign}(e_1)$ is replaced by its equivalent value $\operatorname{sign}(e_1)_{eq}$ which can be calculated using the first equation of (4.35) and using $\dot{e}_1 = 0$. This is yields to

$$\operatorname{sign}(e_1) = \frac{e_2}{w_1}$$

if we substitute this equality in (4.34) for $i = 1$ we obtain

$$\begin{aligned} \xi_2 &= \hat{x}_2 + w_1 \text{ sign}(\xi_1 - \hat{x}_1) \\ &= \hat{x}_2 + w_1 \text{ sign}(e_1) \\ &= \hat{x}_2 + e_2 \\ &= x_2 \ . \end{aligned}$$

Therefore ξ_2 is equal to x_2 after $t \geq t_r^1$ and we have

$$\dot{e}_2 = e_3 - w_2 \text{ sign}(e_2) \ , \quad \forall\, t > t_r^1$$

similarly if $w_2 > |e_3|_{\max}$ sliding mode occur on the surface $\sigma_2 \ : \ e_2 = 0$, then we can continue until we obtain sliding mode on the surface $\sigma_{n-1} \ : \ e_{n-1} = 0$. Using the $(n-1)^{th}$ equation of (4.35) and the fact that $\dot{e}_{n-1} = 0$ after sliding mode on σ_{n-1} has occurred, we get

$$x_n = \hat{x}_n + w_{n-1} \text{ sign}(\xi_{n-1} - \hat{x}_{n-1}) = \xi_n$$

thus the last equation in (4.35) together with $\xi_n = x_n$ results in

$$\dot{e}_n = -w_n \text{ sign}(e_n)$$

hence sliding mode occur on the sliding surface $\sigma_n \ : \ e_n = 0$ simply by choosing $w_n > 0$.

Interpreting the foregoing results, it was shown in [83] that for real-life system $\text{sign}(.)_{eq}$ is physically an average value of the chattering with high frequency variable sign(.). Thus for the design purpose the equivalent $\text{sign}(.)_{eq}$ can be obtained by low pass filtering the result of the sign function. Moreover, one can notice that the observer convergence is obtained on the basis of a step by step algorithm, where at each step one sliding surface is reached, that is one observer state converges to its corresponding system state in finite time. Therefore, we have

$$\begin{aligned} & \text{for each step } i \ , \quad i = 1, \ldots, n-1 \\ \dot{e}_i &\leq -\Big(w_i - |e_{i+1}|_{\max}\Big) \text{ sign}(e_i) \ , \quad w_0 = 1 \\ &\leq -\delta_i \text{ sign}(e_i) \ , \quad \delta_i > 0 \end{aligned}$$

From the last equation we can obtain

$$t_r^i = \frac{|e_i(t_r^{(i-1)})|}{\delta_i} \ , \ t_r^0 = 0 \quad i = 1, \ldots, n \ .$$

Therefore, the sliding manifold $e = 0$ $(x = \hat{x})$ is reached after time

$$t_r = \sum_{i=1}^{n} t_r^i$$

whereas the estimations ξ become equal to x after $t_r^\xi = t_r - t_r^n$.

We also note that this result is founded on the assumption that the error $e = x - \hat{x}$ is bounded, to allow the choice of the observer gain $w_i \;\; i = 1, \ldots, n-1$.

Generalization of this technique to the controlled systems is possible. However, in general the observation depends on the control. Nevertheless, one can consider a class of dynamical systems that can fit to many real systems.

Consider for instance the class of systems described by

$$\begin{bmatrix} \dot{x}_1 \\ \dot{x}_2 \\ \vdots \\ \dot{x}_{n-1} \\ \dot{x}_n \end{bmatrix} = \begin{bmatrix} x_2 \\ x_3 \\ \vdots \\ x_n \\ \varphi(x) \end{bmatrix} + \begin{bmatrix} g_1(x_1) \\ g_2(x_1, x_2) \\ \vdots \\ g_{n-1}(x_1, \ldots, x_{n-1}) \\ g_n(x_1, \ldots, x_n) \end{bmatrix} u = F(x) + G(x)u \;, \tag{4.36a}$$

$$y = x_1 = Cx \;. \tag{4.36b}$$

using the same technique as for the autonomous case, a sliding mode observer for this system can be

$$\begin{bmatrix} \dot{\hat{x}}_1 \\ \dot{\hat{x}}_2 \\ \vdots \\ \dot{\hat{x}}_{n-1} \\ \dot{\hat{x}}_n \end{bmatrix} = \begin{bmatrix} \hat{x}_2 \\ \hat{x}_3 \\ \vdots \\ \hat{x}_n \\ \varphi(\xi) \end{bmatrix} + \begin{bmatrix} g_1(\xi_1) \\ g_2(\xi_1, \xi_2) \\ \vdots \\ g_{n-1}(\xi_1, \ldots, \xi_{n-1}) \\ g_n(\xi_1, \ldots, \xi_n) \end{bmatrix} u + \begin{bmatrix} w_1 \operatorname{sign}(\xi_1 - \hat{x}_1) \\ w_2 \operatorname{sign}(\xi_2 - \hat{x}_2) \\ \vdots \\ w_{n-1} \operatorname{sign}(\xi_{n-1} - \hat{x}_{n-1}) \\ w_n \operatorname{sign}(\xi_n - \hat{x}_n) \end{bmatrix} , \tag{4.37}$$

where ξ_i is as described in (4.34).

4.5 Adaptive nonlinear observers

For the sake of completeness of this bibliographic study, we will give herein a brief idea on a kind of nonlinear adaptive observer design that was suggested by Hedrick [62], which is merely a generalization of the work done by Marino [49]. Adaptive observers help to identify the parameters simultaneously with the system states, a fact that made them widely used in many applications [62].

We consider the class of single-output nonlinear systems, that can be described by the following dynamics

$$\dot{x} = Ax + f(x, u) + b\Phi^T(x, u)\theta \;, \tag{4.38a}$$

$$y = Cx \;, \tag{4.38b}$$

where $x \in \mathbb{R}^n$, $u \in \mathbb{R}^m$, $y \in \mathbb{R}$, $b \in \mathbb{R}^n$, $\theta \in \mathbb{R}^s$ and $\Phi : \mathbb{R}^n \times \mathbb{R}^m \to \mathbb{R}^s$. We suppose that the following hypothesis are verified

($\mathcal{H}1$) There exists a positive symmetric matrix P such that

$$b^T P = \alpha\, C$$

for some real α.

($\mathcal{H}2$) f and ϕ are Lipschitz in x with Lipschitz constants γ_1 and γ_2 respectively, i.e. for all x, $\hat{x} \in \mathbb{R}^n$

$$\begin{aligned}\|f(x,u) - f(\hat{x},u)\| &\leq \gamma_2 \|x - \hat{x}\| \ , \\ \|\Phi(x,u) - \Phi(\hat{x},u)\| &\leq \gamma_1 \|x - \hat{x}\| \ .\end{aligned}$$

($\mathcal{H}3$) The vector of unknown parameters θ is bounded in the sense $\|\theta\|_2 \leq \gamma_3$

($\mathcal{H}4$) A gain matrix L can be chosen such that

$$\gamma_1 + \gamma_2\gamma_3\|b\| < \frac{\lambda_{\min}(Q)}{2\lambda_{\max}(P)}$$

where Q is a positive definite symmetric matrix satisfying the Lyapunov equation

$$(A - LC)^T P + P(A - LC) = -Q$$

Theorem 4.8 *Consider the system described by (4.38) satisfying ($\mathcal{H}1$) – ($\mathcal{H}4$), then the adaptive observer*

$$\begin{aligned}\dot{\hat{x}} &= A\hat{x} + f(\hat{x},u) + b\Phi^T(\hat{x},u)\hat{\theta} + L(y - C\hat{x}) \ , &\text{(4.39a)}\\ \dot{\hat{\theta}} &= \frac{1}{\mu}\Phi(\hat{x},u)(y - C\hat{x}) \ , \quad \mu > 0 &\text{(4.39b)}\end{aligned}$$

is stable, $e_x = x - \hat{x} \to 0$ *as* $t \to \infty$ *and* $\left(b\Phi^T(x,u)\theta - b\Phi^T(\hat{x},u)\hat{\theta}\right) \to 0$ *as* $t \to \infty$ □

Proof : Let $e_x = x - \hat{x}$ be the estimation error and $e_\theta = \theta - \hat{\theta}$ be the parameter error. The error dynamics are given by

$$\dot{e}_x = (A - LC)e_x + f(x,u) - f(\hat{x},u) + b\Phi^T(x,u)\theta - b\Phi^T(\hat{x},u)\hat{\theta} \ . \tag{4.40}$$

Consider the Lyapunov function candidate

$$V = e_x^T P e_x + \mu e_\theta^T e_\theta$$

with P chosen so as to satisfy $(\mathcal{H}1)$ and $(\mathcal{H}4)$.

$$\begin{aligned}
\dot{V} &= e_x^T\Big((A-LC)^TP + P(A-LC)\Big)e_x + 2e_x^TP\Big(f(x,u)-f(\hat{x},u)\Big) \\
&\quad +2\Big(b\Phi^T(x,u)\theta - b\Phi^T(\hat{x},u)\hat{\theta}\Big)^TPe_x + 2\mu e_\theta^T\dot{e}_\theta \\
\dot{V} &\leq -e_x^TQe_x + 2\gamma_1\lambda_{\max}(P)e_x^Te_x + 2\Big(b\Phi^T(x,u)\theta - b\Phi^T(\hat{x},u)\theta\Big)^TPe_x \\
&\quad +2\Big(b\Phi^T(\hat{x},u)e_\theta\Big)^TPe_x + 2\mu e_\theta^T\dot{e}_\theta \\
\dot{V} &\leq -e_x^TQe_x + 2\gamma_1\lambda_{\max}(P)e_x^Te_x + 2\|b\|\gamma_2\gamma_3\lambda_{\max}(P)e_x^Te_x \\
&\quad +2\Big(b\Phi^T(\hat{x},u)e_\theta\Big)^TPe_x + 2\mu e_\theta^T\dot{e}_\theta
\end{aligned}$$

Choose L such that

$$\gamma_1 + \|b\|\gamma_2\gamma_3 < \frac{\lambda_{\min}(Q)}{2\lambda_{\max}(P)}$$

so

$$\gamma_1 + \|b\|\gamma_2\gamma_3 - \frac{\lambda_{\min}(Q)}{2\lambda_{\max}(P)} = -M < 0\ .$$

Then

$$\dot{V} = -Me_x^Te_x + 2e_\theta^T\Big(\Phi(\hat{x},u)b^TPe_x + \mu\dot{e}_\theta\Big)$$

Choose $\dot{e}_\theta$ to annihilate the right most term in the above equation

$$\begin{aligned}
\dot{e}_\theta &= -\frac{1}{\mu}\Phi(\hat{x},u)b^TPe_x\ , \\
&= -\frac{\alpha}{\mu}\Phi(\hat{x},u)Ce_x\ , \\
&= -\frac{\alpha}{\mu}\Phi(\hat{x},u)(y-C\hat{x})\ .
\end{aligned}$$

Hence

$$\dot{V} \leq -Me_x^Te_x$$

and so the system is Lyapunov stable. this implies that $e_x \in L_\infty$ and $e_\theta \in L_\infty$.

Now, from the last result, we have

$$V(t) \leq V(0) - M\int_0^t e_x^Te_x dt.$$

Since $V(t) \in L_\infty$ and $V(0)$ is finite, this implies that $e_x \in L_2$. Also, from (4.40) we see that $\dot{e}_x \in L_\infty$. Thus from Barbalat's lemma [41], e_x converges to zero.

Next, we investigate the convergence of e_θ

$$\int_0^\infty \dot{e}_x\ dt = \lim_{t\to\infty} e_x(t) - e_x(0) = -e_x(0)$$

which is finite. Also, from (4.40) and using the Lipschitz continuity of f, $\dot{e}_x$ is uniformly continuous. Therefore, by Barbalat's lemma $\dot{e}_x \to \infty$, and with (4.40) this implies $\left(b\Phi^T(x,u)\theta - b\Phi^T(\hat{x},u)\hat{\theta}\right) \to 0$. This ends the proof.

Lemma 4.2 *(Barbalat's Lemma [41, page 186]) Let $f : \mathbb{R} \to \mathbb{R}$ be a uniformly continuous function on $[0, \infty)$. Suppose that*

$$\lim_{t\to\infty} \int_0^t f(\tau)d\tau$$

exists and is finite. Then

$$f(t) \to 0 \quad as \quad t \to \infty$$

□

4.6 Summary

In summary, let us see the advantages and the disadvantages of the stated observers.

The Linearization technique is very interesting due to its simplicity, whenever a linearizing diffeomorphism is easy to determine. However finding a non linear transformation that linearizes the system is not always evident, and this constitutes the main drawback of this method.

The observer suggested by Thau guarantees that the observer error is globally asymptotically convergent to zero. Yet, as we have explained in Remark 4.2 the necessary condition (4.9) cannot always be satisfied, for instance with systems having high Lipschitz constant.

This fact was remedied by the approach of the high-gain observers. Nevertheless, the observer suggested by Gauthier *et. al.* has a slightly restrictive structure, and many applications systems cannot satisfy the necessary hypotheses. We have also seen that an attempt to generalize that approach by Hammami leaded to fulling in the same problem as Thau's observer though the problem of determining the observer gain is solved. An interesting study will be a design of a high-gain observer for general nonlinear systems having as large as possible Lipshitz constant. This will be a part of our work presented in the next section.

The observer that shows high practical interest is the sliding observer, due to its robustness and finite time convergence. In the next chapter we will present a contribution to the theory of nonlinear sliding observer design, with application to electrohydraulic manipulators.

Chapitre 5

Nonlinear observer design : New approach

In this chapter we try to contribute to the theory of nonlinear observers. Our work is motivated by the need to estimate different states of the electrohydraulic manipulator model presented in chapter 2, a system that proved to defy some observers existing in literature. We start by modifying an observer available in [35]. The modification brought to this observer improves the speed of convergence of the observer, in addition it enlarges its domain of application as it can cover systems with stiffer nonlinearities. Next, we introduce a new simple type of observers, though it does not have a systematic design method, whenever the system in question helps in finding such observer, exponential or at least asymptotic convergence is reached. In the case of our application exponential stability was attained. Finally, we present a sliding observer for a class of nonlinear systems with unknown inputs. We show that in presence of bounded matched uncertainties, sliding observer still correctly estimates the systems states. This observer was applied to the electrohydraulic system, and showed advantages compared to the other observers.

5.1 High-gain nonlinear observer

5.1.1 Observer synthesis

We consider the nonlinear system described by the following equations on $\mathbb{R}^n$.

$$
\begin{aligned}
\dot{x} &= Ax + Bu + f(x,u) \qquad ; \ u \in \mathbb{R}^m, && (5.1a)\\
y &= Cx \qquad ; \ y \in \mathbb{R}^p, && (5.1b)
\end{aligned}
$$

where A, B and C are constant matrices of appropriate dimensions and the nonlinear vector field $f = (f_1, f_2, \dots, f_n)^T$ (T stands for the transpose) is Lipschitz and smooth, with $f(0,0) = 0$.

The high-gain observer presented by Hammami in [35], namely

$$\dot{\hat{x}} = A\hat{x} + Bu + f(\hat{x}, u) + S^{-1}C^T(y - C\hat{x}) \quad (5.2a)$$
$$0 = -\theta S - A^T S - SA + C^T C \quad (5.2b)$$

gives a bound on the Lipschitz constant which limits the domain of application of the observer. In this work, we try to bring a slight modification to increase the bound on the Lipschitz constant [24].

Then Let's consider the following system

$$\dot{\hat{x}} = A\hat{x} + Bu + f(\hat{x}, u) + \zeta S^{-1}C^T(y - C\hat{x}) \quad (5.3a)$$
$$0 = -\theta S - A^T S - SA + C^T C \quad (5.3b)$$

where θ is large enough, $\zeta \geq 1$

Remark 5.1 *The matrix $S(\theta)$ can be seen as the stationary solution of the differential equation*

$$\dot{S}_t(\theta) = -\theta S_t(\theta) - A^T S_t(\theta) - S_t(\theta)A + C^T C \ ,$$

with initial condition S_0 being positive definite. $S(\theta) = \lim_{t\to\infty} S_t(\theta)$, where $S_t(\theta) \in S^+$ the cone of symmetric positive definite matrices.

Theorem 5.1 *If the system defined by (5.1) satisfies the following hypotheses*

($\mathcal{H}1$) *there exists a positive constant γ_1 such that*

$$\|f(x,u) - f(\hat{x},u)\| \leq \gamma_1 \|x - \hat{x}\|$$

$\forall (x, \hat{x}) \in \mathbb{R}^{n\times n}$ *and* $\forall u \in \mathbb{R}^m$

($\mathcal{H}2$) *the pair (C, A) is observable*

($\mathcal{H}3$) *we can chose $\theta > 0$ and $\zeta \geq 1$ such that*

$$\gamma_1 < \frac{\lambda_{\min}(\theta S + (2\zeta - 1)C^T C)}{2\lambda_{\max}(S)} \quad (5.4)$$

$\lambda_{\min}(.)$ and $\lambda_{\max}(.)$ denote the smallest and largest eigenvalues of the matrix $(.)$.

Then the system defined by (5.3) is an observer for the system described by (5.1) with

$$\|x(t) - \hat{x}(t)\| \leq \sqrt{\frac{\lambda_{\max}(S)}{\lambda_{\min}(S)}} \exp(-\alpha_0 t)\|x(0) - \hat{x}(0)\| \ ,$$

where $\alpha_0 = \dfrac{\lambda_{\min}(\theta S + (2\zeta - 1)C^T C)}{2\lambda_{\max}(S)} - \gamma_1$. □

proof :
If we express equation (5.3b) in the form of a Lyapunov equation

$$(-A^T - \frac{\theta}{2}I)S + S(-\frac{\theta}{2}I - A) = -C^T C$$

then the matrix $A_\theta = -\frac{\theta}{2}I - A$ is Hurwitz stable if

$$\theta > -2 \ \min\{\mathcal{R}e(\lambda)|\lambda \in spec(A)\} \tag{5.5}$$

where $spec(A)$ is the spectrum of A. For that condition and using [85, page 201] $S(\theta)$ is positive definite.

Let's define $e = x - \hat{x}$ and consider the system of errors

$$\dot{e} = (A - \zeta S^{-1}C^T C)e + f(x,u) - f(\hat{x},u)$$

together with the Lyapunov function $V(e) = e^T S e$

$$\dot{V}(e) = 2e^T SAe - 2\zeta e^T C^T Ce + 2e^T S\Big(f(x,u) - f(\hat{x},u)\Big)$$

using equation (5.3b)

$$\begin{aligned}
\dot{V}(e) &= -\theta e^T Se - (2\zeta - 1)e^T C^T Ce + 2e^T S\Big(f(x,u) - f(\hat{x},u)\Big) \\
&\leq -e^T(\theta S + (2\zeta - 1)C^T C)e + 2\gamma_1\lambda_{\max}(S)\|e\|^2 \\
&\leq -\Big(\lambda_{\min}\big(\theta S + (2\zeta - 1)C^T C\big) - 2\gamma_1\lambda_{\max}(S)\Big)\|e\|^2 \\
&\leq -\left(\frac{\lambda_{\min}(\theta S + (2\zeta - 1)C^T C)}{2\lambda_{\max}(S)} - \gamma_1\right)2V(e)
\end{aligned}$$

hence if $(\mathcal{H}3)$ is satisfied then we can have an exponentially decaying bound on the Lyapunov function.

$$V(t) \leq V(0)\exp(-2\alpha_0 t)$$

where $\alpha_0 = \frac{\lambda_{\min}(\theta S + (2\zeta - 1)C^T C)}{2\lambda_{\max}(S)} - \gamma_1$. Using the following inequality

$$\lambda_{\min}(S)\|e\|^2 \leq e^T Se \leq \lambda_{\max}(S)\|e\|^2 \ ,$$

we have

$$\|e(t)\|^2 \leq \frac{V(t)}{\lambda_{\min}(S)} \leq \frac{V(0)\exp(-2\alpha_0 t)}{\lambda_{\min}(S)} \leq \frac{\lambda_{\max}(S)}{\lambda_{\min}(S)}\exp(-2\alpha_0 t)\|e(0)\|^2 \ ,$$

equivalently

$$\|e(t)\| \leq \sqrt{\frac{\lambda_{\max}(S)}{\lambda_{\min}(S)}}\exp(-\alpha_0 t)\|e(0)\| \ .$$

Therefore, the observer states converge exponentially fast to the system states. □

Remark 5.2 *In [35] the bound on the Lipschitz constant was* $\gamma_1 < \frac{\theta}{2}\frac{\lambda_{\min}(S)}{\lambda_{\max}(S)}$. *It is clear that the bound is larger here for* $\zeta > 1$. *Unfortunately, this bound cannot be increased abundantly but there exists* $\bar{\theta}$ *for which it is maximized, with the maximum reached asymptotically as* ζ *goes to infinity.*

Remark 5.3 *We can see from the proof of Theorem 5.1 that for the special cases where the nonlinear function* $f(x,u)$ *is decreasing with respect to the state* x *then there is* $\gamma_2 \in [0,\gamma_1]$ *such that*

$$f(x,u) - f(\hat{x},u) \leq -\gamma_2(x-\hat{x}) \ ,$$

and so the observer converges for any value of γ_1.

5.1.2 Application to the electrohydraulic manipulator

We recall the model of the electrohydraulic manipulator presented in the second chapter is given by the following system of differential equations

$$\begin{aligned} \dot{P}_L &= \frac{4B}{V_t}\left(ku\sqrt{\frac{P_s - P_r - sign(u)P_L}{2}} - \frac{\alpha}{1+\gamma|u|}P_L - Sv\right) \ , && (5.6a) \\ \dot{v} &= \frac{1}{m_t}\Big(SP_L - bv - k_l(x_p - x_{p0})\Big) \ , && (5.6b) \\ \dot{x}_p &= v \ . && (5.6c) \end{aligned}$$

where C_{il} is the internal leakage coefficient of the piston. Without loss of generality we will consider $x_{p0} = 0$. The parameter values are stated in Table 5.1.

If we use SI units, i.e. pressure in *pascal (Pa)*, displacement in *meter (m)*, and velocity in *meter per second (m/s)*, then we can note that the state variables have different ranges of operation that may lead to numerical instability. Therefore we will scale our variables as follows

$$x_1 = P_L/Ps \ ; \ x_2 = v/\bar{v} \ ; \ x_3 = x_p/l \ ; \ \bar{v} = 1m/s \ .$$

thus the above system can be expressed as follows

$$\begin{aligned} \dot{x} &= Ax + f(x,u) \ , \\ y &= Cx \ . \end{aligned}$$

where

$$A = \begin{bmatrix} 0 & -\frac{4BS}{P_sV_t} & 0 \\ \frac{SP_s}{m_t} & -\frac{b}{m_t} & -\frac{k_l l}{m_t} \\ 0 & \frac{1}{l} & 0 \end{bmatrix}$$

Parameter	value	unit
fluid		
B	2.2×10^9	Pa
P_s	300×10^5	Pa
P_r	1×10^5	Pa
piston		
m_0	50	kg
S	1.5×10^{-3}	m^2
V_t	1×10^{-3}	m^3
load		
m	20	kg
b	590	kg/s
k_l	125000	N/m
servovalve		
k	5.12×10^{-5}	$m^3s^{-1}A^{-1}Pa^{-1/2}$
α	4.1816×10^{-12}	$m^3s^{-1}Pa^{-1}$
γ	8571	s^{-1}

TAB. 5.1 – Numerical values used for simulations.

$$f(x,u) = \begin{pmatrix} \frac{4B}{P_sV_t}\left(ku\sqrt{\frac{P_s-P_r-sign(u)P_sx_1}{2}} - \frac{\alpha}{1+\gamma|u|}P_sx_1\right) \\ 0 \\ 0 \end{pmatrix}$$

Clearly, the nonlinearity

$$\mathcal{N}(x_1) = ku\sqrt{\frac{P_s - P_r - sign(u)P_sx_1}{2}} \tag{5.7}$$

is not globally Lipschitz. The results of the previous analysis are not directly applicable to this system. However, the input control $u(t)$ can be properly chosen so that the square root term is Lipschitz within the operating range. Indeed, the square root term is Lipschitz if x_1 is kept outside of a ball of radius $r > 0$ around $P_s - P_r$.

Under the foregoing constraints and if we use a sensor to measure the displacement that is having $y = x_3$ and $y = Cx$ means $C = [0 \ \ 0 \ \ 1]$. We can easily check that the pair (C, A) is observable. A sinusoidal exponentially decaying signal is used as an input control. The amplitude of the input is 10 mA, its frequency is 40 Hz and the damping coefficient is 10 s^{-1}. The maximum pressure difference attained with this input is about 230 bar. Hence, for these conditions the Lipschitz constant is 0.0087.

Remark 5.4 *The square root function in equation (5.6a) is usually substituted by a rather Lipschitz function to ease the numerical integration in hydraulic simulating softwares. Take for instance AMESim uses a* tanh(.) *a steep but Lipschitz function around the origin.*

$$\varphi(x) = \begin{cases} \tanh(50x) & x < 0.99 \\ \sqrt{|x|}sign(x) & x \geq 0.99 \end{cases}$$

In Figure 5.1 we have plotted the upper bounds on γ_1 across $\theta > 10$, in fact according to equation (5.5) $\theta_{\min} = 8.4515$. We see that for a proper choice of θ ($\theta = 400$ with $\zeta = 4$) we can have maximum upper bound for the Lipschitz constant γ_1. We can also observe the effect of the parameter ζ which raised the bound from 0.0128 to 0.0168. We can also check the convergence of the observer states in a very short time in Figure 5.2.

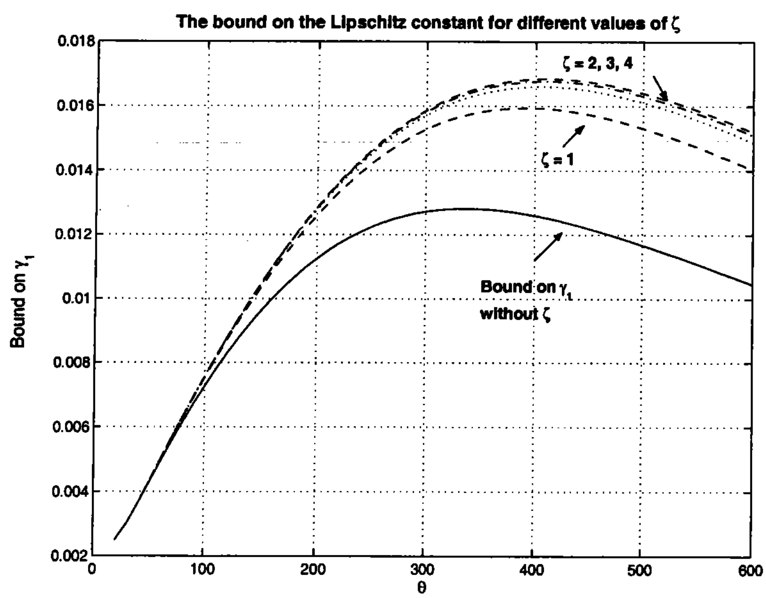

FIG. 5.1 – The upper bound on the Lipschitz constant with different design parameters.

5.2 Drive-response observer

The drive-response observer approach is strongly dependent on the system model. Nevertheless, it was verified that it can be applied to several real applications, we cite for instance our application to electrohydraulic systems [24][25].

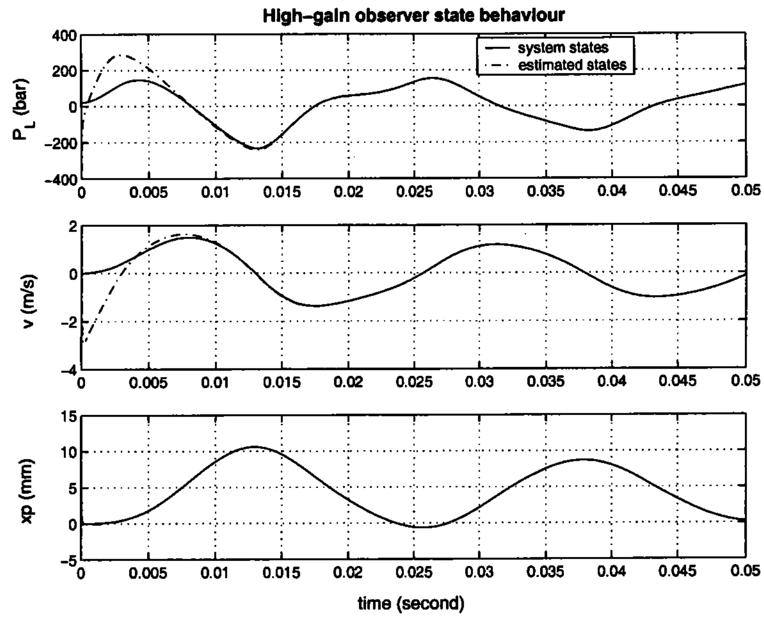

FIG. 5.2 – The observer states behaviour.

We consider systems on $\mathbb{R}^n$ of the form

$$\begin{aligned}\dot{x}_1 &= f_{11}(x_1, u) + f_{12}(x_2, u) , && (5.8a)\\ \dot{x}_2 &= f_2(x_1, x_2, u) , && (5.8b)\\ y &= x_2 . && (5.8c)\end{aligned}$$

where $x_1 \in \mathbb{R}^{n_1}$, $x_2 \in \mathbb{R}^{n_2}$, $u \in \mathbb{R}^p$, f_{11}, f_{12} and f_2 are smooth vector fields. A dynamic observer of (5.8), based on the drive-response concept and the error feedback is a control system

$$\begin{aligned}\dot{\hat{x}}_1 &= f_{11}(\hat{x}_1, u) + f_{12}(x_2, u) , && (5.9a)\\ \dot{\hat{x}}_2 &= f_2(\hat{x}_1, \hat{x}_2, u) + \eta(\hat{x}_1, \hat{x}_2)(x_2 - \hat{x}_2) , && (5.9b)\end{aligned}$$

that uses the input u and the output $y = x_2$ to perform the state determination of (5.8). It can be seen that equation (5.9a), is driven by x_2 to realize the state $\hat{x}_1$, and equation (5.9b) contains the error feedback term and performs the state $\hat{x}_2$. Let $e_1 = x_1 - \hat{x}_1$ and $e_2 = x_2 - \hat{x}_2$ so the error system is

$$\begin{aligned}\dot{e}_1 &= \tilde{f}_1(x_1, \hat{x}_1, u) && = f_{11}(x_1, u) - f_{11}(\hat{x}_1, u)\\ \dot{e}_2 &= \tilde{f}_2(x_1, \hat{x}_1, x_2, \hat{x}_2, u) && = f_2(x_1, x_2, u) - f_2(\hat{x}_1, \hat{x}_2, u) - \eta(\hat{x}_1, \hat{x}_2)(x_2 - \hat{x}_2)\end{aligned}$$

As a matter of fact, there is not much that can be done with the above equations when $\tilde{f}_1$ and $\tilde{f}_2$ are general functions. However, if we can express the error system in the following form

$$\dot{e}_1 = g_1(e_1) , \tag{5.10a}$$

$$\dot{e}_2 = g_2(e_1, e_2) , \tag{5.10b}$$

then under mild conditions and by proper choice of the driving signal x_2, the stability of the error system can be attained. Within the following theorems there are interesting results on the stability of system (5.10).

Theorem 5.2 *[65] we consider system (5.10). Under the assumption that g_1 and g_2 are Lipschitz, if $e_1 = 0$ is asymptotically stable (AS) for (5.10a) and $e_2 = 0$ is AS for $\dot{e}_2 = g_2(0, e_2)$ then $(e_1, e_2) = (0, 0)$ is AS for (5.10).* □

Furthermore, if we consider system (5.10), we notice that due to the smoothness property it is always possible to decompose $g_2(e_1, e_2)$ in the form

$$g_2(e_1, e_2) = g_2(0, e_2) + G(e_1, e_2).e_1$$

where a choice of the function G can be taken as

$$G(e_1, e_2) = \int_0^1 \frac{\partial g_2}{\partial e_1}(\tau e_1, e_2) d\tau.$$

Theorem 5.3 *Suppose that g_1, g_2 are globally Lipschitz functions, $e_1 = 0$ is globally exponentially stable (GES) for (5.10a), $e_2 = 0$ is GES for $\dot{e}_2 = g_2(0, e_2)$ and G satisfies*

$$||G(e_1, e_2)|| \leq \Gamma(||e_1||) , \quad \forall \ e_1, \ e_2$$

where Γ is a nondecreasing, strictly positive, scalar function, and bounded for all bounded e_1. Then $(e_1, e_2) = (0, 0)$ is GES for system (5.10). □

Proof :

Using the fact that, $\dot{e}_1 = g_1(e_1)$ and $\dot{e}_2 = g_2(0, e_2)$ are GES, there exist some Lyapunov functions V_1, V_2 such that :

$$V_1(e_1) > 0 , \ \forall \ e_1 \neq 0 , \ V_1(0) = 0 , \ \lim_{||e_1|| \to +\infty} V_1(e_1) = +\infty$$

$$V_2(e_2) > 0 , \ \forall \ e_2 \neq 0 , \ V_2(0) = 0 , \ \lim_{||e_2|| \to +\infty} V_2(e_2) = +\infty$$

and some positive constants a_i , $i = 1, \ldots, 4$; b_i , $i = 1, \ldots, 4$ such that for all e_1, V_1 satisfies

$$a_1 ||e_1||^2 \leq V_1(e_1) \leq a_2 ||e_1||^2$$
$$||\nabla V_1(e_1)|| \leq a_3 ||e_1||$$
$$\nabla V_1(e_1).g_1(e_1) \leq -a_4 ||e_1||^2$$

and for all e_2, V_2 satisfies

$$b_1\|e_2\|^2 \leq V_2(e_2) \leq b_2\|e_2\|^2$$
$$\|\nabla V_2(e_2)\| \leq b_3\|e_2\|$$
$$\nabla V_2(e_2).g_2(0,e_2) \leq -b_4\|e_2\|^2$$

These properties are result of the converse of Lyapunov theorems for the GES systems $\dot{e_1} = g_1(e_1)$ and $\dot{e_2} = g_2(0,e_2)$ (see [85]).

Consider now

$$W(e_1,e_2) = V_1(e_1) + \eta V_2(e_2)\ , \quad \eta > 0$$

as a Lyapunov function candidate for system (5.10), then the derivative of W along the trajectories of the system is given by :

$$\begin{aligned}
\dot{W}(e_1,e_2) &= \dot{V_1}(e_1) + \eta\dot{V_2}(e_2)\\
&= \nabla V_1(e_1).g_1(e_1) + \eta\nabla V_2(e_2).\Big(g_2(0,e_2) + G(e_1,e_2).e_1\Big)\\
&\leq -a_4\|e_1\|^2 + \eta\nabla V_2(e_2).G(e_1,e_2).e_1 - b_4\eta\|e_2\|^2\\
&\leq -a_4\|e_1\|^2 + \eta b_3\|e_2\|.\|e_1\|.\Gamma(\|e_1\|) - \eta b_4\|e_2\|^2
\end{aligned}$$

since we have $\dot{e_1} = g_1(e_1)$ GES, then $\|e_1(t)\| \leq M\|e_1(0)\|e^{-\lambda t} \leq M\|e_1(0)\|,\ \ M > 0$, which yields

$$\dot{W}(e_1,e_2) \leq -a_4M^2\|e_1(0)\|^2 + \eta b_3M\|e_1(0)\|.\Gamma(M\|e_1(0)\|).\|e_2\| - \eta b_4\|e_2\|^2. \tag{5.11}$$

Therefore, should we choose η such that

$$0 < \eta < \frac{4a_4b_4}{b_3^2\Gamma^2(M\|e_1(0)\|)},$$

the above quadratic term is definite negative on $\mathbb{R}^{n_1} \times \mathbb{R}^{n_2}$. It follows that $(e_1,e_2) = (0,0)$ is GES for system (5.10). □

5.2.1 Application to the electrohydraulic manipulator

For the drive-response observer we shall again measure the displacement of the piston x_p, and use it to drive the observer. We recall

$$\begin{aligned}
\dot{P}_L &= \frac{4B}{V_t}\left(ku\sqrt{\frac{P_s - P_r - sign(u)P_L}{2}} - \frac{\alpha}{1+\gamma|u|}P_L - Sv\right)\ ,\\
\dot{v} &= \frac{1}{m_t}\Big(SP_L - bv - k_lx_p\Big)\ ,\\
\dot{x}_p &= v\ .
\end{aligned}$$

and using (5.9) we will postulate the following observer

$$\begin{aligned}
\dot{\hat{P}}_L &= \frac{4B}{V_t}\left(ku\sqrt{\frac{P_s - P_r - sign(u)\hat{P}_L}{2}} - \frac{\alpha}{1+\gamma|u|}\hat{P}_L - S\hat{v}\right) , \\
\dot{\hat{v}} &= \frac{1}{m_t}\left(S\hat{P}_L - b\hat{v} - k_l x_p\right) , \\
\dot{\hat{x}}_p &= \hat{v} + \kappa(x_p - \hat{x}_p) .
\end{aligned}$$

Let's consider the function defined in (5.7), thus the error system is written as

$$\begin{aligned}
\dot{e}_{P_L} &= \frac{4B}{V_t}\left(\mathcal{N}(P_L) - \mathcal{N}(\hat{P}_L) - \frac{\alpha}{1+\gamma|u|}e_{P_L} - Se_v\right) , \\
\dot{e}_v &= \frac{1}{m_t}(Se_{P_L} - be_v) , \\
\dot{e}_{x_p} &= e_v - \kappa e_{x_p} .
\end{aligned}$$

The first two equations are independent of e_{x_p}. In addition to its being decreasing function, following the argument of the preceding section, $\mathcal{N}(P_L)$ is Lipschitz within the operating range. Then,

$$\begin{aligned}
\dot{e}_{P_L} &= \frac{4B}{V_t}\left(-\gamma_2 e_{P_L} - \frac{\alpha}{1+\gamma|u|}e_{P_L} - Se_v\right) , \\
\dot{e}_v &= \frac{1}{m_t}(Se_{P_L} - be_v) ,
\end{aligned}$$

where $\gamma_2 \in [0, \gamma_1]$. Now we consider the Lyapunov function

$$\begin{aligned}
V(e_{P_L}, e_v) &= \frac{1}{2}\left(\frac{V_t}{4B}e_{P_L}^2 + m_t e_v^2\right) \\
\dot{V}(e_{P_L}, e_v) &= -\gamma_2 e_{P_L}^2 - \frac{\alpha}{1+\gamma|u|}e_{P_L}^2 - be_v^2
\end{aligned}$$

thus the above subsystem is exponentially stable. Now, if we let $\kappa > 0$, deducing the exponential stability of the overall error system is a straight forward application of Theorem 5.3 after considering Remark 5.4.

Remark 5.5 *The convergence of e_{x_p} to its origin is exponentially fast, so $e_{x_p} \to 0$ as $t \to \infty$. However if we choose*

$$\dot{\hat{x}}_p = \hat{v} + \kappa \ sign(x_p - \hat{x}_p),$$

then

$$\dot{e}_{x_p} = e_v - \kappa \ sign(e_{x_p}) .$$

so that if we choose $\kappa > |e_v|_{\max}$ then e_{x_p} will fade to zero in finite time $t_r = \frac{|e_{x_p}(0)|}{\kappa}$. We can verify that κ exists since $e_v(t)$ is exponentially stable.

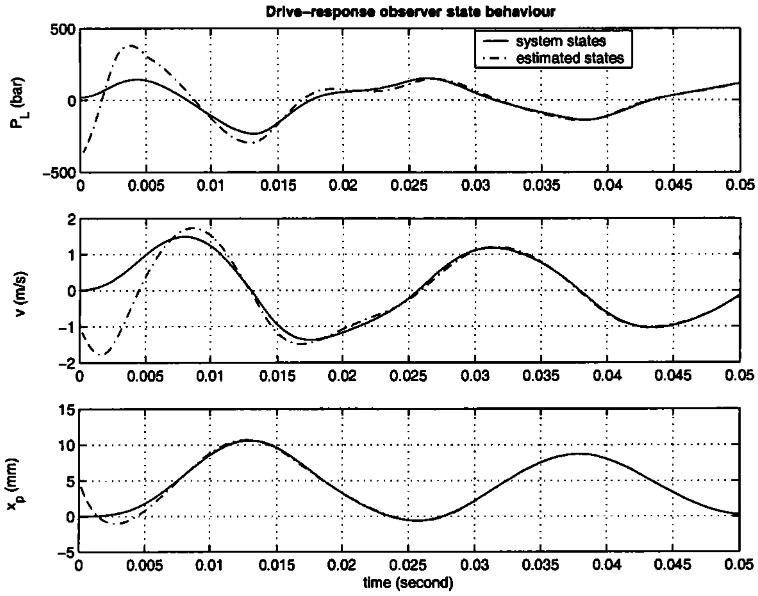

FIG. 5.3 – The drive-response observer states behaviour.

In Figure 5.3 we show the convergence of the drive-response observer states. Though the drive-response observer is strongly dependent on the system structure, its synthesis is very simple and does not require hard design computations. Indeed, this observer is free from the hypotheses ($\mathcal{H}2$) and ($\mathcal{H}3$) of proposition 5.1, and only requires a choice of positive feedback gain, namely $\kappa > 0$, to obtain an exponential convergence rate.

5.3 Sliding observer for systems with unknown inputs

In general nonlinear observer design, the plant model is reproduced with an addition of a feedforward term which is usually a function of the error between the system output and the observer output. However in many practical domains an unknown set of parameters might interfere into the system plant such as noise, hard-to-measure nonlinear parameters... Whenever such unknowns are present the usual design procedures no longer lead in general to the convergence of the obtained observers. In this section we present sufficient conditions to design a sliding observer for a class of nonlinear systems. We show that under suitable choice of the observation gain the observer states will asymptotically converge to the original states even in the presence of bounded modelling errors . We first start by stating the observer, then we give methods to design the feedforward injection map that makes the observer insensitive to parameter uncertainties, and next we develop sufficient conditions for the existence of the sliding mode.

5.3.1 Sliding observer design

Part A : Observer statement

Consider the class of nonlinear uncertain systems, transformable into dynamical systems affine with respect to uncertain parameters, described as follows :

$$\dot{x} = Ax + f(x,u) + B\Phi(x)\mu \,, \tag{5.12a}$$
$$y = Cx \,. \tag{5.12b}$$

where $x \in \mathbb{R}^n$ is the state vector, $u \in \mathbb{R}^m$ is the input control and $y \in \mathbb{R}^p$ is the system output $p < n$. A and C are two constant matrices of appropriate dimensions, $f : \mathbb{R}^n \times \mathbb{R}^m \to \mathbb{R}^n$ is a smooth vector field. $B \in \mathbb{R}^{n \times p}$ is the uncertainty injection map $\Phi : \mathbb{R}^n \to \mathbb{R}^{p \times p}$ is a bounded function, and $\mu \in \mathbb{R}^p$ is the unknown parameter vector. Here x^T denotes the transpose of the vector x and $\|x\|$ its Euclidean norm.

Remark 5.6 *We will assume without loss of generality that the observability matrix C and the uncertainty injection map B to be of full column rank, $rank(C) = p$ and $rank(B) = p$. In fact, if C is not full rank then there is redundancy in the observation and C should be modified until it is full rank. With similar reasoning B can be modified to be full rank.*

We assume that system (5.12) satisfies the following hypotheses

($\mathcal{H}1$) (C, A) is an observable pair.

($\mathcal{H}2$) $f(x,u)$ is uniformly Lipschitz with respect to x, i.e.

$$\|f(x,y) - f(\hat{x},u)\| \leq \gamma_f \|x - \hat{x}\| \,.$$

($\mathcal{H}3$) The uncertain parameters are bounded

$$\sup_{t>0} \|\mu(t)\| \leq \gamma_\mu \,.$$

($\mathcal{H}4$) $\|\Phi(x)\| \leq \gamma_\Phi \qquad \forall x \in \mathbb{R}^n$.

A sliding observer for system (5.12) is the following

$$\dot{\hat{x}} = A\hat{x} + f(\hat{x},u) + \zeta S^{-1}C^T(y - C\hat{x}) + \Lambda v \,, \tag{5.13a}$$
$$\hat{y} = C\hat{x} \,, \tag{5.13b}$$
$$0 = -\theta S - A^T S - SA + CC^T \,. \tag{5.13c}$$

where $v \in \mathbb{R}^p$ is a discontinuous feedforward compensation signal and $\Lambda \in \mathbb{R}^{n \times p}$ is the feedforward injection map such that $C\Lambda$ is a nonsingular matrix, thus by purview of remark 5.6 $rank\Lambda = p$. And $\zeta > 1$ and $\theta > 0$ are two real numbers with θ large enough such that S is a positive definite matrix.

Define $e = x - \hat{x}$ and $e_y = y - \hat{y}$, then the state reconstruction error is

$$\dot{e} = \big(A - \zeta S^{-1}C^T C\big)e + f(x,u) - f(\hat{x},u) + B\Phi(x)\mu - \Lambda v \,, \tag{5.14a}$$

$$e_y = Ce \,. \tag{5.14b}$$

we wish to determine ζ, θ, Λ and v such that (5.14) is at least asymptotically stable in the sense of Lyapunov.

Part B : Design of ζ and θ

To choose ζ and θ we consider the system

$$\begin{aligned} \dot{\xi} &= A\xi + f(\xi,u) \,, \\ \mathcal{O} &= C\xi \,, \end{aligned}$$

and its observer

$$\dot{\hat{\xi}} = A\hat{\xi} + f(\hat{\xi},u) + \zeta S^{-1}C^T(y - C\hat{\xi}) \,,$$

where S is as described in (5.13c), which can also be expressed in the form of a Lyapunov equation

$$\Big(- A^T - \frac{\theta}{2}I\Big)S + S\Big(- \frac{\theta}{2}I - A\Big) = C^T C \,.$$

It has been shown in Section 5.1 that this observer converges exponentially fast if

$$\gamma_f < \frac{\lambda_{\min}\Big(\theta S + (2\zeta - 1)C^T C\Big)}{2\lambda_{\max}(S)} \tag{5.15}$$

with $\zeta > 1$ and

$$\theta > -2\ \min\{\mathcal{R}e(\lambda) | \lambda \in spec(A)\} \tag{5.16}$$

where $spec(A)$ is the spectrum of A. We also note that there exist $\bar{\theta}$ for which this bound on γ_f is maximized when ζ goes to infinity. Hereafter, we assume that the following is true.

($\mathcal{H}5$) Given the system (5.12) we can choose $\theta = \bar{\theta}$ and $\zeta = \bar{\zeta}$ such that

$$\gamma_f < \frac{\bar{\theta}}{2}\frac{\lambda_{\min}(S)}{\lambda_{\max}(S)} < \frac{\lambda_{\min}\Big(\bar{\theta} S + (2\bar{\zeta} - 1)C^T C\Big)}{2\lambda_{\max}(S)}$$

($\bar{\zeta}$ is large enough such that any value of $\zeta > \bar{\zeta}$ does not bring significant change on the bound (5.15))

Part C : Design of Λ and v

The aim of the observer is to bring $e = 0$, that is to have stable origin in the dynamics represented by equation (5.14). For this aim, and since we only measure $y = Cx$, we would choose $e_y = 0$ as an attractive and sliding surface. The ideal sliding mode for the system (5.14) is obtained if $e_y = 0$ and $\dot{e}_y = 0$, but

$$\begin{aligned}
&\dot{e}_y = 0 \\
\Leftrightarrow &C\dot{e} = 0 \\
\Leftrightarrow &C\big(A - \zeta S^{-1}C^T C\big)e + C\Big(f(x,u) - f(\hat{x},u)\Big) + CB\Phi(x)\mu - C\Lambda v = 0
\end{aligned}$$

thus according to the equivalent control method we have a feedforward input

$$v_{eq} = (C\Lambda)^{-1}CAe + (C\Lambda)^{-1}C\Big(f(x,u) - f(\hat{x},u)\Big) + (C\Lambda)^{-1}CB\Phi(x)\mu\ . \tag{5.17}$$

Substituting (5.17) in (5.14a), then when sliding mode occur, the state reconstruction error system has the following form

$$\begin{aligned}
\dot{e} = \big(I - \Lambda(C\Lambda)^{-1}C\big)Ae + \big(I - \Lambda(C\Lambda)^{-1}C\big)\big(f(x,u) - f(\hat{x},u)\big) \\
+\big(I - \Lambda(C\Lambda)^{-1}C\big)B\Phi(x)\mu\ .
\end{aligned}$$

Now $\Pi = I - \Lambda(C\Lambda)^{-1}C$ is a projection onto the kernel space of C in the direction of the range space of Λ. Consequently, if we choose Λ such that the columns of B lie in the range space of Λ, that is there exist a nonsingular matrix $D \in \mathbb{R}^{p\times p}$ such that

$$\Lambda D = B \tag{5.18}$$

then the term $\big(I - \Lambda(C\Lambda)^{-1}C\big)B\Phi(x)\mu$ will be annihilated and the state reconstruction error system becomes independent of the uncertain vector μ, particularly

$$\dot{e} = \big(I - \Lambda(C\Lambda)^{-1}C\big)Ae + \big(I - \Lambda(C\Lambda)^{-1}C\big)\big(f(x,u) - f(\hat{x},u)\big)\ .$$

Remark 5.7 *Note that the existence of Λ depends on the observation matrix C. Indeed, $\Lambda D = B \Rightarrow C\Lambda D = CB$, then if CB is singular then D is also singular, since $C\Lambda$ is necessarily a nonsingular matrix. If we refer to (5.18) this in turn contradicts the fact that Λ and B are matrices of full column rank.*

In the sequel we assume that the following hypothesis is satisfied

($\mathcal{H}6$) There exists a $p \times p$ matrix D such that

$$\Lambda D = B$$

The existence of the sliding mode requires v to be a discontinuous function. Let for instance

$$v = W\text{sign}(Ce)$$

where W is a positive definite matrix, $W \in \mathbb{R}^{p\times p}$.

Our aim is to find conditions under which the state reconstruction error dynamics are stable, i.e.

$$\lim_{t\to\infty} e(t) = 0 \ .$$

Set

$$\Lambda = S^{-1}C^T W^{-1} \ , \tag{5.19}$$

thus for this choice of Λ, we can check that $C\Lambda$ is nonsingular, indeed we have

$$C\Lambda = CS^{-1}C^T W^{-1}$$

but we know that W^{-1} is positive definite, then to show that $C\Lambda$ is nonsingular we only need to show that $CS^{-1}C^T$ is nonsingular. To this aim we will proceed by contradiction. Suppose there is $z \in \mathbb{R}^p$, $z \neq 0$ such that $CS^{-1}C^T z = 0$ then

$$\begin{aligned}
CS^{-1}C^T z &= 0 \\
z^T CS^{-1}C^T z &= 0 \\
z^T CS^{-1/2}S^{-1/2}C^T z &= 0 \quad (\text{ since } S^{-1} \text{ is positive definite }) \\
\left(S^{-1/2}C^T z\right)^T \left(S^{-1/2}C^T z\right) &= 0 \\
S^{-1/2}C^T z &= 0 \\
C^T z &= 0 \quad (\text{ since } S^{-1/2} \text{ is positive definite }) \\
z &= 0 \quad (\text{ since } C^T \text{ is full column rank })
\end{aligned}$$

The fact that z is necessarily zero, contradicts our assumption of $z \neq 0$, and shows that $CS^{-1}C^T$ is nonsingular. Furthermore, since S^{-1} is positive definite and $CS^{-1}C^T$ is symmetric it follows that $CS^{-1}C^T$ is also positive definite. Eventually,

$$C\Lambda = CS^{-1}C^T W^{-1}$$

is a nonsingular matrix.

We should now investigate the conditions under which

$$\Lambda = S^{-1}C^T W^{-1}$$

can satisfy $(\mathcal{H}6)$.

Since $\Lambda D = B$ with D nonsingular, then

$$\begin{aligned} Image(\Lambda) &= Image(B) \\ \Lambda(\mathbb{R}^p) &= B(\mathbb{R}^p) \\ S^{-1}C^T W^{-1}(\mathbb{R}^p) &= B(\mathbb{R}^p) \\ S^{-1}C^T(\mathbb{R}^p) &= B(\mathbb{R}^p) \quad (\text{ since } W^{-1} \text{ is nonsingular }) \\ C^T(\mathbb{R}^p) &= SB(\mathbb{R}^p) \\ Image(C^T) &= Image(SB) \end{aligned}$$

Let us consider, without loss of generality, that

$$C = (I_p \quad 0)$$

that is we directly observe the states and not an algebraic combination of them.

Remark 5.8 *This assumption is not restrictive, since by linear coordinate change $\bar{x} = \mathbf{T}x$ we can obtain*

$$\bar{C} = C\mathbf{T} \ , \quad \text{with } \bar{C} = (I_p \quad 0)$$

$$\bar{A} = \mathbf{T}^{-1}A\mathbf{T} \ , \quad \bar{B} = \mathbf{T}^{-1}B \ , \quad \bar{f}(x,u) = \mathbf{T}^{-1}f(x,u)$$

Now

$$C^T = \begin{pmatrix} I_p \\ 0 \end{pmatrix}$$

Set

$$S = \begin{pmatrix} S_{11} & S_{12} \\ S_{12}^T & S_{22} \end{pmatrix} \quad \text{and} \quad B = \begin{pmatrix} B_1 \\ B_2 \end{pmatrix}$$

where $S_{11} \in \mathbb{R}^{p\times p}$, $S_{22} \in \mathbb{R}^{(n-p)\times(n-p)}$, $B_1 \in \mathbb{R}^{p\times p}$, $B_2 \in \mathbb{R}^{(n-p)\times p}$, with B_1 nonsingular.

$$SB = \begin{pmatrix} S_{11} & S_{12} \\ S_{12}^T & S_{22} \end{pmatrix} \begin{pmatrix} B_1 \\ B_2 \end{pmatrix} = \begin{pmatrix} S_{11}B_1 + S_{12}B_2 \\ S_{12}^T B_1 + S_{22}B_2 \end{pmatrix}$$

to satisfy the equality $Image(C^T) = Image(SB)$ we need to have $S_{11}B_1 + S_{12}B_2$ nonsingular and

$$S_{12}^T B_1 + S_{22}B_2 = 0 \ . \tag{5.20}$$

Equation (5.20) involve conditions on the matrix S which is a solution of

$$\theta S = -A^T S - SA - CC^T \ . \tag{5.21}$$

If we set

$$A = \begin{pmatrix} A_{11} & A_{12} \\ A_{21} & A_{22} \end{pmatrix}$$

then

$$SA = \begin{pmatrix} S_{11} & S_{12} \\ S_{12}^T & S_{22} \end{pmatrix} \begin{pmatrix} A_{11} & A_{12} \\ A_{21} & A_{22} \end{pmatrix} = \begin{pmatrix} S_{11}A_{11} + S_{12}A_{21} & S_{11}A_{12} + S_{12}A_{22} \\ S_{12}^T A_{11} + S_{22}A_{21} & S_{12}^T A_{12} + S_{22}A_{22} \end{pmatrix}$$

thus (5.21) yields to

$$\theta S_{11} = -\big(A_{11}^T S_{11} + S_{11}A_{11}\big) - \Big((S_{12}A_{21}) + (S_{12}A_{21})^T\Big) - I_p \tag{5.22a}$$

$$\theta S_{12} = -\big(A_{11}^T S_{12} + S_{12}A_{22}\big) - \big(A_{21}^T S_{22} + S_{11}A_{12}\big) \tag{5.22b}$$

$$\theta S_{22} = -\big(A_{22}^T S_{22} + S_{22}A_{22}\big) - \Big((S_{12}^T A_{12}) + (S_{12}^T A_{12})^T\Big) \tag{5.22c}$$

Therefore, to satisfy hypothesis ($\mathcal{H}6$) with the choice of Λ as in (5.19), and $C = (I_p \;\; 0)$, all matrices A, B and S should satisfy equations (5.20) and (5.22).

Example : If we let for instance, B_1 nonsingular and $B_2 = 0$, then according to (5.20) we get $S_{12} = 0$, and to obtain a unique positive definite solution S_{11} from (5.22a) we need to have

$$\Big(\frac{\theta}{2}I_p + A_{11}\Big) \quad \text{Hurwitz stable}$$

Similarly, to obtain unique positive definite solution S_{22} from (5.22c) we need to have

$$\Big(\frac{\theta}{2}I_{(n-p)} + A_{22}\Big) \quad \text{Hurwitz stable}$$

And from (5.22b) we need to have

$$A_{21}^T S_{22} + S_{11}A_{12} = 0 \; .$$

Therefore, should $\Lambda = S^{-1}C^TW^{-1}$ lead to asymptotic stability, then it is considered as a suitable choice, since according to the previous analysis it satisfies two necessary conditions, namely $C\Lambda$ nonsingular, and columns of B in the range space of Λ.

Let's then investigate the stability of the error dynamics. To this aim we consider the Lyapunov function candidate $V(e) = e^TSe$, and we distinguish two cases :

Case 1 : if $Ce \neq 0$

$$\begin{aligned}
\dot{V} &= 2e^TSAe - 2\zeta e^TC^TCe + 2e^TS\big(f(x,u) - f(\hat{x},u)\big) + 2e^TSB\Phi(x)\mu - 2e^TS\Lambda v \\
&= -\theta e^TSe - (2\zeta - 1)e^TC^TCe + 2e^TS\big(f(x,u) - f(\hat{x},u)\big) \\
&\quad +2e^TS\Lambda D\Phi(x)\mu - 2e^TS\Lambda v \\
&= -\theta e^TSe - (2\zeta - 1)e^TC^TCe + 2e^TS\big(f(x,u) - f(\hat{x},u)\big) \\
&\quad +2e^TC^TW^{-1}D\Phi(x)\mu - 2e^TC^T\mathrm{sign}(Ce) \\
&\leq -\Big(\lambda_{\min}\Big(\theta S + (2\zeta - 1)C^TC\Big) - 2\gamma_f\lambda_{\max}(S)\Big)\|e\|^2 \\
&\quad +2\big(\|W^{-1}D\|\gamma_\Phi\gamma_\mu - 1\big)\|Ce\|
\end{aligned}$$

Hence if ($\mathcal{H}5$) is satisfied and besides we choose W such that

$$\lambda_{\min}(W) \geq \|D\|\gamma_\Phi\gamma_\mu \ , \tag{5.23}$$

we obtain

$$\begin{aligned}
\dot{V} &\leq -\Big(\frac{\lambda_{\min}\Big(\theta S + (2\zeta - 1)C^TC\Big)}{2\lambda_{\max}(S)} - \gamma_f\Big)2V - \Big(1 - \frac{\|D\|\gamma_\Phi\gamma_\mu}{\lambda_{\min}(W)}\Big)2\|Ce\| \\
&< -2\alpha_1 V
\end{aligned}$$

where $\alpha_1 = \frac{\lambda_{\min}(\theta S + (2\zeta-1)C^TC)}{2\lambda_{\max}(S)} - \gamma_f > 0$, that is we have an exponentially decaying bound on the Lyapunov function.

$$V(t) \leq V(0)\exp(-2\alpha_1 t)$$

Using the following inequality

$$\lambda_{\min}(S)\|e\|^2 \leq e^TSe \leq \lambda_{\max}(S)\|e\|^2 \ ,$$

we have

$$\|e(t)\|^2 \leq \frac{V(t)}{\lambda_{\min}(S)} \leq \frac{V(0)\exp(-2\alpha_1 t)}{\lambda_{\min}(S)} \leq \frac{\lambda_{\max}(S)}{\lambda_{\min}(S)}\exp(-2\alpha_1 t)\|e(0)\|^2 \ ,$$

equivalently

$$\|e(t)\| \leq \sqrt{\frac{\lambda_{\max}(S)}{\lambda_{\min}(S)}}\exp(-\alpha_1 t)\|e(0)\| \ .$$

Therefore,

$$\lim_{t\to\infty} e(t) = 0$$

Case 2 : if $Ce = 0 \ \Rightarrow \ v = v_{eq}$

$$\begin{aligned}
\dot{V} &= -\theta e^TSe + 2e^TS\big(f(x,u) - f(\hat{x},u)\big) + 2e^TC^TW^{-1}D\Phi(x)\mu - 2e^TC^TW^{-1}v_{eq} \\
&\leq -\theta\lambda_{\min}(S)\|e\|^2 + 2\gamma_f\lambda_{\max}(S)\|e\|^2 \\
&\leq -\Big(\theta\lambda_{\min}(S) - 2\gamma_f\lambda_{\max}(S)\Big)\|e\|^2
\end{aligned}$$

We recall from ($\mathcal{H}5$) that

$$\gamma_f < \frac{\theta}{2}\frac{\lambda_{\min}(S)}{\lambda_{\max}(S)},$$

then

$$\begin{aligned}\dot{V} &\leq -\left(\frac{\theta}{2}\frac{\lambda_{\min}(S)}{\lambda_{\max}(S)} - \gamma_f\right)2V \\ &\leq -2\alpha_2 V\end{aligned}$$

and similar to the previous case this leads to

$$\|e(t)\| \leq \sqrt{\frac{\lambda_{\max}(S)}{\lambda_{\min}(S)}}\exp(-\alpha_2 t)\|e(0)\|\,.$$

Therefore, from ($\mathcal{H}5$) it results that

$$\lim_{t\to\infty} e(t) = 0$$

Now that we have proved the stability of the error system, it follows that $\lim\limits_{t\to\infty} e_y(t) = 0$ that is a convergent sliding mode exists. We shall next investigate the conditions for the existence of the sliding mode. The necessary condition for sliding mode to occur is $e_y^T\dot{e}_y \leq 0$ but we have

$$\begin{aligned}e_y^T\dot{e}_y &= e^T C^T C\dot{e} \\ &= e^T C^T C\Big((A-\zeta S^{-1}C^T C)e + f(x,u) - f(\hat{x},u) + B\Phi(x)\mu - \Lambda v\Big) \\ &= e^T C^T\Big(C(A-\zeta S^{-1}C^T C)\Big)e + e^T C^T C\Big(f(x,u) - f(\hat{x},u)\Big) \\ &\quad + e^T C^T C S^{-1}C^T W^{-1}D\Phi(x)\mu - e^T C^T C S^{-1} C^T W^{-1} W\mathrm{sign}(Ce) \\ &\leq \|Ce\|\;\|C\|\;\|(A-\zeta S^{-1}C^T C)\|\;\|e\| + \|Ce\|\;\|C\|\gamma_f\|e\| \\ &\quad + \|Ce\|\lambda_{\max}(CS^{-1}C^T)\|W^{-1}D\|\gamma_\Phi\gamma_\mu - \|Ce\|\lambda_{\min}(CS^{-1}C^T) \\ &\leq \|Ce\|\Bigg(\sigma_{\max}(C)\sigma_{\max}(A-\zeta S^{-1}C^T C)\|e\| + \gamma_f\sigma_{\max}(C)\|e\| \\ &\quad + \lambda_{\max}(CS^{-1}C^T)\frac{\|D\|}{\lambda_{\min}(W)}\gamma_\Phi\gamma_\mu - \lambda_{\min}(CS^{-1}C^T)\Bigg)\end{aligned}$$

where $\sigma_{\max}(.)$ is the largest singular value of the matrix in question. A sufficient condition for the sliding mode to occur is that the term on the right of the previous equation must be negative, that is

$$\|e\| < \frac{\lambda_{\min}(CS^{-1}C^T)\lambda_{\min}(W) - \lambda_{\max}(CS^{-1}C^T)\|D\|\gamma_\Phi\gamma_\mu}{\lambda_{\min}(W)\;\;\sigma_{\max}(C)\Big(\sigma_{\max}(A-\zeta S^{-1}C^T C) + \gamma_f\Big)}$$

but this inequality requires that the numerator be positive that is

$$\lambda_{\min}(W) > \|D\|\gamma_\Phi\gamma_\mu \frac{\lambda_{\max}(CS^{-1}C^T)}{\lambda_{\min}(CS^{-1}C^T)} \tag{5.24}$$

with this condition we have

$$\|e\| < \frac{\lambda_{\min}(CS^{-1}C^T)\lambda_{\min}(W) - \lambda_{\max}(CS^{-1}C^T)\|D\|\gamma_\Phi\gamma_\mu}{\lambda_{\min}(W)\ \ \sigma_{\max}(C)\Big(\sigma_{\max}(A - \zeta S^{-1}C^T C) + \gamma_f\Big)} = r_s$$

therefore if the state error trajectory lies within the vicinity of the sliding surface inside a ball of radius r_s then the system behaves in sliding mode and slides along the hyperplane $e_y = 0$ until it reaches the origin.

Remark 5.9 *We have seen that the stability of the error system requires*

$$\lambda_{\min}(W) > \|D\|\gamma_\Phi\gamma_\mu$$

and the existence of sliding mode requires

$$\lambda_{\min}(W) > \|D\|\gamma_\Phi\gamma_\mu \frac{\lambda_{\max}(CS^{-1}C^T)}{\lambda_{\min}(CS^{-1}C^T)} .$$

Hence if W is chosen to satisfy the second inequality the first is simultaneously satisfied.

Eventually we summaries our main result in the following theorem

Theorem 5.4 *Given a nonlinear dynamical system of the form*

$$\Sigma \begin{cases} \dot{x} & = Ax + f(x,u) + B\Phi(x)\mu \ , \\ y & = Cx \ . \end{cases}$$

with B and C full rank matrices, and consider the following auxiliary system

$$\hat{\Sigma} \begin{cases} \dot{\hat{x}} & = A\hat{x} + f(\hat{x},u) + \zeta S^{-1}C^T(y - C\hat{x}) + \Lambda v \ , \\ \hat{y} & = C\hat{x} \ , \\ 0 & = -\theta S - A^T S - SA + CC^T \ . \end{cases}$$

if all the hypotheses $(\mathcal{H}1) - (\mathcal{H}6)$ are satisfied and

$$\Lambda = S^{-1}C^T W^{-1}$$

with W a positive definite matrix satisfying

$$\lambda_{\min}(W) > \|D\|\gamma_\Phi\gamma_\mu \frac{\lambda_{\max}(CS^{-1}C^T)}{\lambda_{\min}(CS^{-1}C^T)} .$$

Then $\hat{\Sigma}$ is an exponential observer for Σ. □

5.3.2 Application to the electrohydraulic manipulator

In here we will consider the electrohydraulic manipulator model with some slight differences. Namely, we will consider that there is an internal piston leakage between the two chambers ($C_{il} = 3.3^{-12}$ is the internal leakage coefficient) , and we will also assume that the mass is subjected to abrupt instantaneous dry friction of unknown amplitude a_c ($\max(a_c) = 2100\ N$).

$$\begin{aligned}
\dot{P}_L &= \frac{4B}{V_t}\left(ku\sqrt{\frac{P_s - P_r - sign(u)P_L}{2}} - \frac{\alpha}{1+\gamma|u|}P_L - C_{il}P_L - Sv\right) , && (5.25a)\\
\dot{v} &= \frac{1}{m_t}\left(SP_L - bv - k_l x_p - a_c\text{sign}(v)\right) , && (5.25b)\\
\dot{x}_p &= v . && (5.25c)
\end{aligned}$$

By scaling it as in the previous section, the above system can be expressed as follows

$$\begin{aligned}
\dot{x} &= Ax + f(x,u) + B\Phi(x)\mu ,\\
y &= Cx .
\end{aligned}$$

where

$$A = \begin{bmatrix} -\frac{4BC_{il}}{V_t} & -\frac{4BS}{P_sV_t} & 0 \\ \frac{SP_s}{m_t} & -\frac{b}{m_t} & -\frac{k_l l}{m_t} \\ 0 & \frac{1}{l} & 0 \end{bmatrix}$$

$$f(x,u) = \begin{pmatrix} \frac{4B}{P_sV_t}\left(ku\sqrt{\frac{P_s - P_r - sign(u)P_s x_1}{2}} - \frac{\alpha}{1+\gamma|u|}P_s x_1\right) \\ 0 \\ 0 \end{pmatrix}$$

$$B = \begin{bmatrix} 0 \\ -\frac{1}{m_t} \\ 0 \end{bmatrix} , \quad \Phi(x) = \text{sign}(x_2) , \quad \mu = a_c .$$

Again we will consider suitable inputs $u(t)$ that yield to local Lipschitz nonlinear function. In this application we will use a sensor to measure piston velocity that is having $y = x_2$ and $y = Cx$ means $C = [0\ \ 1\ \ 0]$. We can easily check that the pair (C, A) is observable. The same sinusoidal exponentially decaying signal is used as an input control. The values $\bar{\theta} = 320$ and $\bar{\zeta} = 4$ satisfy $(\mathcal{H}5)$.

We check that $CB \neq 0$, and we set $\Lambda = [0\ \ 1\ \ 0]^T$ so $C\Lambda = 1 \neq 0$ and we have $\frac{-1}{m_t}\Lambda = B$ that is $|D| = \frac{1}{70}$. We also have $\gamma_\Phi = 1$ and $\gamma_\mu = 2100$, hence according to Theorem 5.4, W should be larger than 30, set $W = 50$. Using all the foregoing data a system and observer were designed and simulated using MATLAB®5.3 and we have obtained the results shown in the figures shown here.

A second unknown parameter that can be considered is the spring stiffness, in fact the spring here represents the stiffness of the environment, which is quite hard to model or at least cannot be exactly modeled by a linear spring. Therefore we will consider that the exact value of the stiffness is $k_l + \Delta k_l$ where $\Delta k_l = 49000 N/m$, thus equation (5.25b) will be replaced by the following one

$$\dot{v} = \frac{1}{m_t}\left(SP_L - bv - k_l x_p - \Delta k_l x_p\right) .$$

Consequently, $\Phi(x) = x_3$ and $\theta = \Delta k_l$. Set matrices C and Λ as before, so $|D| = \frac{1}{70}$. In this case $\gamma_\phi = 0.3$ which corresponds to half cylinder length, as x is measured relative to the middle of the stroke of the piston, and $\gamma_\theta = 49000$. According to Theorem 5.4 W should be larger than 210, we have set $W = 250$ and we simulated the above system and observer.

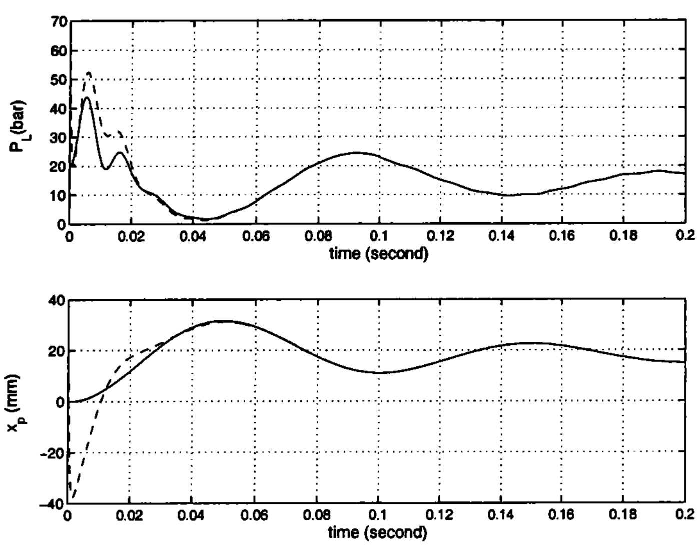

FIG. 5.4 – The high-gain observer states behaviour under no unknown inputs.

In Figure 5.4 we show the results of the high-gain observer shown in Part B of section 5.3.1 for the unperturbed system. Figure 5.5 delineates the behaviour of the same observer if a sudden dry friction of magnitude 1500 N acts on the load during 10 ms starting from $0.05s$ to $0.06s$. We clearly see the degradation in the estimation of the observer. This observer also fails to track the states, if the system had uncertainties in the spring stiffness. Actually, the exact value of the spring stiffness changes as time elapses in the following manner $k_l + \Delta k_l$ if $t < 0.03s$, then $k_l - \Delta k_l$ if $0.03s < t < 0.06s$, finally k_l if $t > 0.06s$ see Figure 5.6.

Finally, in Figures 5.7 and 5.8 the estimations of the sliding observer are shown in the presence of the same dry friction action, and spring stiffness variations. One can obviously notice the robustness of the sliding observer. From the first simulations (dry friction unknown) we can see that while the sliding observer was not significantly perturbed in estimating the pressure and retrieved the correct value of the displacement 20 ms after the perturbation has stopped, the high-gain observer was significantly perturbed in estimating the pressure and the displacement could only converge 120 ms after the end of the perturbation. Similarly in the second simulations (spring stiffness variation), the high-gain observer was severely perturbed whereas the sliding mode observer smoothly converged to the actual states of the system. In the next figures observers behaviours are represented by dashed lines and the solid lines show the behaviours of the system.

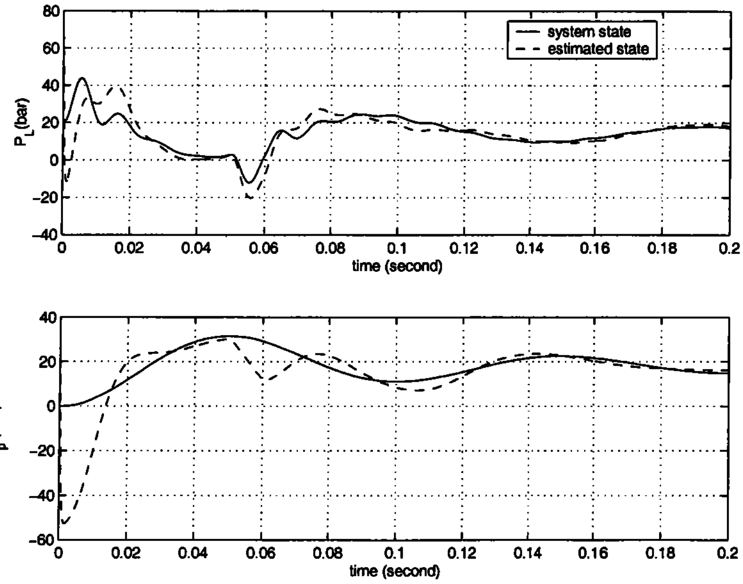

FIG. 5.5 – The high-gain observer states response to dry friction perturbation.

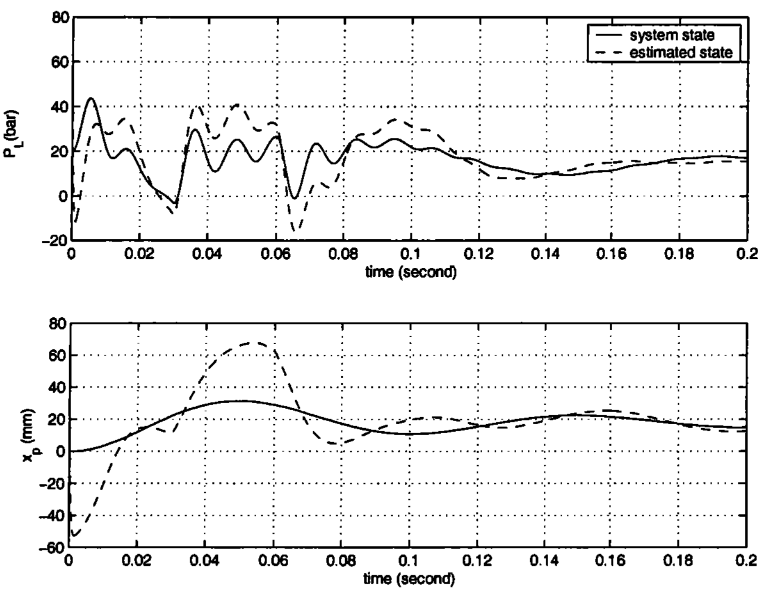

FIG. 5.6 – The high-gain observer states response to stiffness variations.

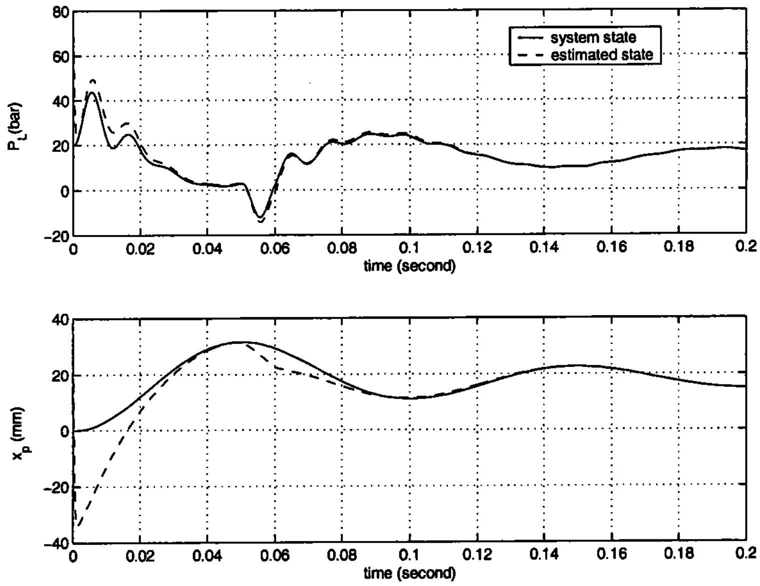

FIG. 5.7 – The sliding observer states robustness to dry friction perturbation.

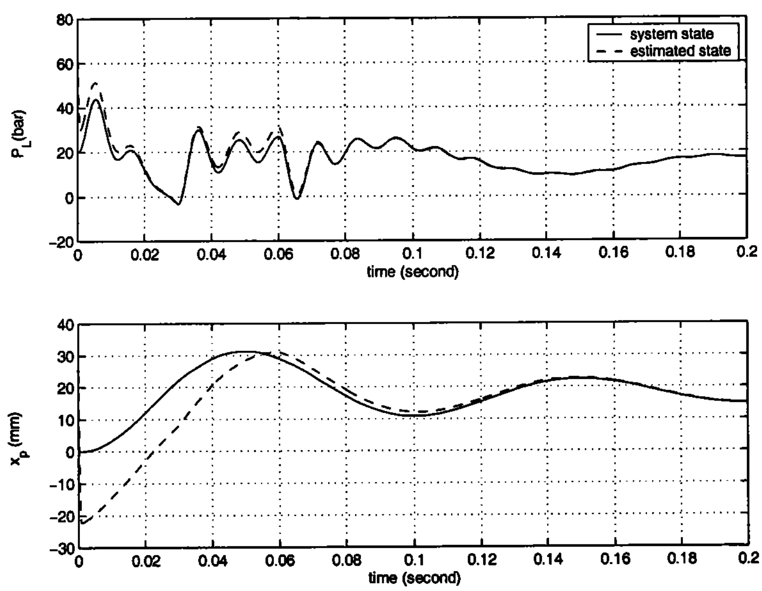

FIG. 5.8 – The sliding observer states robustness to stiffness variations.

Chapitre 6

Stabilization of nonlinear systems by state detection

State feedback control of nonlinear dynamical systems has been considered by many researchers, see chapter 3. Most of the works stated therein premise the complete accessibility to the state variables. In general, this assumption is not satisfied and only a few of the states are measurable. One way to obtain the nonmeasurable states is to construct an auxiliary system the role of which is to estimate the missing states knowing only the input to the system in question as well as the available states provided by direct measurements. The feedback control law is thereafter constructed using the estimated states. Should the estimated states be exactly equal to the real states, then one can expect that the feedback control law derived from the estimated states to stabilize the dynamic system in question.

However, in general, the initial conditions of the observer (state estimator) are not equal to those of the system, thus the estimated state are not exactly equal but exponentially tend to the real states. Therefore, the stability of the system, controlled via estimated states is not a straightforward conclusion, but rather needs further analysis.

The question that rises here is, under what conditions can we separately design a feedback stabilizing controller and an observer and we obtain a stabilizing estimated-states based feedback control law ? This has been called the *separation principle* problem. While in the linear case the results were well developed, its counterpart in the nonlinear case is still intriguing many researchers, since there is dependency between the stabilizability and observability of nonlinear systems.

The separation principle for nonlinear systems has been studied by Vidyasagar in [84] where he has shown that if the stabilizing control law is continuously differentiable, then the same control law derived from the observer states can also stabilize the system.

This work was then generalized by Tsinias in [81] where he dropped the differentiability assumption, and only considered stabilization by continuous feedback controllers. Some more results on the separation principle for some particular classes of nonlinear systems have been obtained by Khalil [4] and Praly [75].

In some cases however, it is easier or may be necessary to design a discontinuous controller in order to stabilize a given system using feedback control. This fact motivated our need to find conditions under which discontinuous controllers constructed by observer states can also stabilize the system in question [26] [27].

6.1 Feedback stabilization via observer states

We consider nonlinear systems of the form

$$\dot{x} = f(x,u) \,, \tag{6.1a}$$

$$y = h(x) \,. \tag{6.1b}$$

where $x \in \mathbb{R}^n$ is the state vector, $u \in \mathcal{U} \subseteq \mathbb{R}^m$ is the input, and $y \in \mathbb{R}^k$ is the output of the system. The mappings $f : \mathbb{R}^n \times \mathbb{R}^m \to \mathbb{R}^n$ and $h : \mathbb{R}^n \to \mathbb{R}^k$ are continuous, the origin $(0,0) \in \mathbb{R}^n \times \mathbb{R}^m$ is assumed to be an equilibrium point of (6.1), and the input space consists of functions $u : \mathbb{R}^+ \to \mathbb{R}^m$.

We recall from chapter 2 that a function $\phi : \mathbb{R}^+ \to \mathbb{R}^+$ is of class $\mathcal{K}$ $(\phi \in \mathcal{K})$, if it is continuous, strictly increasing and $\phi(0) = 0$; it is of class $\mathcal{K}^\infty$ $(\phi \in \mathcal{K}^\infty)$ if $\phi \in \mathcal{K}$, and also $\phi(r) \to \infty$ as $r \to \infty$.

Definition 6.1 *We say that (6.1) is weakly detectable, if there exists a continuous mapping $g : \mathbb{R}^n \times \mathbb{R}^k \times \mathbb{R}^m \to \mathbb{R}^n$ with $g(0,0,0) = 0$, a continuously differentiable function $W : \mathbb{R}^n \times \mathbb{R}^n \to \mathbb{R}^+$ and real functions $\psi_i \in \mathcal{K}^\infty (\psi_i \in \mathcal{K})$ $i = 1,2,3$, such that*

$$f(x,u) = g(x,h(x),u),$$

for all $(x,u) \in \mathbb{R}^n \times \mathbb{R}^m$ and further

$$\psi_1(\|x-z\|) \leq W(x,z) \leq \psi_2(\|x-z\|) \,, \tag{6.2}$$

$$\frac{\partial W}{\partial x} f(x,u) + \frac{\partial W}{\partial z} g(z,h(x),u) \leq -\psi_3(\|x-z\|) \,, \tag{6.3}$$

for all $u \in \mathcal{U} \subseteq \mathbb{R}^m$ and sufficiently small $e = x - z \in \mathbb{R}^n$ □

According to Definition 6.1, if (6.1) is weakly detectable, then the system $\dot{z} = g(z, h(x), u)$ is an observer for (6.1), namely $0 \in \mathbb{R}^n$ is asymptotically stable with respect to the error system

$$\dot{e} = f(x,u) - g(x - e, h(x), u) ,$$

uniformly on x and u.

We now start by stating the results given by Vidyasagar in [84]. We consider the nonlinear system described by (6.1) and the following hypotheses.

$(\mathcal{H}1)$ f is continuously differentiable and $f(0,0) = 0$, furthermore, there exist positive constants c_1 and c_2 such that for all x and u

$$\|\nabla_x f(x,u)\| \le c_1 , \quad \|\nabla_u f(x,u)\| \le c_2 .$$

$(\mathcal{H}2)$ h is continuous and $h(0) = 0$.

Theorem 6.1 *Suppose system (6.1) and the assumptions* $(\mathcal{H}1)$ *and* $(\mathcal{H}2)$ *pertaining to it. If we can find a feedback control* $u = \gamma(x)$ *such that*

(i) γ *is continuously differentiable,* $\gamma(0) = 0$ *and*

$$\|\nabla_x \gamma(x)\| \le \phi(\|x\|)$$

where $\phi \in \mathcal{K}$.

(ii) $x = 0$ *is a uniformly asymptotically stable equilibrium point of*

$$\dot{x} = f(x, \gamma(x)) .$$

If furthermore, (6.1) is weakly detectable, then $x = 0$ *and* $z = 0$ *is a uniformly asymptotically stable equilibrium point of the system*

$$\begin{aligned} \dot{x} &= f(x, \gamma(z)) , \\ \dot{z} &= g(z, h(x), \gamma(z)) . \end{aligned}$$

□

Proof : See Vidyasagar [84].

Tsinias has relaxed condition (i) in Vidyasagar's theorem, and only considered $\gamma(x)$ to be continuous.

Theorem 6.2 *If system (6.1) is weakly detectable and* $\dot{x} = f(x, \gamma(x))$ *is (locally) asymptotically stable at* $0 \in \mathbb{R}^n$ *then the output feedback* $u = \gamma(z)$ *asymptotically stabilizes*

$$\begin{aligned} \dot{x} &= f(x, \gamma(z)) , \\ \dot{z} &= g(z, h(x), \gamma(z)) . \end{aligned}$$

at $(0,0) \in \mathbb{R}^n \times \mathbb{R}^n$. □

Proof : See Tsinias [81].

Since we need sometimes to design discontinuous feedback controllers to stabilize nonlinear dynamic systems we will give conditions under which we can further relax the continuity condition, and only assume the controller to be piecewise continuous. For this aim we need first to give the input-to-state stability definition introduced by Sontag [72], and other definitions needed in the sequel.

Definition 6.2 *Sontag [72] We say that (6.1) is input-to-state stable (ISS) if and only if it admits an ISS-Lyapunov function. Namely, there exists a continuously differentiable function* $V : \mathbb{R}^n \to \mathbb{R}^+$, $\alpha_1, \alpha_2 \in \mathcal{K}^\infty$ *and* $\alpha_3, \eta \in \mathcal{K}$ *such that*

$$\alpha_1(\|x\|) \leq V(x) \leq \alpha_2(\|x\|) , \tag{6.4}$$

for any $x \in \mathbb{R}^n$ *and*

$$\nabla V(x).f(x,u) \leq -\alpha_3(\|x\|) , \tag{6.5}$$

for any $x \in \mathbb{R}^n$ *and any* $u \in \mathbb{R}^m$ *verifying* $\|x\| \geq \eta(\|u\|)$. □

Remark 6.1 *[72] A function V is an ISS-Lyapunov function for (6.1) if and only if there exists* $\alpha_i \in \mathcal{K}^\infty$ $i = 1, 2, 3, 4$ *such that (6.4) holds, and*

$$\nabla V(x).f(x,u) \leq -\alpha_3(\|x\|) + \alpha_4(\|u\|) . \tag{6.6}$$

Definition 6.3 *[88, page 19] A function* $\Gamma : \mathrm{X} \to \mathbb{R}$ *is upper semi-continuous at* x_0 *if*

$$\lim_{x \to x_0} \inf \Gamma(x) = \Gamma(x_0) .$$

□

We say that Γ is *upper semi-continuous* if it is upper semi-continuous at x_0 for every $x_0 \in \mathrm{X}$. We then verify that the set $\{x \in \mathrm{X} | \Gamma(x) < r\}$ is open for every $r \in \mathbb{R}$

Let $\gamma(x)$ be an admissible feedback control law for system (6.1). We will mean by admissible, any control law for which the differential equation $\dot{x} = f(x, \gamma(x))$ is well posed, that is for each initial state $x(0) \in \mathbb{R}^n$ there is an absolutely continuous solution. Let $\rho \in \mathcal{K}^\infty$, a feedback law will be said to be bounded by ρ if for each $x \in \mathbb{R}^n$, $\|\gamma(x)\| \leq \rho(\|x\|)$.(and the equality holds only if $x = 0$)

The main result of our work will be stated in the following theorem

Theorem 6.3 *If system (6.1) is weakly detectable and is ISS then there exists a bounded feedback control law* $u = \gamma(x)$, $\gamma(0) = 0$ *which stabilizes (6.1) and such that the augmented system*

$$\dot{x} = f(x, \gamma(z)) , \tag{6.7a}$$

$$\dot{z} = g(z, h(x), \gamma(z)) . \tag{6.7b}$$

is asymptotically stable. □

Proof : system (6.1) is ISS, then let V be an ISS-Lyapunov function and α_i $(i = 1, 2, 3)$ and η be as in Definition 6.2, without loss of generality we assume that $\eta \in \mathcal{K}^\infty$. Let $\rho(s) = \eta^{-1}(r)$; then $\rho \in \mathcal{K}^\infty$ as well, and we have

$$\nabla V(x).f(x,u) \leq -\alpha_3(\|x\|) ,$$

for any $x \in \mathbb{R}^n$ and any $u \in \mathbb{R}^m$ such that $\|u\| \leq \rho(\|x\|)$, which implies that :

$$\nabla V(x).f(x,\gamma(x)) \leq -\alpha_3(\|x\|) ,$$

for any $x \in \mathbb{R}^n$ for any feedback law γ bounded by ρ. Choose $u = \gamma(x)$ for which $\dot{x} = f(x, \gamma(x))$ is well posed and γ is bounded by ρ, observe that $\gamma(0) = 0$. Now there exists a neighborhood $\mathrm{X} \subset \mathbb{R}^n$ of zero, such that $\forall x \in \mathrm{X}$, $\|\gamma(x)\| \leq \rho(\|x\|)$. Next, since (6.1) is weakly detectable, it follows by definition that $\forall\ \epsilon > 0\ \exists\ \delta(\epsilon)$ such that $\|x_0 - z_0\| < \delta(\epsilon) \Rightarrow \|x(t, x_0, u) - z(t, z_0, u)\| < \epsilon\ \forall\ t > 0$. Therefore there exist an open neighborhood $\hat{\mathrm{X}} \subset \mathbb{R}^n$ of zero, contained in X such that $\|\gamma(z)\| \leq \rho(\|z\|)\ \forall z \in \hat{\mathrm{X}}$. Now from Remark 1 we have (6.1) is ISS then

$$\begin{aligned} \nabla V(x).f(x,u) &\leq -\alpha_3(\|x\|) + \alpha_4(\|u\|) \\ \nabla V(x).f(x,\gamma(z)) &\leq -\alpha_3(\|x\|) + \alpha_4(\|\gamma(z)\|) \\ &\leq -\alpha_3(\|x\|) + \alpha_4 \circ \rho(\|z\|) . \end{aligned}$$

For each $x \in \mathrm{X}$ we define

$$a(x) = \sup\{| - \alpha_3(\|x\|) + \alpha_4 \circ \rho(\|z\|)|; z \in \hat{\mathrm{X}}\} . \tag{6.8}$$

The function $a(x)$ is continuous and nonnegative on X.

Now we define $\bar{\gamma}(x) = \|\gamma(x)\|$ and we suppose that $\bar{\gamma}(x)$ is piecewise continuous and moreover it is upper semi-continuous.

Let $\mathbb{X} = \mathrm{X} \times \hat{\mathrm{X}}$ and consider a subset $\Delta = \{(x,z) \in \mathbb{X} : x = z\}$. For any $x_0 \in \mathrm{X} \setminus \{0\}$ we have $\bar{\gamma}(x_0) < \rho(\|x_0\|)$ and there exists $r \in \mathbb{R}$ such that $\bar{\gamma}(x_0) < r < \rho(\|x_0\|)$. In addition, due to upper semi-continuousness of $\bar{\gamma}$, there also exist two subsets,

$$\mathcal{U}_{x_0} \text{ an open neighborhood of } x_0 \text{ such that } \forall z \in \mathcal{U}_{x_0} \quad \bar{\gamma}(z) < r .$$

$$\mathcal{V}_{x_0} \text{ an open neighborhood of } x_0 \text{ such that } \forall x \in \mathcal{V}_{x_0} \quad \rho(\|x\|) > r .$$

next we define

$$\mathbb{U} = \bigcup_{(x_0,x_0)\in\Delta\setminus\{0\}} \mathcal{V}_{x_0} \times \mathcal{U}_{x_0} ,$$

clearly $\mathbb{U}$ is an open subset of $\mathbb{X}$ that contains Δ.

We finally define

$$b(x) = \inf\{\psi_3(\|x-z\|); (x,z) \in \mathbb{X} \setminus \mathbb{U}\} . \tag{6.9}$$

Since $\psi_3 \in \mathcal{K}$ and $x - z = 0$ only if $(x,z) \in \Delta$, it follows that $b(x)$ is strictly positive on $\mathrm{X} \setminus \{0\}$. Therefore there exists a strictly increasing function $\sigma : \mathbb{R}^+ \to \mathbb{R}^+$, such that

$$\sigma(\|x\|)a(x) < b(x) . \tag{6.10}$$

Now, we define

$$\tilde{V}(x) = \int_0^{V(x)} \sigma \circ \alpha_2^{-1}(\xi) d\xi . \tag{6.11}$$

It is obvious that $\tilde{V}$ is positive definite and $\tilde{V}(0) = 0$. Next, we show that

$$\Phi(x,z) = \tilde{V}(x) + W(x,z) \tag{6.12}$$

is a Lyapunov function candidate of $(0,0) \in \mathbb{R}^n \times \mathbb{R}^n$ with respect to (6.7). Observe that $\Phi(x,z)$ is positive definite, indeed $\Phi(x,z) \geq 0 \ \forall \ (x,z) \neq 0$ and $\Phi(x,z) = 0$ if and only if $(x,z) = (0,0)$. It remains to show that the time derivative of $\Phi(x,z)$ along the trajectories of (6.7) is negative.

$$\begin{aligned}\dot{\Phi}(x,z) &= \nabla V(x) f(x,\gamma(z)).\sigma \circ \alpha_2^{-1}(V(x)) + \frac{\partial W}{\partial x} f(x,\gamma(z)) + \frac{\partial W}{\partial z} g(z,h(x),\gamma(z)) \\ &\leq \nabla V(x) f(x,\gamma(z)).\sigma \circ \alpha_2^{-1}(V(x)) - \psi_3(\|x-z\|)\end{aligned} \tag{6.13}$$

case 1 : $(x,z) \in \mathbb{X} \setminus \mathbb{U}$ and $x \neq 0$
using (6.8), (6.9) and (6.10)

$$\dot{\Phi}(x,z) \leq a(x)\sigma(\|x\|) - b(x) < 0 \tag{6.14}$$

case 2 : $(x,z) \in \mathbb{U}$ and $x \neq 0$
since in the set $\mathbb{U}$ we have $\bar{\gamma}(z) = \|\gamma(z)\| < \rho(\|x\|)$ then using (6.5) we get

$$\begin{aligned}\dot{\Phi}(x,z) &\leq \nabla V(x) f(x,\gamma(z))\sigma(\|x\|) - \psi_3(\|x-z\|) \\ &\leq -\alpha_3(\|x\|)\sigma(\|x\|) \\ &< 0\end{aligned} \tag{6.15}$$

since α_3 and σ are strictly positive for $x \neq 0$.

case 3 : $x = 0$ and $z \neq 0$

$$\dot{\Phi}(x,z) \leq -\psi_3(\|z\|) < 0 \tag{6.16}$$

Thus $\dot{\Phi}(x,z) < 0 \ \ \forall \ (x,z) \neq 0$ near zero. Finally, using (6.14), (6.15) and (6.16) we can conclude that Φ is a Lyapunov function of $(0,0) \in \mathbb{R}^n \times \mathbb{R}^n$ with respect to (6.7) and consequently the origin $(0,0) \in \mathbb{R}^n \times \mathbb{R}^n$ is asymptotically stable.

6.2 Example : A robot arm

In this section we consider a system describing the dynamics of a robot arm that can be in general stabilized by a continuous feedback control law. However, in the case of tracking a trajectories having piecewise continuous derivatives, the control law needed is piecewise continuous.

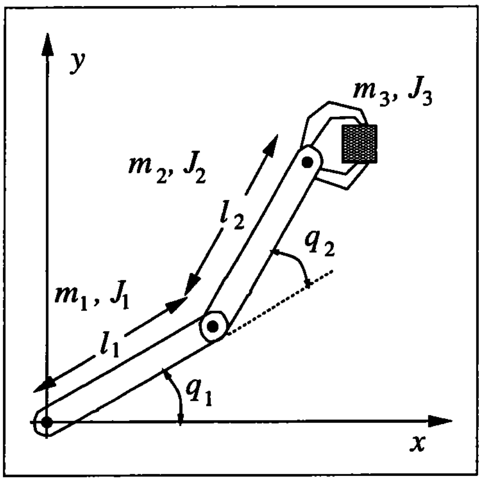

FIG. 6.1 – Two-link planar robot arm

In the model of the robot arm we will discard the vertical translation degree of freedom due to its being completely decoupled from the other coordinates. We will also neglect the movement of the hand and consider it together with the load as a single unit with mass m_3 and inertia J_3. the remaining degrees of freedom are the angular rotations of the inner and outer links of the arm. The dynamic equations of the robot arm are (see [28])

$$u_1 = (H_1 + 2H_2 \cos q_2)\ddot{q}_1 + (H_3 + H_2 \cos q_2)\ddot{q}_2 - H_2(2\dot{q}_1\dot{q}_2 + \dot{q}_2^2)\sin q_2 \quad (6.17a)$$

$$u_2 = (H_3 + H_2 \cos q_2)\ddot{q}_1 + H_3\ddot{q}_2 + H_2\dot{q}_1^2 \sin q_2 \quad (6.17b)$$

with

$$\begin{aligned} H_1 &= J_1 + J_2 + J_3 + m_2 l_1^2 + m_3(l_1^2 + l_2^2) + \frac{m_1 l_1^2 + m_2 l_2^2}{4} \\ H_2 &= l_1 l_2 \left(m_3 + \frac{m_2}{4}\right) \\ H_3 &= J_2 + J_3 + l_2^2\left(m_3 + \frac{m_2}{4}\right) \end{aligned}$$

where m_i, l_i and J_i ; $i = 1, 2$ are respectively the i^{th} link mass, length and moment of inertia with respect to its center of mass. q_i and u_i are the joint position and the torque applied to the i^{th} link. We will assume that the outputs of the system are $y_1 = q_1$ and $y_2 = q_2$ *i.e.* the measured joint positions.

$$\begin{array}{ccc} m_1 = 30kg & m_2 = 15kg & m_3 = 6kg \\ J_1 = 0.4kgm^2 & J_2 = 0.1075kgm^2 & J_3 = 0.01kgm^2 \\ l_1 = 0.4m & l_2 = 0.25m & \end{array}$$

If we define

$$x_1 \triangleq q_1 \ , \quad x_2 \triangleq q_2 \ , \quad x_3 \triangleq \dot{q}_1 \ , \quad x_4 \triangleq \dot{q}_2 \ ,$$

and

$$x \triangleq (x_1 \ x_2 \ x_3 \ x_4)^T$$

then

$$y_1 = h_1(x) \triangleq x_1 \quad \text{and} \quad y_2 = h_2(x) \triangleq x_2$$

from (6.17) we obtain

$$u_1 = (H_1 + 2H_2 \cos x_2)\dot{x}_3 + (H_3 + H_2 \cos x_2)\dot{x}_4 - H_2(2x_3x_4 + x_4^2)\sin x_2 \tag{6.18a}$$

$$u_2 = (H_3 + H_2 \cos x_2)\dot{x}_3 + H_3\dot{x}_4 + H_2x_3^2 \sin x_2 \tag{6.18b}$$

Consider

$$D(x) \triangleq \begin{bmatrix} H_1 + 2H_2 \cos x_2 & H_3 + H_2 \cos x_2 \\ H_3 + H_2 \cos x_2 & H_3 \end{bmatrix}$$

$$P(x) \triangleq \begin{bmatrix} -H_2(2x_3x_4 + x_4^2)\sin x_2 \\ H_2x_3^2 \sin x_2 \end{bmatrix}$$

one can check that the inertia matrix $D(x)$ is positive definite, hence invertible. Equation (6.18) can be written in matrix form

$$\begin{bmatrix} u_1 \\ u_2 \end{bmatrix} = D(x) \begin{bmatrix} \dot{x}_3 \\ \dot{x}_4 \end{bmatrix} + P(x)$$

thus solving for $\dot{x}_3$ and $\dot{x}_4$ we get

$$\begin{bmatrix} \dot{x}_3 \\ \dot{x}_4 \end{bmatrix} = -D^{-1}(x)P(x) + D^{-1}(x) \begin{bmatrix} u_1 \\ u_2 \end{bmatrix} \tag{6.19}$$

Whence, the dynamical system describing the planar motion of the robot arm is described as follows

$$\dot{x} = f(x) + g(x)u \tag{6.20a}$$

$$y = h(x) \tag{6.20b}$$

with

$$f(x) = \begin{bmatrix} x_3 \\ x_4 \\ -D^{-1}(x)P(x) \end{bmatrix} \ , \quad g(x) = \begin{bmatrix} 0 & 0 \\ 0 & 0 \\ \multicolumn{2}{c}{D^{-1}(x)} \end{bmatrix} \ , \quad h(x) = \begin{bmatrix} x_1 \\ x_2 \end{bmatrix}$$

$$D^{-1}(x) = \frac{1}{H_1H_3 - H_3^2 - H_2^2\cos^2 x_2}\begin{bmatrix} H_3 & -H_3 - H_2\cos x_2 \\ -H_3 - H_2\cos x_2 & H_1 + 2H_2\cos x_2 \end{bmatrix}$$

let $g(x) = \begin{pmatrix} g_1(x) & g_2(x) \end{pmatrix}$.

Feedback controller design

By analogy to the input-output linearization method presented in section 2 of chapter 2, a similar theory was developed by Isidori [38, page 219] for the multi-input multi-output systems.

A multi-variable nonlinear system of the form (6.20) has a vector relative degree (r_1, r_2) at a point x_0 if

(i) $L_{g_j}L_f^k h_i(x) = 0$

for $j = 1, 2$, $i = 1, 2$ and $k < r_i - 1$ and for all x in the neighborhood of x_0.

(ii) the 2×2 matrix

$$R(x) = \begin{bmatrix} L_{g_1}L_f^{r_1-1}h_1(x) & L_{g_2}L_f^{r_1-1}h_1(x) \\ L_{g_1}L_f^{r_2-1}h_2(x) & L_{g_2}L_f^{r_2-1}h_2(x) \end{bmatrix}$$

is nonsingular at $x = x_0$.

Using the foregoing definition, we can easily check that the dynamic system describing the robot arm (6.20), has vector relative degree $(r_1, r_2) = (2, 2)$ and that $R(x) = D^{-1}(x)$. The linearizing feedback controller needed for output tracking can be obtained analogously to the single input single output case, and it is given by

$$u(x) = R^{-1}(x)\left(- \begin{bmatrix} L_f^2 h_1(x) \\ L_f^2 h_2(x) \end{bmatrix} + \begin{bmatrix} \ddot{y}_{1d} \\ \ddot{y}_{2d} \end{bmatrix} - K \begin{bmatrix} y_1 - y_{1d} \\ \dot{y}_1 - \dot{y}_{1d} \\ y_2 - y_{2d} \\ \dot{y}_2 - \dot{y}_{2d} \end{bmatrix} \right)$$

where $K \in \mathbb{R}^{2\times 4}$ is a gain matrix to be chosen to ensure asymptotic output tracking. Set

$$K = \begin{bmatrix} k_{11} & k_{12} & 0 & 0 \\ 0 & 0 & k_{21} & k_{22} \end{bmatrix}$$

thus $u(x)$ can be written

$$u(x) = D(x)\left(D^{-1}(x)P(x) + \begin{bmatrix} \ddot{x}_{1d} \\ \ddot{x}_{2d} \end{bmatrix} - \begin{bmatrix} k_{11}(x_1 - \dot{x}_{1d}) & k_{12}(x_3 - \dot{x}_{3d}) \\ k_{21}(x_2 - \dot{x}_{2d}) & k_{22}(x_4 - \dot{x}_{4d}) \end{bmatrix} \right) \tag{6.21}$$

We can obtain K by substituting (6.21) in (6.20), and imposing the resulting closed loop system to be asymptotically stable.

$$
\begin{aligned}
\dot{x} &= f(x) + g(x)u(x) \\
&= \begin{bmatrix} x_3 \\ x_4 \\ -D^{-1}(x)P(x) \end{bmatrix} + \begin{bmatrix} 0 & 0 \\ 0 & 0 \\ & D^{-1}(x) \end{bmatrix} \times \\
&\quad D(x)\left(D^{-1}(x)P(x) + \begin{bmatrix} \ddot{x}_{1d} \\ \ddot{x}_{2d} \end{bmatrix} - \begin{bmatrix} k_{11}(x_1 - \dot{x}_{1d}) + k_{12}(x_3 - \dot{x}_{3d}) \\ k_{21}(x_2 - \dot{x}_{2d}) + k_{22}(x_4 - \dot{x}_{4d}) \end{bmatrix}\right) \\
&= \begin{bmatrix} x_3 \\ x_4 \\ -D^{-1}(x)P(x) \end{bmatrix} + \begin{bmatrix} 0 \\ 0 \\ D^{-1}(x)P(x) + \begin{bmatrix} \dot{x}_{3d} \\ \dot{x}_{4d} \end{bmatrix} - \begin{bmatrix} k_{11}(x_1 - \dot{x}_{1d}) & k_{12}(x_3 - \dot{x}_{3d}) \\ k_{21}(x_2 - \dot{x}_{2d}) & k_{22}(x_4 - \dot{x}_{4d}) \end{bmatrix} \end{bmatrix} \\
&= \begin{bmatrix} x_3 \\ x_4 \\ \dot{x}_{3d} - k_{11}(x_1 - \dot{x}_{1d}) - k_{12}(x_3 - \dot{x}_{3d}) \\ \dot{x}_{4d} - k_{21}(x_2 - \dot{x}_{2d}) - k_{22}(x_4 - \dot{x}_{4d}) \end{bmatrix}
\end{aligned}
$$

Let us define

$$
e_1 \triangleq x_1 - x_{1d}\ , \quad e_2 \triangleq x_2 - x_{2d}\ , \quad e_3 \triangleq x_3 - x_{3d}\ , \quad e_4 \triangleq x_4 - x_{4d}
$$

this yields to

$$
\begin{bmatrix} \dot{e}_1 \\ \dot{e}_2 \\ \dot{e}_3 \\ \dot{e}_4 \end{bmatrix} = \begin{bmatrix} 0 & 0 & 1 & 0 \\ 0 & 0 & 0 & 1 \\ -k_{11} & 0 & -k_{12} & 0 \\ 0 & -k_{21} & 0 & -k_{22} \end{bmatrix} \begin{bmatrix} e_1 \\ e_2 \\ e_3 \\ e_4 \end{bmatrix} \tag{6.22}
$$

or

$$
\dot{e} = A_c e
$$

k_{11}, k_{12}, k_{21} and k_{22} should be chosen such that A_c has all of its eigenvalues with negative real parts. Actually, the characteristic polynomial is

$$
p(\lambda) = \det(\lambda I - A_c) = \det \begin{bmatrix} 0 & 0 & 1 & 0 \\ 0 & 0 & 0 & 1 \\ -k_{11} & 0 & -k_{12} & 0 \\ 0 & -k_{21} & 0 & -k_{22} \end{bmatrix}
$$

$$
p(\lambda) = \lambda^4 + (k_{12} + k_{22})\lambda^3 + (k_{12}k_{22} + k_{11} + k_{21})\lambda^2 + (k_{12}k_{21} + k_{11}k_{22})\lambda + k_{11}k_{21}
$$

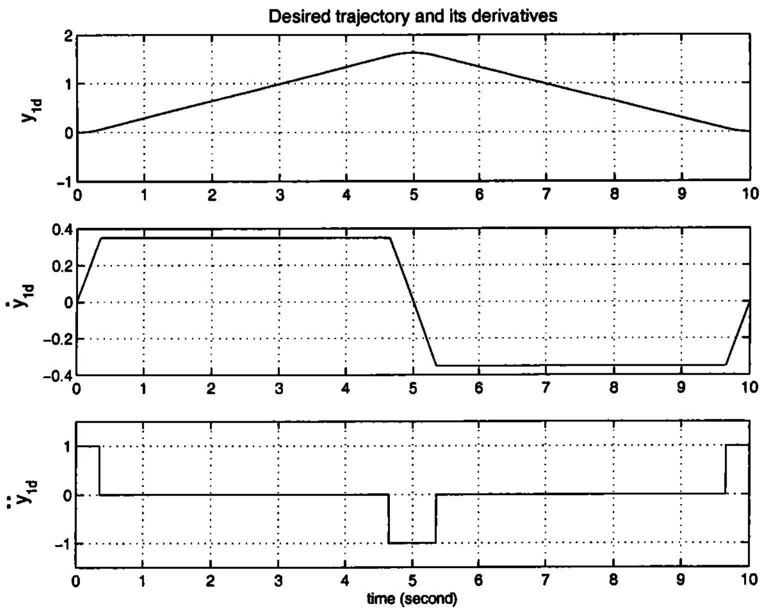

FIG. 6.2 – The desired trajectory.

if we let $k_{11} = k_{12} = k_{21} = k_{22} = 4$

$$\begin{aligned} p(\lambda) &= \lambda^4 + 8\lambda^3 + 24\lambda^2 + 32\lambda + 16 \\ &= (\lambda + 2)^4 \end{aligned}$$

Therefore leading to $\lambda = -2$, and consequently to an exponential output tracking. Figure 6.3 shows the numerical simulation resulting from the above analysis.

The desired trajectory to be tracked is given by

$$\ddot{y}_{1d} = \begin{cases} 1 & 0 \le t < 0.35 \\ 0 & 0.35 \le t < 4.65 \\ -1 & 4.65 \le t < 5.35 \\ 0 & 5.35 \le t < 9.65 \\ 1 & 9.65 \le t < 10 \end{cases}$$

$$\dot{y}_{1d}(0) = y_{1d}(0) = 0$$

$$y_{2d}(t) = y_{1d}(t) \quad \forall\, t \in [0, 10[$$

Note that the desired outputs $\ddot{y}_{1d}$ and $\ddot{y}_{2d}$ that appear in the synthesis of the feedback control law are two piecewise continuous signals, thus yielding a piecewise continuous control. The control signals $u_1(t)$ and $u_2(t)$ are plotted in Figure 6.4

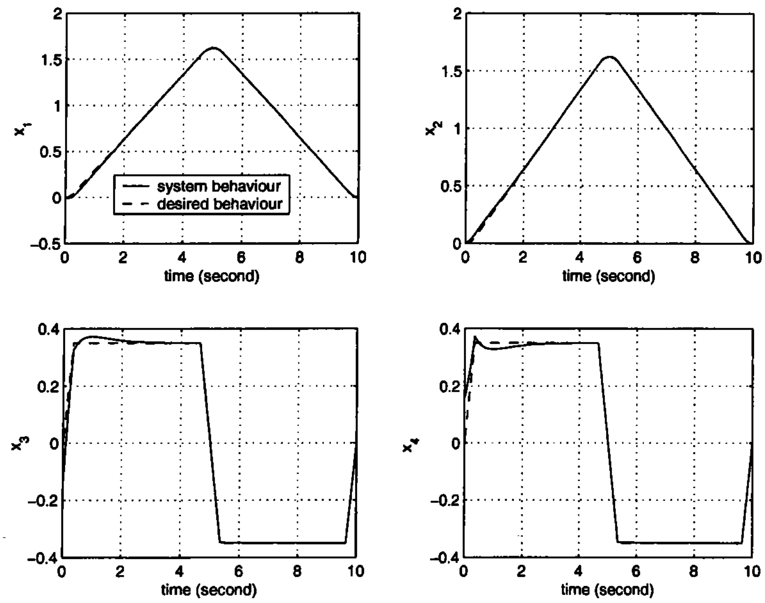

FIG. 6.3 – Output tracking using state feedback.

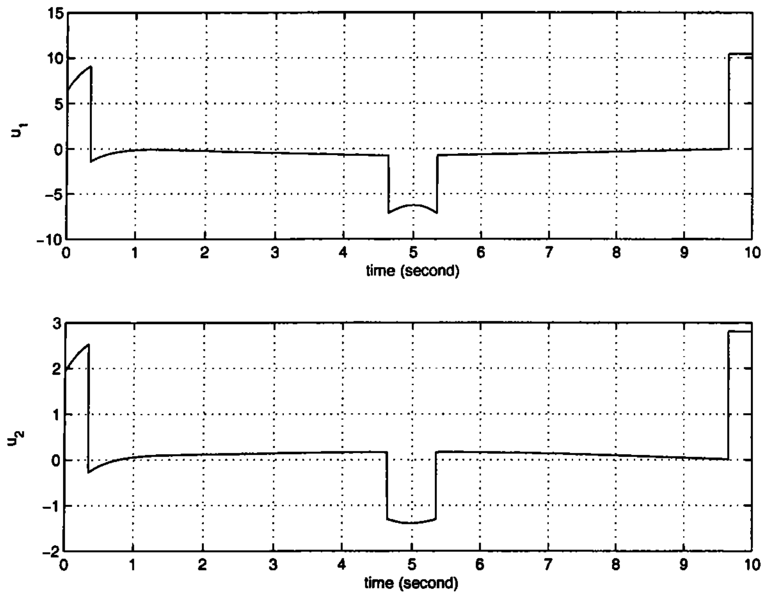

FIG. 6.4 – The needed control constructed using state feedback.

Observer design

The nonlinear system describing the dynamics of the robot arm is the following

$$\begin{bmatrix} \dot{x}_1 \\ \dot{x}_2 \\ \dot{x}_3 \\ \dot{x}_4 \end{bmatrix} = \begin{bmatrix} x_3 \\ x_4 \\ -D^{-1}(x)P(x) \end{bmatrix} + \begin{bmatrix} 0 & 0 \\ 0 & 0 \\ \multicolumn{2}{c}{D^{-1}(x)} \end{bmatrix} u \tag{6.23}$$

$$h(x) = \begin{bmatrix} x_1 \\ x_2 \end{bmatrix}$$

this system can be written in the form

$$\begin{aligned} \dot{x} &= Ax + f(x,u) \\ y &= Cx \end{aligned}$$

with

$$A = \begin{bmatrix} 0 & 0 & 1 & 0 \\ 0 & 0 & 0 & 1 \\ 0 & 0 & 0 & 0 \\ 0 & 0 & 0 & 0 \end{bmatrix}, \quad C = \begin{bmatrix} 1 & 0 & 0 & 0 \\ 0 & 1 & 0 & 0 \end{bmatrix}, \quad f(x,u) = \begin{bmatrix} 0 \\ 0 \\ D^{-1}(x)\big(u - P(x)\big) \end{bmatrix}$$

we can easily check that (C, A) is an observable pair, and by using the results of section 1 from chapter 4

$$\dot{\hat{x}} = A\hat{x} + f(\hat{x}, u) + \zeta S^{-1} C^T (y - C\hat{x}) \tag{6.24}$$

where S is the solution of the equation

$$0 = -\theta S - A^T S - SA + C^T C$$

is an observer for the system (6.23), with $\theta = 7$ and $\zeta = 10$. Figure 6.5 show the behaviour of the observer and that of the real system. The initial conditions used for the simulations are

$$x_1(0) = 0\ , \quad x_2(0) = 0\ , \quad x_3(0) = -0.16\ , \quad x_4(0) = 0.16$$

$$\hat{x}_1(0) = 0\ , \quad \hat{x}_2(0) = 0\ , \quad \hat{x}_3(0) = 0\ , \quad \hat{x}_4(0) = 0$$

We have seen in previous figures how output tracking was achieved and how the observer correctly estimates the real states. In the next figures 6.6 and 6.7 we will show the output tracking and the feedback control resulting from a control via estimated states.

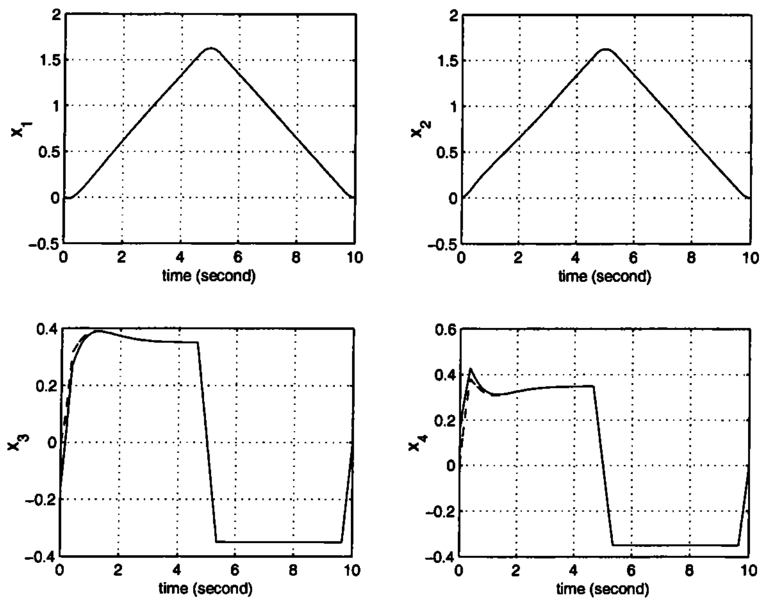

FIG. 6.5 – The observer behaviour, x(—), $\hat{x}$(- - -).

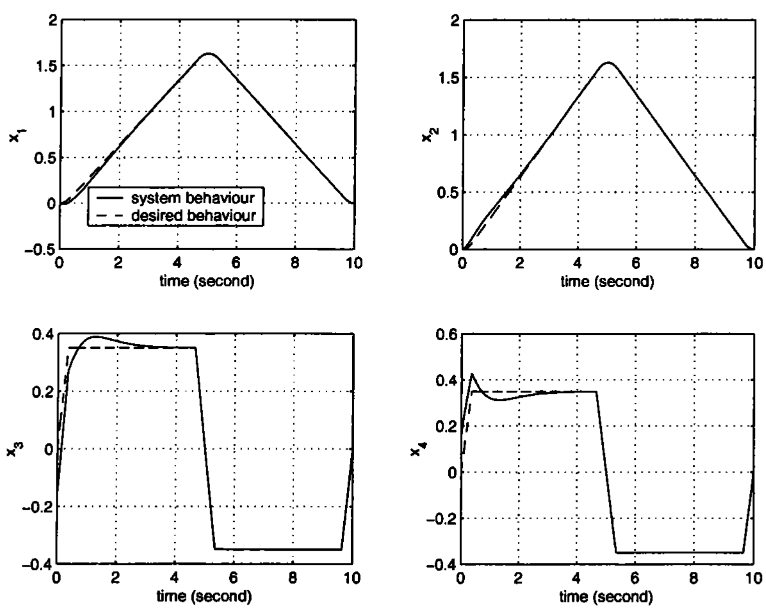

FIG. 6.6 – Tracking via observer states feedback.

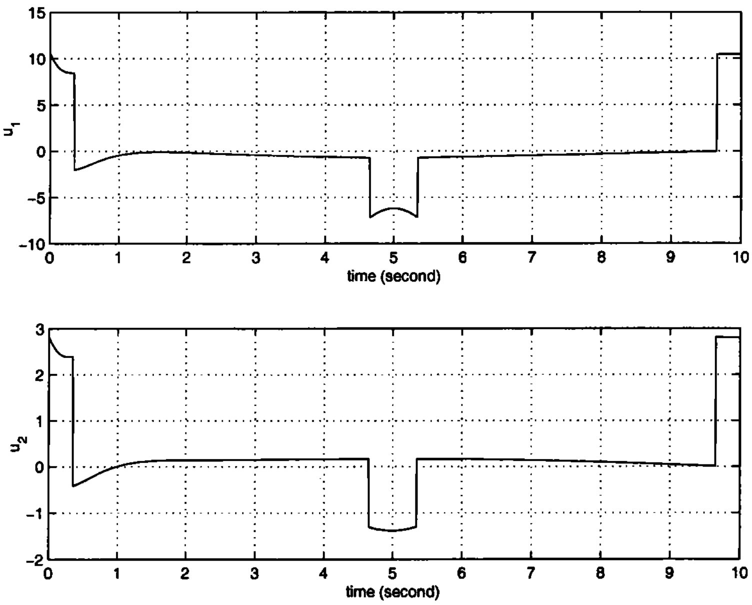

FIG. 6.7 – Feedback control constructed using observer states.

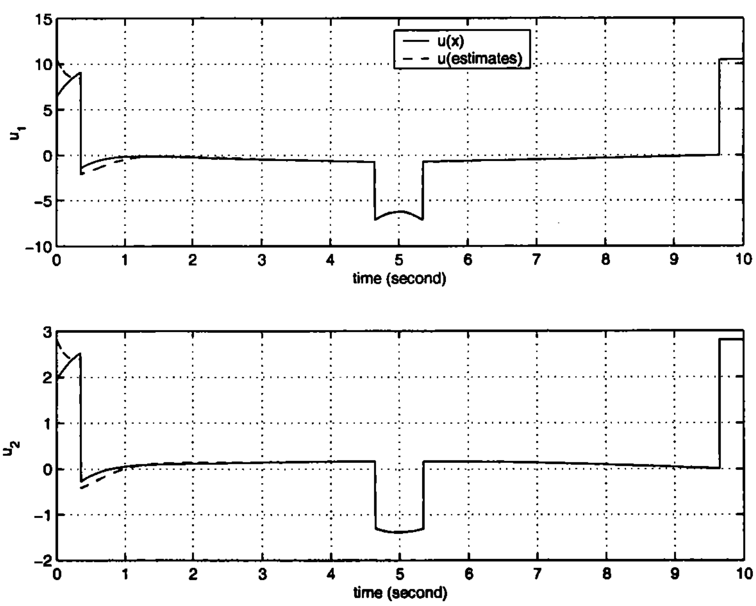

FIG. 6.8 – Comparing $u(x)$ and $u(\hat{x})$

Chapitre 7

Conclusions and future work

In this dissertation the problem of investigating hydraulically driven manipulators has been addressed from two viewpoints. The first point consists in modeling the system to be studied, and the second one was to design observers and controllers that help to automatically control such systems.

7.1 Conclusions

In the development of a mathematical model for the electrohydraulic system we conceived the idea of obtaining a model that can reflect the real behaviour of the system meanwhile being appropriate for easy mathematical analysis. the approach stem from the fact of taking into consideration the servovalve leakages which were more often than not neglected in theoretical analysis. To check the validity of the model, simulations were subjected to comparison with experimental results. The graphs of section 2.5.3 confirmed the applicability and performance of our model.

Having obtained a proper model for the system that constitute the root of our research, we were than ready to tackle the controller and observer design issues.

From the very first inspection of the system model, it appeared that electrohydraulic systems introduce aspects such as higher order dynamics, with increased nonlinearities. These aspects complicate the control design. Therefore direct application of known nonlinear control methods is not straightforward.

Designing a nonlinear controller, from the nonlinear methods existing in literature, to a simplified version of our model helped in fixing the drawbacks of these methods. Thus from the theories of sliding mode and that of the passive approach we have developed a new way to design a sliding surface. Such an approach contributes to designing robust controllers for non-affine nonlinear systems.

As it has been always the case, the controller design topic often recalls the observer design topic, since it has been shown that the feedback control expression involves all the state variables. The answer to the question of observer design has been addressed in chapter 5, from where we deduce the following conclusions.

The electrohydraulic system including a symmetric piston is observable if we only measure the displacement of the piston.

We have improved the performance of a high-gain observer and developed another simple one based on drive-response approach. however, as these observers consider the exact knowledge of parameters, their field of application is restricted and it is expected that their performance will be degraded in the presence of parameters change. This was illustrated in section 5.4.2. Consequently, we have designed a robust observer based on sliding method. The sliding observer is founded on the assumption that the uncertainties in the model are bounded and are matched with the observations.

We finally, studied the problem of stabilization using estimated states. Our main concern raised from the fact that some stabilizing controllers, and especially those constructed using sliding mode method, may be discontinuous functions of time. Hence we aimed to prove that under mild conditions the stabilizing controller built using estimated states will also stabilize the system is question. the application chosen for this theoretical result was the robot arm since the simulations were clearer.

7.2 Future works and open issues

Although we have brought answers to the problems which have been raised in the introduction, improvements are still possible. Actually, from this research the following aspects seem to be worthwhile to be investigated in more details.

The use of a dynamic model of the servovalve, rather than a static model, as explained in the summary of chapter 3, may lead to better controller results and further enlarge the applicability of the model, for instance in the case of relatively high frequency applications (*i.e.* applications where the servovalve spool has to switch position following a high frequency input signal).

Related to robustness, one can think of parameter estimation such as developing an adaptive observer. This work is presently being done to estimate Coulomb friction parameter only by measuring the displacement of the rod.

The design of a sliding observer showed a number of open issues. Although the assumption of bounded uncertainties is not restrictive, the matching condition is not always verified in practice, hence searching in this direction can be of great value. Robustness with respect to measurement inaccuracy is also worth analyzing.

Bibliographie

[1] K. H. Adjallah. *Contribution au diagnostic de systèmes par observateur d'état.* Phd thesis, L'Institue National Polytechnique de Lorraine, France, 1993.

[2] A. Alleyne and J.K. Hedrick. Nonlinear adaptive control of active suspensions. *IEEE Trans. on Control Systems Technology*, 3(3) :94–102, 1995.

[3] A. Alleyne, R. Liu, and H. Wright. On the limitation of force tracking control for hydraulic active suspensions. In *Proceedings of American Control Conference*, pages 43–47, Philadelphia, 1998.

[4] Ahmad N. Atassi and Hassan K. Khalil. A separation principle for the stabilization of a class of nonlinear systems. *IEEE Trans. on Automatic Control*, 44(9) :1672–1687, 1999.

[5] Saman Behtash. Robust output tracking for nonlinear systems. *International Journal of Control*, 51(6) :1381–1407, 1990.

[6] O. Bernard, G. Sallet, and A. Sciandra. Nonlinear observers for a class of biological systems : Application to validation of a phytoplanktonic growth model. *IEEE Trans. on Automatic Control*, 43(8) :1056–1065, 1998.

[7] T. Boukhobza, M. Djemai, and J. P. Barbot. Nonlinear sliding observer for systems in output and output derivative injection form. In *Proceedings of IFAC World Congress*, pages 299–305, San Antonio, 1996.

[8] C. I. Byrnes and A. Isidori. Local stabilization of minimum-phase nonlinear systems. *Systems & Control Letters*, 11 :9–17, 1988.

[9] Christopher I. Byrnes and Alberto Isidori. Asymptotic stabilization of minimum phase nonlinear systems. *IEEE Trans. on Automatic Control*, 36(10) :1122–1137, 1991.

[10] F. Celle, J. P. Gauthier, D. kazakos, and G. Sallet. Synthesis on nonlinear observers : A harmonic analysis approach. *Mathematical Systems Theory*, 22 :291–322, 1989.

[11] J. N. Chiasson and R.T. Novotnak. Nonlinear speed observer for the pm stepper motor. *IEEE Trans. on Automatic Control*, 38(10) :1584–1588, 1993.

[12] G. Ciccarella, M. Dalla Mora, and A. Germani. A luenberger-like observer for nonlinear systems. *International Journal of Control*, 57(3) :537–556, 1993.

[13] S. V. Drakunov and I. V. Utkin. Sliding mode control in dynamic systems. *International Journal of Control*, 55(4) :1029–1037, 1992.

[14] Sergey Drakunov and Vadim Utkin. Sliding mode observers tutorial. In *Proceedings of 34th IEEE Conference on Decision and Control*, pages 3376–3378, New Orleans, 1995.

[15] C. Edwards and S. K. Spurgeon. On the development of discontinuous observers. *International Journal of Control*, 59(5) :1211–1229, 1994.

[16] C. Edwards, S. K. Spurgeon, and R. J. Patton. Sliding mode observers for fault detection and isolation. *Automatica*, 36 :541–553, 2000.

[17] A. Ellman. Leakage behaviour of four-way servovalve. In *Proceedings of the ASME fluid power systems and technology division*, pages 163–167, Anaheim, 1998.

[18] A. Ellman and T. Virvalo. Formation of pressure gain in hydraulic servovalves and its significance in system behaviour. In *Proceedings of the ASME fluid power systems and technology division*, pages 77–81, Atlanta, 1996.

[19] Bora Eryilmaz and Bruce H. Wilson. Combining leakage and orifice flows in a hydraulic servovalve model. *Transactions of the ASME - Journal of Dynamic Systems Measurement and Control*, 122 :576–579, 2000.

[20] M. Feki and E Richard. Including leakage flow in the servovalve steady state model. submitted to Transactions of the ASME - Journal of Dynamic Systems Measurement and Control, March 2001.

[21] M. Feki, E. Richard, and F. Gomes Almeida. Commande en effort d'un vérin hydraulique par linéarization entrée/sortie. In *Journées Doctorales d'Automatiques, JDA'99.*, pages 181–184, Nancy-France, 1999.

[22] M. Feki and J-C Vivalda. Sliding observer for a class of nonlinear systems with uncertainties. submitted to Systems & Control Letters, April 2001.

[23] Moez Feki. Robust control of a hydraulic system force. In *Second Nonlinear Control Network (NCN) Workshop*, Paris, 2000.

[24] Moez Feki and Mohamed Ali Hammami. Observer design for an electrohydraulic manipulator. In *IASTED Intl. Conf. on Control Applications*, Banff - Canada, 2001.

[25] Moez Feki and J-C. Vivalda. Nonlinear observer design application to an electrohydraulic system. In *3rd Intl. Conf. on Applied Mathematics and Engineering Sciences*, Morocco, 2000.

[26] Moez Feki and J-C. Vivalda. Sur la stabilisation des systèmes non linéaires par retour d'états estimés. In *Actes de Société de Mathématiques Tunisienne*, Sousse - Tunisie, 2000.

[27] Moez Feki and Jean-Claude Vivalda. A result on the stabilization of nonlinear systems by state detection. In *Fourth Nonlinear Control Network (NCN) Workshop*, Shefield, 2001.

[28] Rafael A. Garcia and Carlos E. D'Attellis. Trajectory tracking in nonlinear systems via nonlinear reduced-order observers. *International Journal of Control*, 62(3) :685–715, 1995.

[29] J. P. Gauthier and G. Bornard. *Outils et modèles mathématiques pour l'automatique et la théorie des signals*, chapter Stabilization des systèmes non linéaires, pages 307–324. Edition du CNRS, 1981.

[30] J. P. Gauthier and I. A. K. Kupka. Observability and observer for nonlinear systems. *SIAM Journal on Control and Optimization*, 32(4) :975–994, 1994.

[31] J.P. Gauthier and G. Bornard. Observability for any $u(t)$ of a class of nonlinear systems. *IEEE Trans. on Automatic Control*, AC-26(4) :922–926, 1981.

[32] J.P. Gauthier, H. Hammouri, and S. Othman. A simple observer for nonlinear systems applications to bioreactors. *IEEE Trans. on Automatic Control*, 37(6) :875–880, 1992.

[33] Vivek Grag. *Fault detection in nonlinear systems : An application to automated highway systems.* Phd in mechanical engineering, University of California at Berkeley, USA, 1995.

[34] W. Hahn. *Stability of Motion.* Springer-Verlag, Berlin, 1967.

[35] M. A. Hammami. Stabilization of a class of nonlinear systems using an observer design. In *Proceedings of 32nd IEEE Conference on Decision and Control*, pages 1954–1959, San Antonio, 1993.

[36] H. Hammouri, K. Busawon, and M. Farza. Nonlinear observers for local uniform observable systems. *SIAM Journal on Control and Optimization*, pages –, 1999.

[37] H. Hammouri, M Kinnaert, and E. H. El Yaagoubi. Observer-based approach to fault detection and isolation for nonlinear systems. *IEEE Trans. on Automatic Control*, 44(10) :1879–1884, 1999.

[38] Alberto Isidori. *Nonlinear Control Systems.* Springer-Verlag, United Kingdom, 3rd edition, 1995.

[39] V. Jurdjevic and J.P. Quinn. Controllability and stability. *Journal of Differential Equations*, 28 :381–389, 1978.

[40] Thomas Kailath. *Linear Systems.* Printice-Hall, USA, 1980.

[41] Hassan K. Khalil. *Nonlinear Systems.* Macmillan, New York, 1992.

[42] K. K. Lee and A. Arapostathis. Remarks on smooth feedback stabilization of nonlinear systems. *Systems & Control Letters*, 10 :41–44, 1988.

[43] Wei Lin. Feedback stabilization of general nonlinear control systems : A passive system approach. *Systems & Control Letters*, 25 :41–52, 1995.

[44] Wei Lin. Global asymptotic stabilization of general nonlinear systems with stable free dynamics via passivity and bounded feedback. *Automatica*, 32(6) :915–924, 1996.

[45] Xiao-Yun Lu and Sarah K. Spurgeon. Robust sliding mode control of uncertain nonlinear systems. *Systems & Control Letters*, 32 :75–90, 1997.

[46] David G. Luenberger. Observer for multivariable systems. *IEEE Trans. on Automatic Control*, AC-11(2) :190–197, 1966.

[47] David G. Luenberger. An introduction to observers. *IEEE Trans. on Automatic Control*, AC-16(6) :596–602, 1971.

[48] Ricardo Marino. Feedback stabilization of single-input nonlinear systems. *Systems & Control Letters*, 10 :201–206, 1988.

[49] Ricardo marino. Adaptive observers for single output nonlinear systems. *IEEE Trans. on Automatic Control*, 35(9) :1054–1058, 1990.

[50] Ricardo marino and Patrizio Tomei. Global adaptive observers for nonlinear systems via filtered transformations. *IEEE Trans. on Automatic Control*, 37(8) :1239–1245, 1992.

[51] Ricardo marino and Patrizio Tomei. Adaptive observers with arbitrary exponential rate of convergence for nonlinear systems. *IEEE Trans. on Automatic Control*, 40(7) :1300–1304, 1995.

[52] Herbert E. Merritt. *Hydraulic Control Systems.* John Wiley & Sons, USA, 1967.

[53] S. Nicosia, P. Tomei, and A. Tornambè. Observer-based control law for a class of nonlinear systems. *International Journal of Control*, 51(3) :355–566, 1990.

[54] A. J. Nijmeijer, H.Vander Schaft. *Nonlinear Dynamical Control Systems.* Springer-Verlag, USA, 1990.

[55] N. Niksefat and N. Sepehri. Design and experimental evaluation of a robust force controller for an electrohydraulic actuator via quantitative feedback theory. *Control Engineering Practice*, 8 :1335–1345, 2000.

[56] J. O'Reilly. *Observers for Linear Systems*, volume 170 of *Mathematics in Science and Engineering.* Academic Press, New york, 1983.

[57] R. Outbib and E. Richard. State feedback stabilization of an electropneumatic system. *Transactions of the ASME - Journal of Dynamic Systems Measurement and Control*, 122 :410–415, 2000.

[58] R. Outbib and G. Sallet. Stabilizability of the angular velocity of a rigid body revisited. *Systems & Control Letters*, 18 :93–98, 1992.

[59] William J. Palm III. *Modeling Analysis and Control of Dynamical Systems.* Jhon Wiley & Sons, Canada, 1983.

[60] R.V. Patel and M. Toda. Quantitative measures of robustness in multivariable systems. In *Proceedings of American Control Conference*, San Francisco, 1980.

[61] S. Raghavan and J.K. Hedrick. Observer design for a class of nonlinear systems. *Int. J. Control*, 59(2) :515–528, 1994.

[62] Rajesh Rajamani and J. Karl Hedrick. Adaptive observers for active automotive suspensions : Theory and experiment. *IEEE Trans. on Control Systems Technology*, 3(1) :86–93, 1995.

[63] E. Richard and R. Outbib. State feedback stabilization of an electrohydraulic system. In *Proceedings of Third European Control Conference*, pages 330–335, Roma, 1995.

[64] E. Richard, S. Scavarda, D. Thomasset, and A. Oustaloup. Modélisation et commande des systèmes à fluide sous pression. Technical report, PRC-GDR Automatique, Paris, Mai 1999.

[65] Peter Seibert and Rodolfo Suarez. Global stabilization of nonlinear cascade systems. *Systems & Control Letters*, 14 :347–352, 1990.

[66] H. Sira-Ramirez. On the dynamical sliding mode control of nonlinear systems. *International Journal of Control*, 57(5) :1039–1261, 1993.

[67] J. J. E. Slotine, J. K. Hedrick, and E. A. Misawa. Nonlinear state estimation using sliding observers. In *Proceedings of 25th IEEE Conference on Decision and Control*, pages 332–339, Athens, 1986.

[68] Jean-Jacques E. Slotine. Sliding controller design for nonlinear systems. *International Journal of Control*, 40(2) :421–434, 1984.

[69] Jean-Jacques E. Slotine and Weiping Li. *Applied Nonlinear Control.* Prentice Hall, USA, 1991.

[70] G. A. Sohl and J. E. Bobrow. Experiments and simulations on the nonlinear control of a hydraulic servosystem. *IEEE Trans. on Control Systems Technology*, 7(3) :238–247, 1999.

[71] Eduardo D. Sontag. *Mathematical Control theory.* Springer-Verlag, New York, 1990.

[72] Eduardo D. Sontag and Yuan Wang. On characterizations of the input-to-state stability property. *Systems & Control Letters*, 24 :351–359, 1995.

[73] H. J. Sussman and P. V. Kokotovic. The peaking phenomenon and the global stabilization of nonlinear systems. *IEEE Trans. on Automatic Control*, 36(4) :424–440, 1991.

[74] S. Tafazoli, C. W. De Silva, and P. D. Lawrence. Tracking control of an electro-hydraulic manipulator in the presence of friction. *IEEE Trans. on Control Systems Technology*, 6(3) :401–411, 1998.

[75] Andrew Teel and Laurent Praly. Global stabilizability and observability imply semi-global stabilizability by output feedback. *Systems & Control Letters*, 22 :313–325, 1994.

[76] F.E. Thau. Observing the state of nonlinear dynamical systems. *International Journal of Control*, 17(3) :471–479, 1973.

[77] William J. Thayer. Specification standards for electrohydraulic flow control servovalves. Technical Bulletin 117, MOOG Inc. Control Division, New York, 1962.

[78] M. L. Thein and E. A. Misawa. Comparison of the sliding observer to several state estimators using a rotational inverted pendulum. In *Proceedings of 34th IEEE Conference on Decision and Control*, pages 3385–3390, New Orleans, 1995.

[79] A. Tornambè. Use of asymptotic observers having high-gains in the state and parameter estimation. In *Proceedings of 28th IEEE Conference on Decision and Control*, pages 1791–1794, Tampa, Florida, 1989.

[80] John Tsinias. Further results on the observer design problem. *Systems & Control Letters*, 14 :411–418, 1990.

[81] John Tsinias. A generalization of vidyasagar's theorem on stabilizability using state detection. *Systems & Control Letters*, 17 :37–42, 1991.

[82] Vadim I. Utkin. variable structure systems with sliding modes. *IEEE Trans. on Automatic Control*, AC-22(4) :212–222, 1977.

[83] Vadim I. Utkin. *Sliding mode in control and optimization.* Springer-Verlag, Berlin, 1992.

[84] M. Vidyasagar. on the stabilization of nonlinear systems using state detection. *IEEE Trans. on Automatic Control*, AC-25(3) :504–509, 1980.

[85] M. Vidyasagar. *Nonlinear Systems Analysis.* Prentice Hall, New Jersey, 2nd edition, 1993.

[86] T. J. Viersma. *Analysis, Synthesis, and Design of Hydraulic Servosystems and Pipelines.* Elsevier, Netherlands, 1980.

[87] B. L. Walcott, M. J. Corless, and S. H. Żak. Comparative study of nonlinear state observation techniques. *International Journal of Control*, 45(6) :2109–2132, 1987.

[88] J. Warga. *Optimal Control of Differential and Functional Equations.* Academic Press, New York, 1972.

[89] John Watton. *Fluid Power Systems.* Printice Hall, United Kingdom, 1989.

[90] Darrell Williamson. Observation of bilinear systems with application to biological control. *Automatica*, 13 :243–254, 1977.

[91] Bartosiewicz Z. Local observability of nonlinear systems. *Systems & Control Letters*, 25 :295–298, 1995.

[92] M. Zeitz. The extended luenberger observer for nonlinear systems. *Systems & Control Letters*, 9 :149–156, 1987.

Résumé

Les systèmes électrohydrauliques se caractérisent par des modèles non-linéaires compliqués, ce qui a fait de leur stabilisation en boucle-fermée (par retour d'état) un objectif difficile. La stabilisation par retour d'état exige, en général, la connaissance de tout l'état, ce qui n'est pas toujours possible. Par conséquence, la conception d'un estimateur d'état est également de grand intérêt.

Cette thèse traite la synthèse de commandes et d'observateurs pour les systèmes non-linéaires avec une application aux systèmes hydrauliques. Pour commencer, un nouveau modèle de système hydraulique, permettant de reproduire correctement les débits de fuite dans la servovalve, est développé. Ensuite, plusieurs méthodes de stabilisation par retour d'état ont été appliquées. Nous proposons une nouvelle méthode de construction d'une commande par mode de glissement qui est connue pour sa robustesse. Puis, le problème de concevoir un observateur non-linéaire est considéré. La contribution de cette thèse consiste en trois observateurs différents, un premier observateur à grand gain, le second est basé sur la méthode "drive-response" et le troisième observateur est basé sur la méthode de glissement. Le dernier est d'intérêt particulier puisqu'il est robuste au variation de paramètres. Par la suite nous avons étudié le problème de la stabilisation par retour d'état estimé.

Mots-clés: Dispositif électrohydraulique, Systèmes non-linéaires, Commandes non-linéaires, Observateurs non-linéaires, Principe de séparation.

Abstract

Electrohydraulic systems are characterized by their complex nonlinear model. This feature has made their stabilization using feedback control a worthwhile endeavor. State feedback stabilization usually requires the direct accessability to different system states, which is not always possible. Hence, the design of a state estimator is also of great interest.

Both controller and observer design are considered in this thesis. First, we start by giving a mathematical model which reflects as best the behaviour of the electrohydraulic system. In our model leakage flow are included meanwhile keeping the model simple enough to be mathematically handled. Next, several methods of designing stabilization feedback control were applied to the electrohydraulic system. In this thesis we present a new simple way to choose the sliding manifold to design a sliding mode controller which is known for its robustness. Then, the problem of designing an observer is considered. The contribution of this thesis consists in designing three different nonlinear observers, a first one based on high-gain method, the second based on drive-response method and the third based on the sliding mode theory. The last observer showed particular interest since it is robust to parameter changes. Eventually, we studied the problem of feedback stabilization using estimated states.

Keywords: Electrohydraulic manipulator, Nonlinear systems, Nonlinear control, Nonlinear observer, Separation principle.